Physico-mechanical, Chemical and Durability Characteristics of Mortar and Concrete Containing Palm Oil Boiler Clinker Aggregate Blended with Rice Husk Ash and Ca-Bentonite

Kamolchanok Kueaket

A Thesis Submitted in Partial Fulfillment of the Requirements for the Degree of Master of Engineering in Mining and Materials Engineering Prince of Songkla University 2021

Physico-mechanical, Chemical and Durability Characteristics of Mortar and Concrete Containing Palm Oil Boiler Clinker Aggregate Blended with Rice Husk Ash and Ca-Bentonite

Kamolchanok Kueaket

A Thesis Submitted in Partial Fulfillment of the Requirements for the Degree of Master of Engineering in Mining and Materials Engineering Prince of Songkla University 2021

Thesis Title   Physico-mechanical, Chemical and Durability Characteristics of Mortar and Concrete Containing Palm Oil Boiler Clinker Aggregate Blended with Rice Husk Ash and Ca-Bentonite

Author   Miss Kamolchanok Kueaket

Major Program   Mining and Materials Engineering

Major Advisor

…………………………………………
(Assoc.Prof.Dr.Danupon Tonnayopas)

Examining Committee:

………………………………….Chairperson
(Asst.Prof.Dr.Vishnu Rachpech)

………………………………...Committee
(Assoc.Prof.Dr.Danupon Tonnayopas)

………………………………...Committee
(Asst.Prof.Dr.Phongpat Sontamino)

………………………………...Committee
(Dr.Abideng Hawa)

The Graduate School, Prince of Songkla University, has approved this thesis as partial fulfillment of the requirements for the Master of Engineering Degree in Mining and Materials Engineering.

………………………………….………
(Prof.Dr.Damrongsak Faroongsarng)
Dean of Graduate School

This is to certify that the work here submitted is the result of the candidate's own investigations. Due acknowledgement has been made of any assistance received.

……………………………….Signature

(Assoc.Prof.Dr.Danupon Tonnayopas)

Major Advisor

…………………………….Signature

(Miss Kamolchanok Kueaket)

Candidate

I hereby certify that this work has not been accepted in substance for any degree, and is not being currently submitted in candidature for any degree.

………………………………… Signature

(Miss Kamolchanok Kueaket)

Candidate

ชื่อวิทยานิพนธ์	คุณลักษณะกายภาพเชิงกล ทางเคมี และความคงทนของมอร์ตาร์และคอนกรีตใส่มวลรวมตะกรันปาล์มน้ำมันผสมกับเถ้าแกลบและเบนโทไนต์ชนิดแคลเซียม
ผู้เขียน	นางสาวกมลชนก เกื้อเกต
สาขาวิชา	วิศวกรรมเหมืองแร่และวัสดุ
ปีการศึกษา	2563

บทคัดย่อ

งานวิจัยนี้มุ่งศึกษาการนำเอาตะกรันปาล์มน้ำมันมาใช้ประโยชน์ในการแทนที่เป็นมวลรวมธรรมชาติผสมกับเถ้าแกลบและเบนโทไนต์ชนิดแคลเซียม เพื่อผลิตเป็นมอร์ตาร์และคอนกรีตรักษ์สิ่งแวดล้อม โดยใช้แคลเซียมเบนโทไนต์และเถ้าแกลบแทนที่ปูนซีเมนต์ปอร์ตแลนด์ประเภท 1 ทั้งสองและสามชนิดที่อัตราส่วนร้อยละ 10 20 และ 30 โดยน้ำหนัก ส่วนผสมทั้งหมดคงที่อัตราส่วนน้ำต่อวัสดุประสานไว้ที่ 0.48 ศึกษาพฤติกรรมเวลาก่อตัวและอุณหภูมิของปฏิกิริยาไฮเดรชันของเพสต์ ศึกษาโครงทางทางจุลภาคและแร่ประกอบของมอร์ตาร์ด้วยกล้องจุลทรรศน์อิเล็กตรอนแบบส่องกราดและเทคนิคการเลี้ยวเบนรังสีเอ็กซ์ ตัวอย่างมอร์ตาร์ทั้งหมดนำไปบ่มในสารละลายน้ำปูนขาวอิ่มตัวที่อุณหภูมิห้อง 29±3 องศาเซลเซียส ความชื้นสัมพัทธ์ร้อยละ 80-90 เป็นระยะเวลา 7 28 และ 56 วัน ก่อนนำไปทดสอบสมบัติต่างๆ ได้แก่ การดูดซึมน้ำ รูพรุนปรากฏ กำลังอัด และความคงทนต่อสารละลายกรดซัลฟูริกและโซเดียมซัลเฟต ทดสอบสภาพการซึมผ่านได้ของประจุคลอไรด์ การดูดซึมน้ำในรูเล็กและกำลังดึงทางอ้อม (แบบบราซิล) ของตัวอย่างคอนกรีต

จากผลการศึกษา พบว่ามวลรวมตะกรันปาล์มน้ำมันสามารถนำมาใช้แทนที่มวลรวมธรรมชาติเพื่อผลิตมอร์ตาร์และคอนกรีตได้ และเมื่อเพิ่มปริมาณวัสดุแทนที่ปูนซีเมนต์ทั้งสองชนิดและสามชนิด ส่งผลให้เวลาก่อตัว อุณหภูมิจากปฏิกิริยาไฮเดรชันของเพสต์ และอัตราการไหลของมอร์ตาร์สดมีค่าลดลง โดยเวลาก่อตัวและอุณหภูมิปฏิกิริยาไฮเดรชันของเพสต์ผสมเถ้าแกลบร้อยละ 30 มีค่าลดลงร้อยละ 16 และ 14 ตามลำดับ เมื่อเทียบกับสูตรควบคุม ทั้งยังพบว่าอัตราการไหลของมอร์ตาร์สดในสูตรดังกล่าวมีค่าลดลงถึงร้อยละ 38 เมื่อเทียบกับสูตรควบคุม นอกจากนี้พบว่าในสูตรแทนที่เถ้าแกลบร้อยละ 20 ให้ค่ากำลังอัด 53 เมกะพาสคัล บ่มที่ 56 วัน ในขณะเดียวกันสมรรถนะความคงทนของมอร์ตาร์ ได้แก่ การดูดซึมน้ำ รูพรุนปรากฏ และความคงทนต่อกรดและโซเดียมซัลเฟตพัฒนาดีขึ้น เมื่อผสมเถ้าแกลบถึงร้อยละ 30 ที่บ่ม 56 วัน ได้ยับยั้งให้ค่าสูญเสียน้ำหนักและกำลังอัด เนื่องจากการกัดกร่อนของสารละลายกรดซัลฟิวริกที่ร้อยละ 0.47 และ 1.58

ตามลำดับ เช่นเดียวกับยับยั้งค่าน้ำหนักที่เพิ่มขึ้นน้อยสุดและกำลังอัดที่ลดลงหลังจากแช่สารละลาย
โซเดียมซัลเฟตเพียงร้อยละ 0.03 และ 0.32 ตามลำดับ ภาพถ่ายโครงสร้างทางจุลภาคและผลกราฟ
การเลี้ยวเบนรังสีเอ็กซ์ของตัวอย่างมอร์ตาร์ พบรูปทรงก้อนเกาะกันและเส้นใยของสารประกอบ
แคลเซียมซิลิเกตไฮเดรตตกตะกอนหนาแน่นในเนื้อและรูโพรงของมอร์ตาร์สูตรผสมเถ้าแกลบเมื่อ
เทียบกับสูตรควบคุม สูตรที่ผสมสองชนิดกับแคลเซียมเบนโทไนต์และสามชนิด จึงส่งผลให้ตัวอย่าง
มอร์ตาร์สูตรที่เติมเถ้าแกลบมีการพัฒนากำลังอัดและความคงทนได้ดีกว่าสูตรอื่นทั้งผสมสองและ
สามชนิด เช่นเดียวกับตัวอย่างคอนกรีตที่ผสมเถ้าแกลบร้อยละ 30 บ่ม 56 วัน มีค่าการซึมผ่านได้
ของประจุคลอไรด์ต่ำสุดที่ 336 คูลอมบ์ และค่าสัมประสิทธิ์การดูดซึมน้ำ 0.06 กิโลกรัมต่อตาราง
มิลลิเมตรต่อรากที่สองของชั่วโมง นอกจากนี้พบว่าค่ากำลังดึงทางอ้อมแบบบราซิลได้พัฒนาเพิ่มขึ้น
เมื่อตัวอย่างคอนกรีตมีอายุบ่มมากขึ้น และสูตรแทนที่ด้วยเถ้าแกลบร้อยละ 10 ให้ค่ากำลังดึงสูงสุดที่
3.80 เมกะพาสคัล บ่ม 56 วัน ดังนั้นเมื่อพิจารณาจากผลการศึกษาดังกล่าวและคำนึงถึงการนำเอา
ของเสียมาใช้ประโยชน์สูงสุด นั้นก็คือสมรรถนะของมอร์ตาร์และคอนกรีตใส่มวลรวมตะกรันปาล์มน้ำมัน
สามารถปรับปรุงดีขึ้นในสูตรที่ผสมสองชนิดกับแคลเซียมเบนโทไนต์ที่ร้อยละ 10 และเถ้าแกลบที่
ร้อยละ 30 และสูตรผสมทั้งสามที่แคลเซียมเบนโทไนต์ร้อยละ 5-10 และเถ้าแกลบร้อยละ 10-20

คำสำคัญ: ตะกรันปาล์มน้ำมัน, แคลเซียมเบนโทไนต์, เถ้าแกลบ, กำลังอัด, ความคงทนต่อกรด
และซัลเฟต, การซึมผ่านได้ของประจุคลอไรด์

Thesis Title   Physico-mechanical, Chemical and Durability Characteristics of Mortar and Concrete Containing Palm Oil Boiler Clinker Aggregate Blended with Rice Husk Ash and Ca-Bentonite

Author   Miss Kamolchanok Kueaket

Major Program   Mining and Materials Engineering

Academic Year   2020

ABSTRACT

This research focused on utilization of palm oil boiler clinker (POBC) as a whole natural aggregate substitution blended with calcium bentonite (CB) and rice husk ash (RHA) for green mortar and concrete productions. The CB and RHA were partially replaced by weight of ordinary Portland cement (OPC), type 1 in three proportions of 10%, 20%, and 30% for binary and ternary blends. All mixtures were taken constant water to binder ratio of 0.48. The behavior of fresh pastes on Vicat setting times and hydration temperature were investigated. The microstructure and mineral phase compositions of mortars were characterized via scanning electron microscope (SEM) and X-ray diffraction technique (XRD). All mortar specimens were cured in lime-saturated water at ambient temperature of 29 ± 3 ℃, RH = 80-90% for periods of 7, 28, and 56 days before each testing. The harden specimens were casted for examination in these following properties: water absorption, apparent porosity, compressive strength, sulfuric acid and sodium sulfate resistance. The cylindrical concrete specimens were prepared for rapid chloride ion permeability test (RCPT), capillary water absorption, and indirect tensile strength test (Brazilian test).

As a result, it was observed that the POBC aggregate can be potentially substituted natural aggregate for mortar and concrete productions. The setting times, hydration temperature of pastes, and percentage flow of fresh mortars were reduced with an increase in binary and ternary blends. The maximum reduction in setting time and hydration temperature was 16% and 14% for the mix incorporating up to 30% RHA. Consequently, an increase in RHA up to 30% decreased the percentage flow by 38%. Moreover, the compressive strength decreased as an increase in ternary blends with prolonged curing ages,

the 56-day highest compressive strength was 53 MPa for the mix incorporating 20% RHA. The durability performances of mortar including water absorption and porosity, sulfuric acid and sodium sulfate resistance improved with an increase in RHA replacement level up to 30% and up to 56-day curing ages. The lowest deteriorating due to sulfuric acid attack was suppressed 0.47% loss in weight and 1.58% loss in compressive strength for the mix incorporating 30% RHA cured for 56 days, as well as the lowest percentage gain in weight and loss in compressive strength due to sodium sulfate attack was 0.03% and 0.32%. The SEM microstructure and XRD patterns of dominant mortars specimens indicated that flocs-like and fibrous- like forms of the C-S-H densely formed in the matrix and filled up the pores of the mortar containing RHA compared to that of control mix, binary and ternary mixes incorporating CB. This findings contributed to the strength and durability improvement. Likewise, an increase in RHA replacement level and curing ages reduced the chloride ion penetrability and capillary absorption coefficient of the concretes containing POBC as a coarse aggregate, while an increase in CB increased those one. The lowest chloride ion penetrability and capillary absorption coefficient was 336 coulombs and 0.06 $kg/mm^2/h^{0.5}$ for the mix incorporating up to 30% RHA at the age of 56 days. The indirect tensile strength of concrete increased with curing ages. The highest indirect tensile strength was 3.80 MPa for the mix incorporating 10% RHA. Therefore, considering in view of practical implication according to the experimental results and waste exploitation, the performances of green mortar and concrete produced with POBC as an aggregate replacement can be improved by the optimum incorporation of binary mixtures of up to 10% CB, 30% RHA, and ternary mixtures of up to 5-10% CB with 10-20% RHA.

Keywords: Palm oil boiler clinker, Calcium bentonite, Rice husk ash, Compressive strength, Acid and sulfate durability, Chloride ion penetrability

Acknowledgements

CONTENTS

CONTENTS (Continue)

LIST OF TABLES

LIST OF TABLES (Continue)

LIST OF FIGURES

LIST OF FIGURES (Continue)

LIST OF ABBREVIATIONS

ACI	American Concrete Institute
ASTM	American Society for Testing and Materials
BS	British Standards
CB	Calcium Bentonite
CH	Calcium hydroxide
C-S-H	Calcium Silicate Hydrate
Ett	Ettringite
ITZ	Interfacial Transition Zone
LOI	Loss on Ignition
LPSA	Laser particle size analyzer
OPC	Ordinary Portland cement
POBC	Palm Oil Boiler Clinker
POBCCA	Palm Oil Boiler Clinker coarse aggregate
POBCFA	Palm Oil Boiler Clinker fine aggregate
RCPT	Rapid Chloride Permeability Test
RHA	Rice Husk Ash
RPM	Round per minute
SAI	Strength Activity Index
SCMs	Supplementary Cementitious Materials
SEM	Scanning Electron Microscope
XRD	X-Ray Diffraction
XRF	X-Ray Fluorescence

LIST OF PUBLICATIONS

1. Kueaket, K., & Tonnayopas, D. (2018). Enhanced properties of palm oil boiler clinker concrete with Sang Yod rice husk ash. *Proceeding of 7th International Conference on Applied Sciences and Engineering (ICASEA, 2018)*, Kota Kinabalu, Sabah, Malaysia, 29-38.

2. Kueaket, K., & Tonnayopas, D. (2019). Palm oil boiler clinker properties used as a green aggregate for construction. *Proceeding of the 13th International Conference on Mining, Materials, and Petroleum Engineering (CMMP 2019)*, Krabi, Thailand, 86-91.

3. Kueaket, K., & Tonnayopas, D. (2021). Compressive strength and durability performance of mortar containing palm oil boiler clinker aggregate, rice husk ash, and calcium bentonite. *Journal of Applied Engineering Science*, 19(1), 193-203. doi: 10.5937/jaes0-27580

4. Kueaket, K., & Tonnayopas, D. (2021). Sustainable mortar and concrete made from palm oil boiler clinker aggregate comprising rice husk ash and calcium bentonite: Compressive strength and durability assessment. *Journal of Applied Science*, 20(1), 39-55. doi: 10.14416/j.appsci.2021.01.004

REPRINTS WERE MADE WITH PERMISSION FROM THE PUBLISHERS

Name	: Ms. Kamolchanok Kueaket
Institution	: Prince of Songkla University
Address	: Faculty of Engineering, Department of Mining ans Materials Engineering, Prince of Songkla University
	15 Karnjanavanich Rd., Hat Yai, Songkhla 90110
	Songkla 90110 Thailand
Paper ID	: 7th ICASEA: 043-025
Author	: Kamolchanok Kueaket
Co-Author	: danupon.t@psu.ac.th
Paper Title	: ENHANCED PROPERTIES OF PALM OIL BOILER CLINKER CONCRETE WITH SANG YOD RICE HUSK ASH
Date	: November 10th, 2018

NOTIFICATION OF PAPER ACCEPTANCE

Dear Ms. Kamolchanok Kueaket,

On behalf of the 7th ICASEA Committee, we are pleased to inform you that your submitted full paper (7th ICASEA: 043-025) entitled "ENHANCED PROPERTIES OF PALM OIL BOILER CLINKER CONCRETE WITH SANG YOD RICE HUSK ASH", has been **ACCEPTED** for the conference. Congratulation!

You may wish to update you Presenter Name. Simply Login > My Submission > Paper Submission > Click on "EDIT".

Please be informed that Conference Fee shall be paid by now. (Login > My Payment). Upload your proof of payment in the system after the payment is made.

As a reminder, the 7th International Conference on Applied Sciences and Engineering Application will be held on 8 & 9 December 2018 at TH Hotel, Kota Kinabalu, Sabah, Malaysia (Tabung Haji Hotel, Kota Kinabalu, Sabah). We look forward to seeing you at the conference.

Please be reminded that the **Conference Fee shall be paid 2 weeks before the conference.**

Again, thank you very much for your submission.

Secretariat 7th ICASEA
Tel: +6010 342 3095 (Nadia)
Fax:
Email: icasea7@gmail.com
Website: https://submit.confbay.com/conf/icasea7

REPRINTS WERE MADE WITH PERMISSION FROM THE PUBLISHERS

CMMP2019 Acceptance Letter

C **CMMP2019 <cmmp2019@easychair.org>**
16/4/2562 15:15

To: Kamolchanok Kueaket

Dear Kamolchanok Kueaket,

Thank you so much for your submission to the CMMP2019.
We are pleased to inform you that your manuscript in the title of "PALM OIL BOILER CLINKER PROPERTIES USED AS A GREEN AGGREGATE FOR CONSTRUCTION" has been accepted for oral presentation.

The schedule of presentations will be informed later. We are looking forward to see you in 13-14 June 2019, Aonang Villa Resort, Krabi, Thailand.

However, the grammar and template of CMMP2019 should be checked again, and if reviewers have some recommended to your manuscript (details below of this email, or login to your EasyChair account), please correct it, and update before 25 April 2019.

Finally, the conference fee for early registration has been extended until 25 April 2019, please check the information for bank transfer and can make registration online at our website: http://cmmp2019.eng.psu.ac.th/

Best regards,
CMMP2019 program chair

REPRINTS WERE MADE WITH PERMISSION FROM THE PUBLISHERS

[JAES][ID 27580] Editor Decision

SA **SCIndeks Asistent** <ceoncees@gmail.com>
26/10/2563 1:05

→

To: KAMOLCHANOK KUEAKET (กมลชนก เกื้อเกต); Danupon Tonnayopas

Dear Kamolchanok Kueaket, Danupon Tonnayopas,

It is my pleasure to inform you that your paper entitled COMPRESSIVE STRENGTH AND DURABILITY PERFORMANCE OF MORTAR CONTAINING PALM OIL BOILER CLINKER AGGREGATE, RICE HUSK ASH, AND CALCIUM BENTONITE is accepted for publication in the Journal of Applied Engineering Science.

With kindly regards,

Prof. Dr Gradimir Danon
Editor in Chief
gdanon@iipp.rs

Journal of Applied Engineering Science - JAES www.engineeringscience.rs

Ovaj mejl je poslat sa sistemskog naloga. Ako želite da odgovorite na njega, molimo Vas da koristite sledeću adresu e-pošte:
This e-mail is sent from system account. To reply, please use the following e-mail address:
"Prof. Dr Gradimir Danon"
gdanon@iipp.rs

REPRINTS WERE MADE WITH PERMISSION FROM THE PUBLISHERS

[JASCI] Editor Decision

AO   **Asst.Prof.Dr.Nonchanutt Chudpooti via Thai Journals Online (ThaiJO) <admin@tci-thaijo.org>**
22/3/2564 18:47

To: Kamolchanok Kueaket; Assoc. Prof. Dr. Danupon Tonnayopas

Save all attachments

COPYRIGHT ASSIGNMENT... 239.96 KB	COPYRIGHT ASSIGNMENT... 206.44 KB	C-Reviewer-Sustainable.pdf 108.52 KB

Dear Kamolchanok Kueaket, Assoc. Prof. Dr. Danupon Tonnayopas,

We have reached a decision regarding your submission to The Journal of Applied Science, "Sustainable mortar and concrete made from palm oil boiler clinker aggregate comprising rice husk ash and calcium bentonite: Compressive strength and durability assessment".

Our decision: Submission accepted

Please fill the copyright form in the attachment and submit the form to ThaiJo system at your earliest convenience.

Best Regards,
Asst.Prof.Dr.Nonchanutt Chudpooti
nonchanutt.c@sci.kmutnb.ac.th

Editorial Board
The Journal of Applied Science
Faculty of Applied Science, King Mongkut's University of Technology North Bangkok

Introduction

Construction materials such as coarse aggregate, sand, and cement are the most important resources for public utility: road, dam, railway, airport, condominium, and other infrastructures that were built for facility and convenience. In Thailand, construction aggregate reserve was estimated at approximately 8,010 million tons from 318 quarries (Innovation in Raw Materials and Primary Industries Division, 2020). Specifically, limestone and shale reserves, which are the fundamental ingredients for cement production, was estimated at 2,245 million tons (Department of Mineral Resources, 2007). It can be seen that the reserve of nonrenewable construction materials was against the demand of aggregate for expanded construction sectors. According to Thailand rural roads standard.231-2562 (2019), 1 m^3 of lean concrete (1:3:5) contained 240 kg cement, 728 kg sand, and 1,218 kg coarse aggregate. Assumed that, the concrete demand is 50,000,000 m^3 each year. Then, 61 million tons of coarse aggregate are consumed, annually. It could be predicted that the aggregate reserved will be completely depleted in AD 2151 (131 years afterwards).

Many researches introduced the sustainable constructions by substitute natural construction materials with industrial and agricultural wastes, recycle aggregates, construction materials with industrial and agricultural wastes i.e. oil palm shell (Ong et al., 2018), palm oil clinker (Huda et al., 2018), recycle aggregates from concrete and construction waste demolitions (Siddique et al., 2020), coal bottom ash, copper, and steel slag (Martínez-Lage et al., 2020) to alleviate the nonrenewable construction materials consumption. Green mortar has been produced by using local wastes for mitigate the environmental problems, land fill used, and disposal expenses (Yague et al., 2021).The green mortar, which contained 100% fly ash as a cement replacement (M-type or geopolymer mortar), also helped reducing carbon dioxide emission by 41% (Alqahtani et al., 2021).

In the southern part of Thailand, palm tree are the important economic plants that covered 7,812.82 square kilometers. Moreover, it was produced by 14,784,987 tons in 2020 (Office of Agricultural Economics, 2020) and fed to 70 local oil palm plants (Department

of industrial works, 2020). Additionally, in Thailand, rice has been planted for $97,600$ square kilometers, provided rice product for approximately 25,500,000 tons (Thai rice exporters association, 2020), and fed to 38,619 local rice mills (Office of agricultural economics, 2014). Thus, it is apparent that the large amount of agricultural and industrial wastes were generated unavoidably.

However, there is no official reports on quantity of wastes that were produced by rice mills and oil palm plants in Thailand. According to Suan et al. (2017) the palm oil wastes in Thailand (palm oil fuel ash (POFA) and palm oil boiler clinker (POBC)) were mentioned that they had a negative impact on environment and caused the disposal area problems. Those wastes are obtained from the burning of shell, bunch, kernel, and fiber of palm fruit.

Rice husk that obtained from rice mills almost utilized as a biomass fuel. Then, the rice husk ash (RHA) was provided after completed burning of rice husk. Chindaprasirt et al. (2008), Tonnayopas & Jitnukul (2013), and Raheem & Kareem (2017) revealed that RHA can be used as partial cement replacement and addressed as pozzolanic materials or supplementary cementitious materials (SCMs) due to the high percentage of amorphous silica component.

Calcium bentonite (CB) is clay mineral, which contained mostly SiO_2 and Al_2O_3 (Velde, 1992). Few researches were conducted by using CB as a cement replacement to reduce the cost of construction (Mirza et al., 2009). Additionally, CB has an interesting properties: high plasticity and lubricity, low permeability and low compressibility (Memon et al., 2012). However, CB was reported that it provided low strength activity index when compared to reference cement mix (Achyutha Kumar Reddy & Ranga Rao, 2019; Al-Hammood et al., 2021; Mesboua et al., 2018).

Thus, in this study was employed the local waste by-products, i.e. POBC as 100% natural aggregate replacement, RHA and CB as partial substitution of ordinary Portland cement (OPC). Likewise, this research aims to impel and develop the green mortar and concrete for nonstructural application and promote waste utilization in local community: local oil palm plants and rice mills, as well as depleting the natural construction material consumption. The comprising between POBC aggregate, RHA, and CB will be studied in compressive

strength, durability properties, and microstructure to characterize the optimum proportion to produce the efficient performance green mortar and concrete for sustainable construction.

Objectives

  1. To investigate physical and chemical properties of palm oil boiler clinker (POBC) as coarse and fine aggregate, rice husk ash (RHA), and calcium bentonite (CB).

  2. To investigate on physico-mechanical of green mortar containing POBC with RHA and CB as secondary cementitious materials (SCMs).

  3. To evaluate on durability properties of green mortar and concrete.

Scope of study

  1. The properties of POBC coarse and fine aggregates were carried out including water absorption, specific gravity, unit weight, aggregate crushing value, Los Angles abrasion, and organic impurity.

  2. The chemical composition and mineral phase compositions of POBC, RHA, and CB were confirmed by X-ray fluorescence spectrometry (XRF) and X-ray diffraction technique (XRD). In addition, the morphologies of POBC, RHA, and CB were observed under scanning electron microscope (SEM).

  3. This study employed POBC as a fine aggregates, RHA and CB as SCMs in partial replacement by weight of OPC, type I at proportion of 10%, 20%, and 30%. All of binary and ternary mixtures will be blended with constant water to binder ratio (w/b) of 0.48 and cured in saturated-lime water at ambient temperature (29 ± 3 ºC, RH=80-90%) for 7, 28, and 56 days.

  4. Fresh properties of pastes and mortars: The fresh pastes of different binary and ternary mix designations were examined heat of hydration and setting time. Additionally, percentage flow and fresh density of fresh mortars were carried out.

  5. Hardened properties of mortars: physical properties (water absorption and apparent porosity), compressive strength, strength activity index (SAI).

6. Durability properties of mortars and concretes blended with RHA and CB were determined sulfuric acid resistance, sodium sulfate resistance, and rapid chloride permeability test.

7. The microstructures and mineral phases of green mortars were investigated via scanning electron microscope (SEM) and X-ray diffraction technique (XRD).

Benefits

1. Obtaining the guideline in sustainable environmental friendly solution for reducing wastes and promote a self-reliance in construction materials production by using local agricultural and industrial wastes for replacing the nonrenewable construction materials.

2. Further development and production of green mortar and concrete that have good performance in strength and durability.

Palm Oil Boiler Clinker (POBC)

The industrial wastes generated from the palm oil mill are divided into two types i.e. fresh waste and biomass fuel waste. The fresh wastes include oil palm shell, empty fruit, and mesocarp fiber which are obtained after the crude palm oil extraction process. Furthermore, these fresh wastes, especially, the oil palm shell and mesocarp fiber were also used as a biomass fuel to generate the electricity for boiler and the palm oil mill. Then, the palm oil fuel ash (POFA) and the palm oil boiler clinker (POBC) were produced in the aftermath of the biomass fuel combustion. The range of the combustion temperature inside the boiler found to be varied from 500 to 1,200 °C (Hamada et al., 2020; Karim et al., 2018; Kueaket & Tonnayopas, 2018). The POBC's properties and characteristics can be varied depending on the temperature condition of the combustion (Kanadasan et al., 2015; Shakir et al., 2019).

1. Characteristics of POBC

1.1 Chemical compositions

According to the number of literature reports, the chemical compositions of POBC mainly consisted of 55 to 60% SiO_2, 10 to 17% K_2O, 4 to 8% CaO, and 2 to 5% MgO as tabulated in Table 1. Besides, the dissimilar chemical compounds of POBC can be found owing to the difference in the boiler operating condition: pressure and temperature, geological setting, and soil characteristics of oil palm cultivating area (Kanadasan et al., 2015; Shakir et al., 2019).

Table 1 Comparison in chemical properties of POBC aggregates

Chemical composition (%)	Ahmmad et al. (2017)	Karim et al. (2017)	Nayaka et al. (2019)	Ismail et al. (2020)
SiO_2	60.00	62.78	60.29	55.39
K_2O	12.00	10.54	-	17.7
CaO	8.00	6.89	4.71	7.05
P_2O_5	5.00	-	-	3.97
MgO	5.00	3.52	-	2
Fe_2O_3	4.00	6.49	5.83	10.81
Al_2O_3	4.00	3.41	3.83	2.18
SO_3	-	0.08	0.2	0.19
Others	2.00	-	-	0.28
Loss on ignition	-	3.67	2.01	0.02

1.2 Physical properties of POBC aggregate

The POBC was widely studied as a substitution of cement, sand, and aggregates for mortar and concrete productions, thus the physical properties of crushed POBC coarse and fine aggregates, included specific gravity, density, fineness modulus, and 24-h water absorption, had been reviewed as shown in Table 2 and Table 3. The POBC have been found in dark grey to greenish gray in color with irregular shape (Kanadasan et

al., 2015; Kanadasan et al., 2018). The ranges of specific gravity of POBC coarse and fine aggregate were between 1.68 to 1.79 and 1.51 to 2.12, respectively. Accordingly, the density of POBC fine aggregate was in the range of 823 to 1,419 kg/m^3.

Table 2 Physical properties of POBC coarse aggregate

Specific gravity	Density (kg/m^3)	Fineness modulus	24-h Water absorption (%)	References
1.78	823	6.23	5.7	Hamada et al. (2019)
1.75	568	-	5.67	Muthusamy et al. (2019)
1.68	813	-	5.56	Kabir et al. (2017)
1.9	1,419	4.99	4.23	Chai et al. (2017)
1.73	-	-	3 ± 2	Abuhata et al. (2016)

Table 3 Physical properties of POBC fine aggregate

Specific gravity	Density (kg/m^3)	Fineness modulus	24-h Water absorption (%)	References
1.51	945	5.89	5.50	Nayaka et al. (2019)
1.7	-	3.16	19.9	Ong et al. (2018)
1.97-2.11	-	2.71	10±5	Kanadasan et al. (2015; 2018)
2.12	1,025	3.12	3.6	Ahmmad et al. (2017)

Utilization of POBC aggregate

1. Use as a coarse aggregate replacement

    Chai et al. (2017) stated that up to 50% of POBC could be used as coarse aggregate substitution for producing semi-lightweight high strength concrete. Utilization of POBC as a palm oil shell (POS) replacement could develop more UPV and compressive strength by 9% and 43% higher than that of the POS concrete due to the improvement of interlocking bonding between POBC particle and cement (Ahmmad et al., 2016). However, an increased in POBC as a coarse aggregate replacement up to 100% reduced the workability and 28-day compressive strength by 50% and 42% compared to that of control concrete (Abutaha et al., 2016). Hamada et al. (2019) recommended that the concrete containing 100% of POBC coarse aggregate had the higher water absorption than that of the control mix by 54% due to the irregular shape and porous of POBC particle, thus the mineral admixture need to be introduced for improving their durability properties. Moreover, Muthusamy et al. (2019) studied the suitable curing condition for POBC concrete and suggested that the POBC concrete need to be cured in water due to it need sufficient water for hydration process and pozzolanic reaction, while the air-cured specimen showed lower strength and durability properties compared to that of water-cured specimen. The comparisons in mix designation, compressive strength, and oven-dry density of concrete containing POBC as a coarse aggregate were tabulated in Table 4.

Table 4 Compressive strength and oven-dry density of concrete containing POBC as a coarse aggregate with different mix designations.

Size of POBC (mm)	w/b ratio	Maximum replacement (%)	28-day Compressive strength (MPa)	Oven-dry density (kg/m^3)	References
>4.75	0.34	50	68	2,202	Chai et al. (2017)
4.75-12.50	0.35	100	62	1,971	Ahmmad et al. (2016)
5-14	0.53	100	33	2,074	Abutaha et al. (2016)
>4.75	0.35	100	41	2,020	Hamada et al. (2019)
>4.75	0.45	100 with 50% of POBC fine aggregate as a sand replacement	60	1,850	Muthusamy et al. (2019)

2. Use as a fine aggregate replacement

The POBC was used to replace fine aggregate in 100% by weight and it provided the lower density mortar than that of the control mix by 11.3%. In addition, the porous content in POBC caused the strength reduction and weak interfacial transition zone (Kanadasan et al., 2018). Meanwhile, some research pointed out that the rougher texture of POBC could improve the bonding connectivity of the interfacial transition zone (Lucas et al., 2016). The porosities of POBC was in the range of lesser than 10 microns to greater than 200 microns, hence an increase in POBC fine aggregate increased more water absorption and sorptivity. Likewise, the sorptivity had a good correlation to the thermal conductivity and thermal diffusivity (Asadi et al., 2021). Darvish et al. (2020) studied the geopolymer mortar comprising POBC as a whole sand replacement with 10wt.% fly ash, and found that an

increase in molarity of NaOH concentration and fly ash contents increased the density of POBC geopolymer mortar. Kanadasan et al. (2015) compared a physical and mechanical properties of POBC mortar by using POBC from different states in Malaysia. They found that the strength properties was directly related to the characteristics of the POBC and the cost of construction could be reduced by 17% when replaced natural sand with the POBC fine aggregate. The comparisons in mix designation, compressive strength, and hardened density of concrete containing POBC as a fine aggregate were tabulated in Table 5.

Table 5 Compressive strength and hardened density of mortar containing POBC as a fine aggregate with different mix designations

Size of POBC (mm)	w/b ratio	Maximum replacement (%)	28-day Compressive strength (MPa)	Hardened density (kg/m^3)	References
0.2-4	0.30	100	65	2,015	Kanadasan et al. (2018)
<4.75	0.5	100	33	1,890	Asadi et al. (2021)
<4.75	-	100	20	1,710	Darvish et al. (2020)
<4.75	0.28	100	80-100	1,950-2,260	Kanadasan et al. (2015)

Calcium bentonite (CB)

CB is a natural pozzolan and absorbent. It is impurity clay, which mostly composed of montmorillonite. The chemical compositions of some investigated CB are shown in Table 6. It can be seen that the $SiO_2+Al_2O_3+Fe_2O_3$ contents of CB ranged between 75.34 to 86.36%. Specifically, the Al_2O_3 contents ranged from 15.00% to 20.19%, where the Al_2O_3 content of zeolite and metakaolin was 13.5% and 35.14% (Chen et al., 2018; Tafraoui et al., 2016). However, the composition of CB can be varied depending on geological setting, weathering process, quantity of Ca-montmorillonite and others minor minerals (Al-Hammood et al., 2021).

Table 6 Comparison in chemical properties of CB

Chemical composition (%)	Mirza et al. (2009)	Memon et al. (2011)	Ahmad et al. (2011)	Liu et al. (2020)
SiO_2	49.44	54.55	65.00	64.32
K_2O	0.69	3.92	0.27	1.74
CaO	7.45	7.28	2.66	7.13
P_2O_5	-	1.11	-	-
MgO	1.61	4.20	6.5	3.68
Na_2O	0.87	1.27	0.12	0.31
Fe_2O_3	6.20	8.60	3.00	3.80
Al_2O_3	19.7	20.19	15.00	18.24
SO_3	-	-	-	0.03
Loss on ignition (%)	13.74	5.46	6	-

The CB was determined by the major mineral phase composition of smectite clay group in them, which is calcium montmorillonite. The mineral structure of CB is similar to the sandwich, revealed by Man et al. (2019), as illustrated in Figure 1. It contained two tetrahedron layers and one octahedral layer. As a result, this structure causes the exchange ion capacity and water absorption ability of CB.
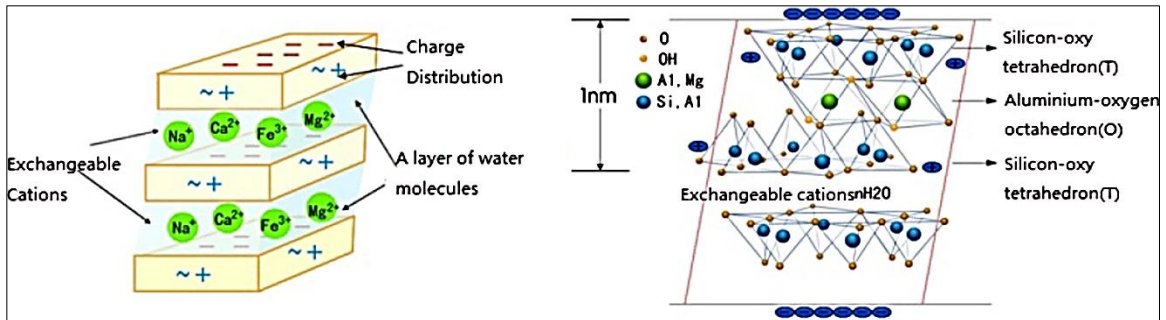
Figure 1 Schematic illustration of bentonite structure (Man et al., 2019).

Utilization of raw calcium bentonite as a supplementary cementitious materials (SCMs)

Cost-reduction and environmental-friendly are the main purpose of using CB as a cement replacement. Thus, utilization of CB had been studied. CB was introduced as a low-cost pozzolanic material according to the study of Mirza et al. (2009), and the recommended CB ratio as a cement substitution was up to 20wt.% to minimize the compressive strength reduction (the 28-day compressive strength was lower than that of control specimen by 18%). Then, Memon et al. (2012) replaced up to 21wt.% of cement by CB and found that an increase in amount of CB decreased density and water absorption of concrete, while showed no significant effect to compressive strength. Ahmad et al. (2011) stated that an increase in amount of CB decreased prolonged compressive strength, which was confirmed by utilization of CB as a substitution of cement by up to 50wt.%. However, mortar containing 30wt.% of CB maintained durability against 5% sodium sulfate attack as compared to mortar without adding CB. Moreover, raw CB could be replaced cement slag by 25wt.% with w/b of 0.445 (2,493 kg of cement) or cement:sand:water ratio of 1:0.9:5. This mixture developed the 28-day compressive strength by 15% with respect to that of control mix, while this mixture with w/b of 0.485 effectively reduced the weight loss due to 5-cycle of sulfuric acid attack (Lee et al., 2021). Additionally, using 5-15% of CB could improve durability properties of eco-friendly concrete due to: (i) decrease water absorption and permeability by pore filling effect, (ii) reduce compressive strength loss after exposed to acid and sulfate attack (Rehman et al., 2020).

Rice husk ash (RHA)

Thailand produced 25.5 million tons of rice in 2020 (*Thai Rice Exporters Association*, 2020). According to Sujivorakul et al. (2011), the rice husk has been estimated as 20wt.% of the total rice production. Then, after the rice husk was taken to use as a biomass fuel, the RHA was estimated as 4wt.% of the total rice production (At incinerated temperature of approximately 800-900 ºC). As a result, the RHA could be estimated as 1.02 million tons in 2020. The chemical composition of RHA contained approximately 80-95% of amorphous SiO_2 depended on the incinerating temperature and burning condition (Fapohunda et al., 2017).

Table 7 Effect of burning condition to SiO_2 content and features of RHA

References	SiO_2 (wt.%)	RHA features	Burning condition	
			temperature (ºC)	Duration (min)
Joshaghani & Moeini (2018)	87.10	Mostly amorphous RHA with density of 2.09 g/cm^2	700	60
Kannan & Ganesan (2016)	87.89	Mostly amorphous RHA with density of 0.51 g/cm^2 and specific surface area of 943 m^2/kg	650	60
Bheel et al. (2020)	86.94	-	600-700	300
Isberto et al. (2021)	93.47	Mostly amorphous RHA with pinkish-white color	400-600	360-480
Sharma & Kumar (2021)	91.90	Black RHA, partly amorphous, contained some crystalline silica	Approx. 600-1,200 (open-air burning)	-
Khan et al. (2020)	96.11	Amorphous RHA with specific gravity of 2.83 g/cm^3	700	1,440

Utilization of RHA as a supplementary cementitious materials (SCMs)

RHA consisted of high amorphous silica content, which could reacted with $Ca(OH)_2$ to form C-S-H phase as recognize as pozzolanic reaction and improve compressive strength and durability (Kumar et al., 2016; Suriyachoto & Tonnayopas, 2013). Tonnayopas & Jitnukul (2013) utilized local RHA (Sang Yod species) that was provided in the rice mill at Phatthalung province, Thailand. The RHA was gray in color with SiO_2 content of 66.13%, which was lower than those of other studies as shown in Table 7. This may be due to open-air burning condition and high residual unburned carbon. As a result, the maximum ratio of RHA replacement of cement was 10wt.% with w/b of 0.40, that could provide the compressive strength of 28-day concrete of 55 MPa. Accordingly, the maximum of 10wt.% of RHA was recommended to replaced cement for production coal bottom ash aggregate concrete with more durability and strength (Bheel et al., 2020). Moreover, the RHA that was burned in appropriate temperature of 700ºC for 60 minutes showed the high amorphousness and low unburned carbon. This RHA was replaced cement by weight in ranges of 10-30%, the mortar contained 20wt.% of RHA showed the highest compressive strength of 72 MPa, while an increase in RHA decreased the water absorption, chloride penetrability and weight loss due to acid attack. This was attributed to the pozzolanic activity of amorphous SiO_2 of RHA that reacted with portlandite $(CaOH_2)$ to produce secondary C-S-H by filled up the pore and lessened pore connectivity (Joshagani & Moeini, 2018). Alex et al. (2016) examined that RHA was derived by 5wt.% of rice husk, the RHA that was prepared for prolonged grinding time showed a lesser particle size with greater specific surface area, bulk density, and pozzolanic activity. Venkatanarayanan & Rangaraju (2014) investigated sulfate resistance properties of mortar containing low-carbon rice husk ash with w/b of 0.40, 0.48, and 0.57. An increase in RHA (up to 15%) with w/b ratio of 0.48 could lessen the 360-day expansion due to 5% sodium sulfate attack by 78% compared to that of control specimen. It could be explained by the pozzolanic activity of RHA improved impermeability matrix and prevented an entering of sulfate ion. Furthermore, the factors that effected the pozzolanicity of RHA were studied by many researchers, which can be concluded as follows (Fapohunda et al., 2017): (i) amorphousness of SiO_2, (ii) specific surface area, (iii) size of RHA particles (fineness), and (iv) carbon contents. Additionally, the factors that effected strength and durability properties of concrete or mortar containing RHA as SCMs can be concluded as follows (Sandhu & Siddique, 2017): (i) ratio of cement substitution, (ii) curing time, (iii) w/b ratio, and (iv) mix design.

Effect of CB and RHA as SCMs on microstructure of hydration products under SEM analysis

Rong et al. (2019) found that ultra-high performance cement-based composite containing the optimum 10-15% of RHA showed the improvement in mechanical properties. It can be seen in Figure 2, the microstructure of 7-day and 28-day's matrix of the mix containing 15% RHA composed of densely flocs-like C-S-H due to the pozzolanic reaction and some hydration products: portlandite ($CaOH_2$) and monosulfate (AFm). Yu et al. (1999) studied the pozzolanic reaction between SiO_2 from RHA and $CaOH_2$. It was confirmed that C-S-H gel was formed in foil-like morphology in 28-day cement paste containing 10% RHA, as depicted in Figure 3. This finding recommended that incorporation of RHA in concrete could lessen the portlandite and increase durability and strength of the specimen due to the formation of C-S-H by this reaction. The fibrous-like C-S-H was clearly observed in microstructure of 4-h autoclaved aerated concrete containing RHA and aluminum powder (mixture containing: 45% OPC, 5% CaO, 45% RHA, 5% sand, and 0.5% aluminum powder) (Kunchariyakun et al., 2015), as presented in Figure 4
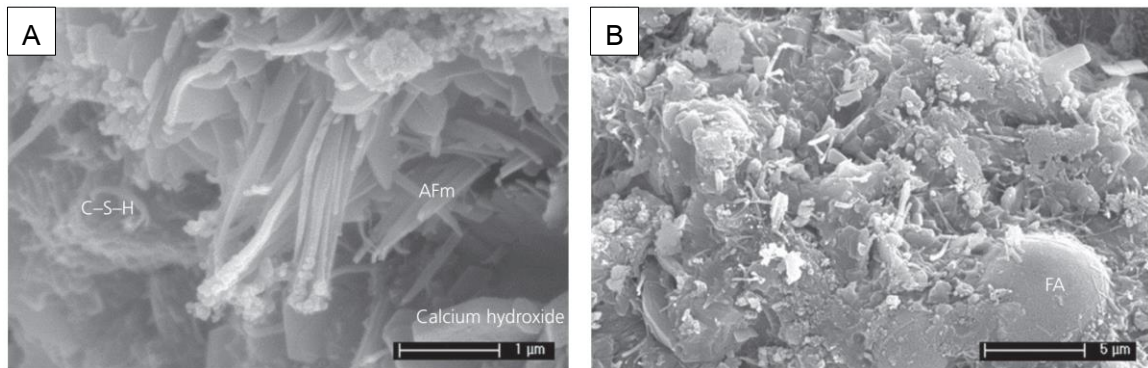
Figure 2 SEM images of ultra-high performance cement-based composite containing 15% RHA at the age of 7 days (A) and 28 days (B) (Rong et al., 2019)
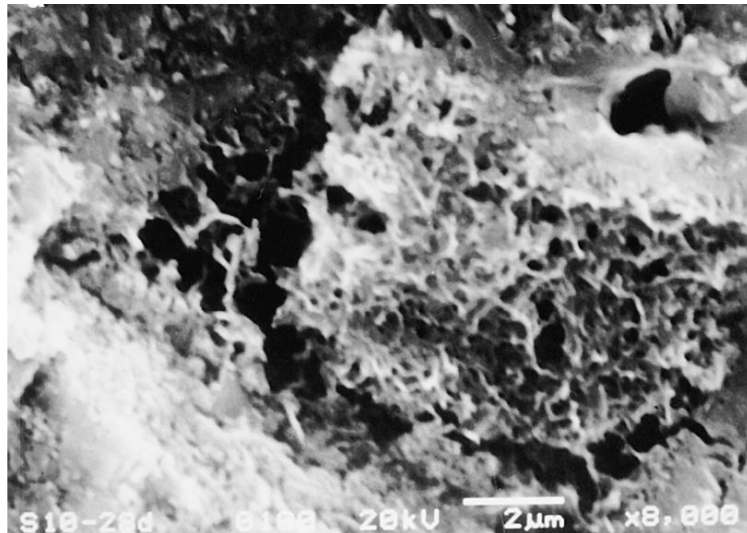
Figure 3 SEM image of floc-like C-S-H found in paste containing 10% RHA at the age of 28 days (Yu et al., 1999)

Figure 4 SEM image of autoclaved aerated concrete containing RHA and aluminum powder (Kunchariyakun et al., 2015)

The microstructure of 28-day cement mortar blended with CB is shown in Figure 5. It can be seen that few flocs-like C-S-H was observed, however, the CB particle played the important role in filled up the large pores in matrix and improve the durability of mortar by filler effect (Liu et al., 2020). Lee et al. (2021) investigated slag mortars containing 0.25% and 0.50% CB. It is apparent that an increase in CB contents enlarged the voids in matrix. However, the C-S-H and ettringite (Aft) was observed in both mixes, as shown in Figure 6. This could be attributed to the layer crystal structure of CB and the absorption capacity, which absorbed more water and hindering the pozzolanic activity.
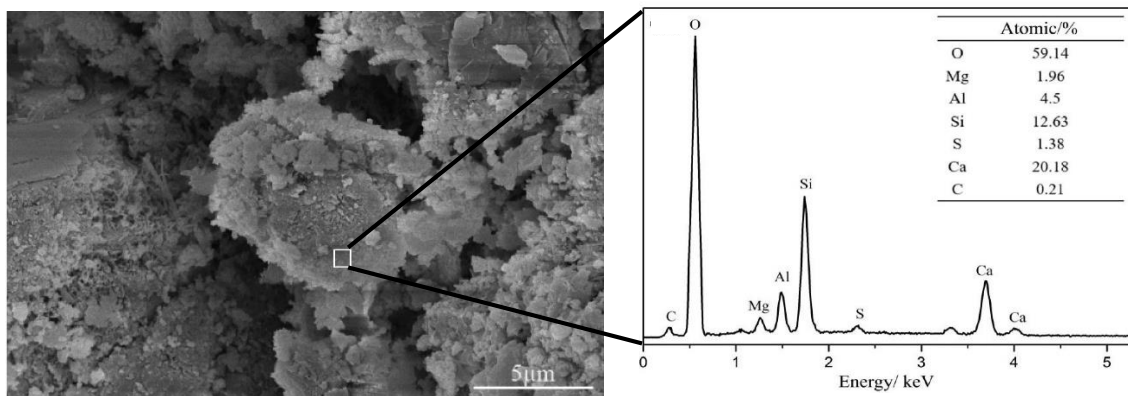
Figure 5 SEM image and EDS analysis of 28-day cement mortar blended with CB

(Liu et al., 2020)
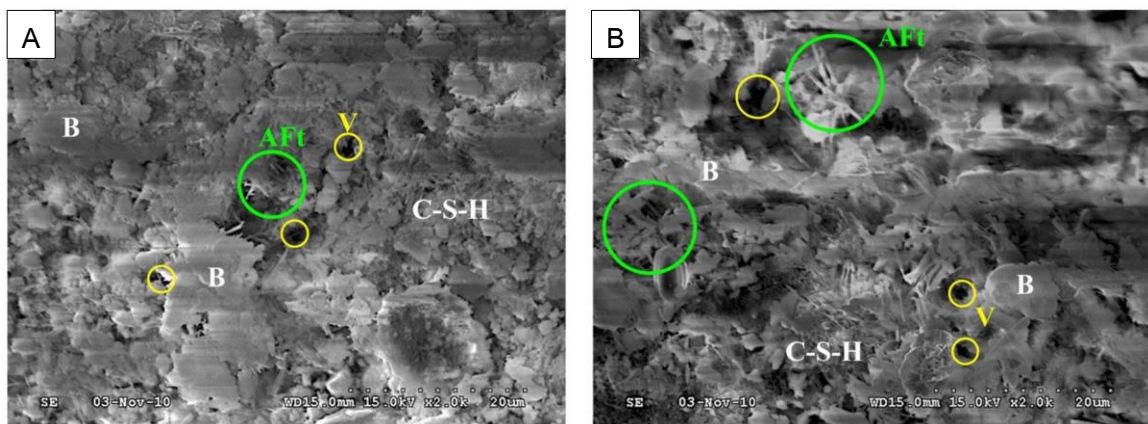
Figure 6 SEM image of slag mortars incorporating 0.25% CB (A) and 0.50% CB (B)

(Lee et al., 2021)

RESULTS AND DISCUSSIONS

Properties of POBC, RHA, and CB

1. The physical properties of POBC aggregate

   The large lumps of POBC as received from the palm oil mill are shown in Figure 7A. Each lump was approximately 10 to 25 cm in size. The POBC was light green to gray in color disseminated with some dark brown to black spots, irregular in shape, very angular, and scentless. The POBC coarse aggregate (POBCCA) and fine aggregate (POBCFA) obtained after crushing process are presented in Figure 7B-C.

Figure 7 Large lumps of POBC (A), POBCCA (B), and POBCFA (C)

   The grading requirement of fine and coarse aggregate was determined conforming to ASTM C33 (2018). The grading analysis and physical properties of POBC aggregate are presented in Figure 8 and Table 8. The mean particle size (d_{50}) of POBCCA and POBCFA was 10 mm and 0.55 mm, respectively. Moreover, the uniform grading analysis curve of POBC aggregate showed medium-graded and poorly-graded for the POBCCA and POBCFA, respectively. The fineness modulus of POBCFA also indicated that it was classified into the same size of coarse sand (0.5 to 1 mm) according to Wentworth scale of rock particle sizes. The Los Angeles abrasion and aggregate impact value of POBCCA represented that the POBC had low resistance to abrasion and crushing. Thus, the POBCCA was not recommended for using in road surfacing, railway ballast, and structural construction purpose. The POBC aggregate contained none of organic impurity, as can be seen in Figure 9.
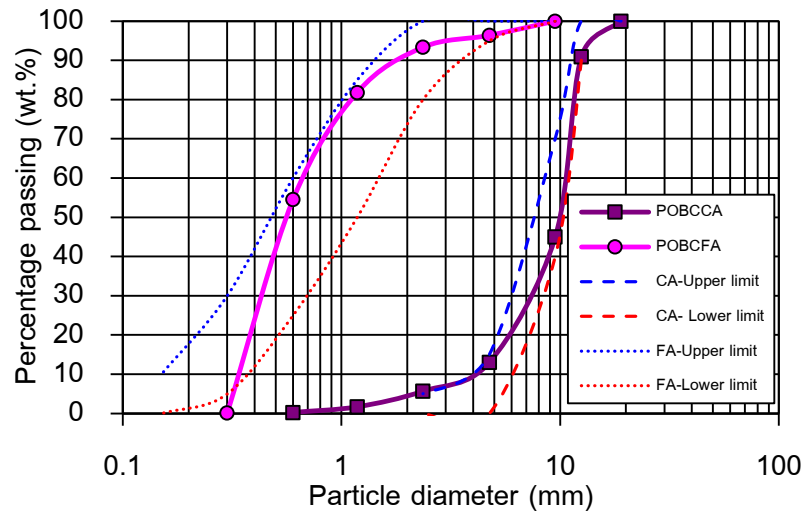
Figure 8 Grading analysis of POBC aggregates

Table 8 Physical properties of POBC aggregates

Properties	POBCCA	POBCFA
Water absorption (%)	1.48	3.15
Specific gravity	2.20	2.40
Unit weight (kg/m^3)	1,182	1,350
Los Angeles abrasion value (%)	37.98	-
Uniformity factor	0.24	-
Aggregate impact value (%)	37.30	-
Particle size distribution		
d_{10} (mm)	4.00	0.35
d_{50} (mm)	10.00	0.55
d_{90} (mm)	15.71	1.86
Fineness modulus	5.42	3.74
Organic impurity	None	

Figure 9 The organic impurity test of POBC aggregate as per ASTM C40

2. The grading analysis and physical properties of RHA and CB

The grading curves of RHA and CB were plotted and compared to that of the OPC, as shown in Figure 10. It is evident that the particle sizes of RHA and CB were finer than the OPC. The mean particle size (d_{50}) of RHA and CB was 12.5 and 2.3 µm, which was lower than that of the OPC by 10% and 84%, respectively. The percentage retained on 45 µm of RHA and CB was 5% and 0.3%, respectively. According to ASTM C618 (2019), the fineness requirement of percentage retained on 45 µm was not exceeded than 34% for the pozzolanic materials class N, C, and F. Thus, the RHA and CB particle sizes were met the fineness requirement. Moreover, the true density (ASTM C604) values of RHA and CB were 2.39 and 2.47, which were lower than that of OPC by 22% and 20%, respectively, as listed in Table 9. Similarly, the OPC also had the highest specific gravity value (3.1) compared to RHA (2.4) and CB (2.5). The true density values conformed to the specific gravity values, as it represented the voids between particles which was directly proportional to the specific gravity of the OPC, RHA, and CB.
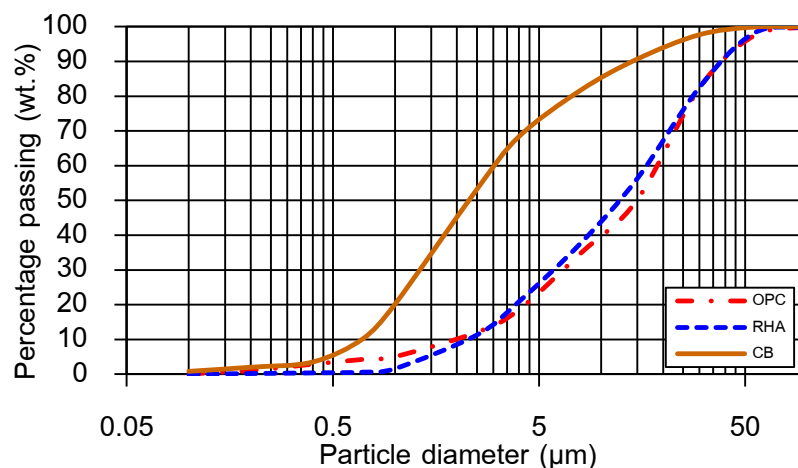
Figure 10 Grading analysis of OPC, RHA, and CB

Table 9 Physical properties of OPC, RHA, and CB

Properties	OPC	RHA	CB
Moisture content (%)	0.33	0.34	0.51
True density (g/cm^3)	3.08	2.39	2.47
Specific gravity	3.10	2.40	2.50
Particle size distribution			
$\quad d_{10}$ (mm)	1.9	2.3	0.6
$\quad d_{50}$ (mm)	13.9	12.5	2.3
$\quad d_{90}$ (mm)	32.7	38.6	14.2
Percentage retained on 45 μm	1.4	5	0.3

3. The chemical compositions of POBC, RHA, and CB

The chemical compositions of POBC, RHA, and CB were analyzed via X-ray fluorescence (XRF) spectrometer, and tabulated in Table 10. It can be seen that the main constituents of POBC, RHA, and CB were SiO_2. In addition, the inferior compositions of POBC were CaO and K_2O, while those of CB was Al_2O_3. Moreover, the composition of CB consisted of more CaO in the proportional of approximately 10% than NaO. Additionally, the XRD patterns of POBC, RHA, and CB were carried out via X-ray diffraction (XRD) spectrometer, and mineral phase compositions are illustrated in Figure 11. The mineral

composition of POBC consisted of quartz (2θ = 26.62° and 50.10°), tridymite (2θ = 20.51° and 23.23°), crystobalite (2θ = 21.95°), whitlockite (2θ = 27.99°, 31.26°, and 34.60°), and diopside (2θ = 29.85°, 35.63°, and 54.79°). The polymorphs of SiO_2 found in XRD pattern also indicated that the temperature in the boiler was in the range of 870°C to 1,470°C, while the POBC was formed after the combustion process of palm oil waste (Di Febo et al., 2020). In addition, the broad hump in the background intensity between 2theta 20° to 30° implied the amorphous phases. The XRD pattern of RHA is presented in Figure 12. It can be clearly seen that RHA composed mainly of amorphous silica (broad peak) and some crystalline silica i. e. , quartz and crystobalite. The mineral phase compositions of CB are demonstrated in Figure 13. CB consisted of quartz (2θ = 20.84° and 26.62°), montmorillonite (2θ = 5.72°, 19.82°, 34.08° and 61.94°), kaolinite (2θ = 12.36° and 24.87°), and gypsum (2θ = 11.63° and 23.39°).

Table 10 Chemical compositions of POBC, RHA, and CB by semi-quantitative XRF analysis

Oxides (wt.%)	POBC	RHA	CB
Al_2O_3	1.66	0.66	19.81
SiO_2	65.23	93.83	56.62
Fe_2O_3	1.78	0.36	0.02
CaO	10.00	0.76	1.16
Na_2O	0.13	0.07	0.18
SO_3	0.04	0.21	0.69
MgO	5.37	0.36	0.55
K_2O	9.56	1.77	0.96
P_2O_5	5.50	1.04	0.05
Loss on ignition	0.04	0.67	10.12
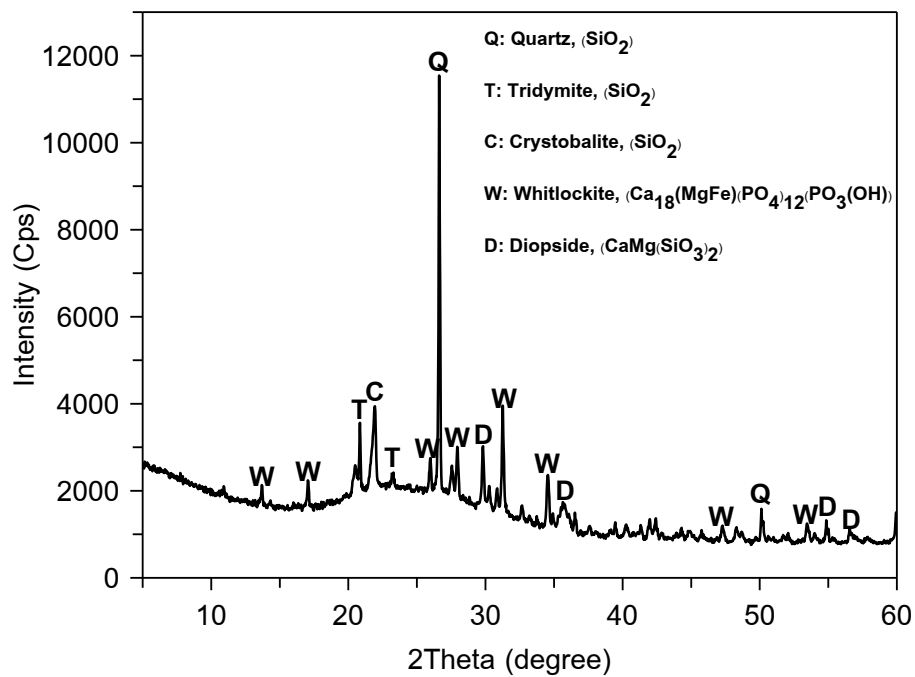
Figure 11 XRD pattern and mineral phase compositions of POBC
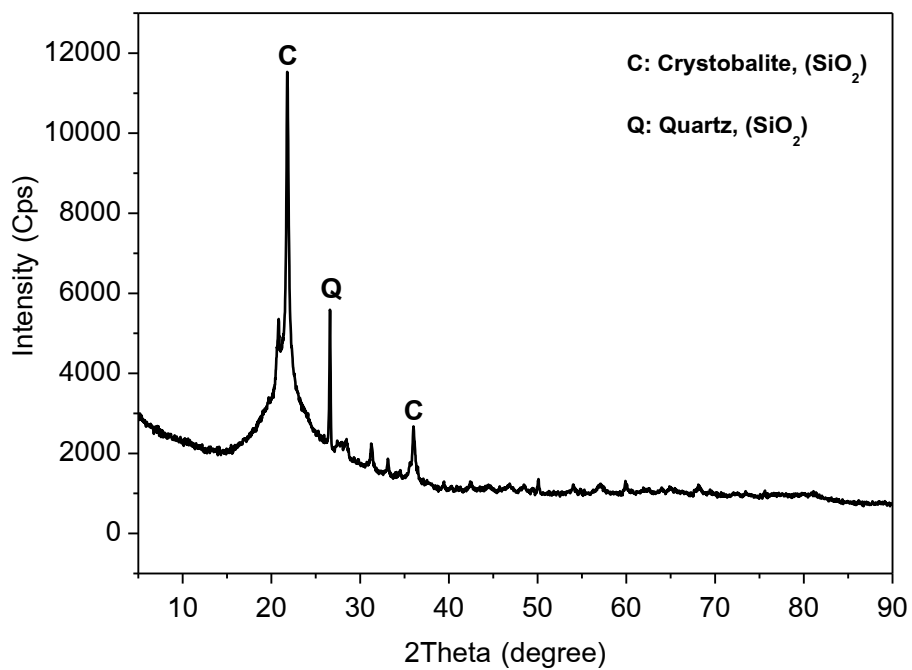
Figure 12 XRD pattern and mineral phase compositions of RHA
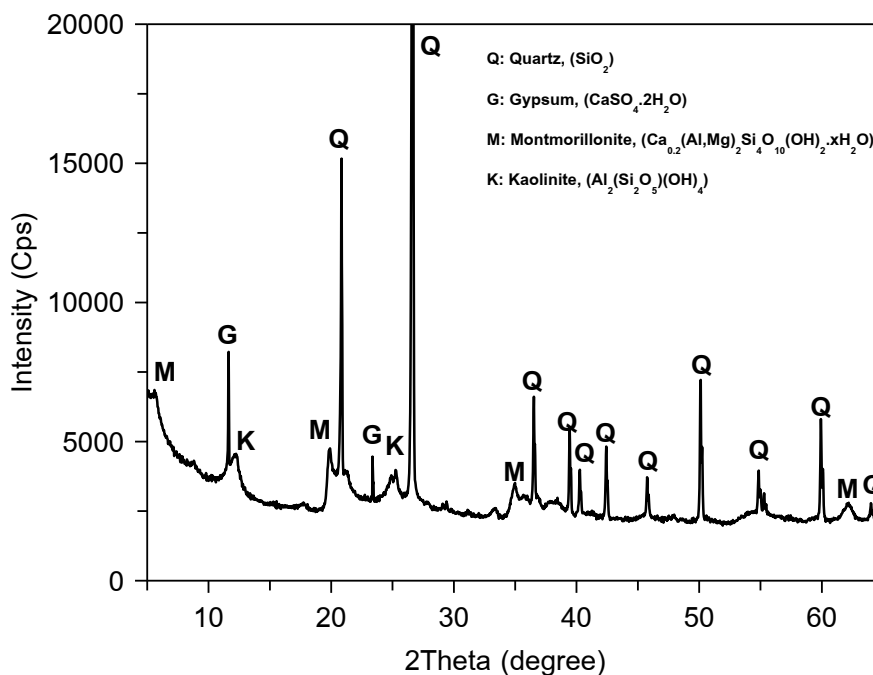
Figure 13 XRD pattern and mineral phase compositions of CB

SEM morphological analysis of POBC, RHA, and CB

The morphological analysis of POBC, RHA, and CB was obtained via scanning electron microscope (SEM), 20 kV. The SEM images of POBC, RHA, and CB are presented in Figure 14A-B. The POBC obtained after crushing to fine aggregate was very angular particle and low sphericity with irregular shape. An enlargement of POBC surface is depicted in Figure 14C. In addition, the POBC had a smooth surface consisted of a few micro porous and the agglomeration of silica component (a smooth rounded shape), as can be seen in Figure 14D.

The RHA (Sang Yod species) obtained after grinding process is shown in Figure 15A-B. The particle shape of RHA was sub-angular to sub-rounded and medium sphericity. It can be noticed that the RHA particle sizes were varied from coarse to very fine particle. An enlargement of RHA surface demonstrated the clustered feature of silica component, which was the principal composition of RHA, as depicted in Figure 15B.
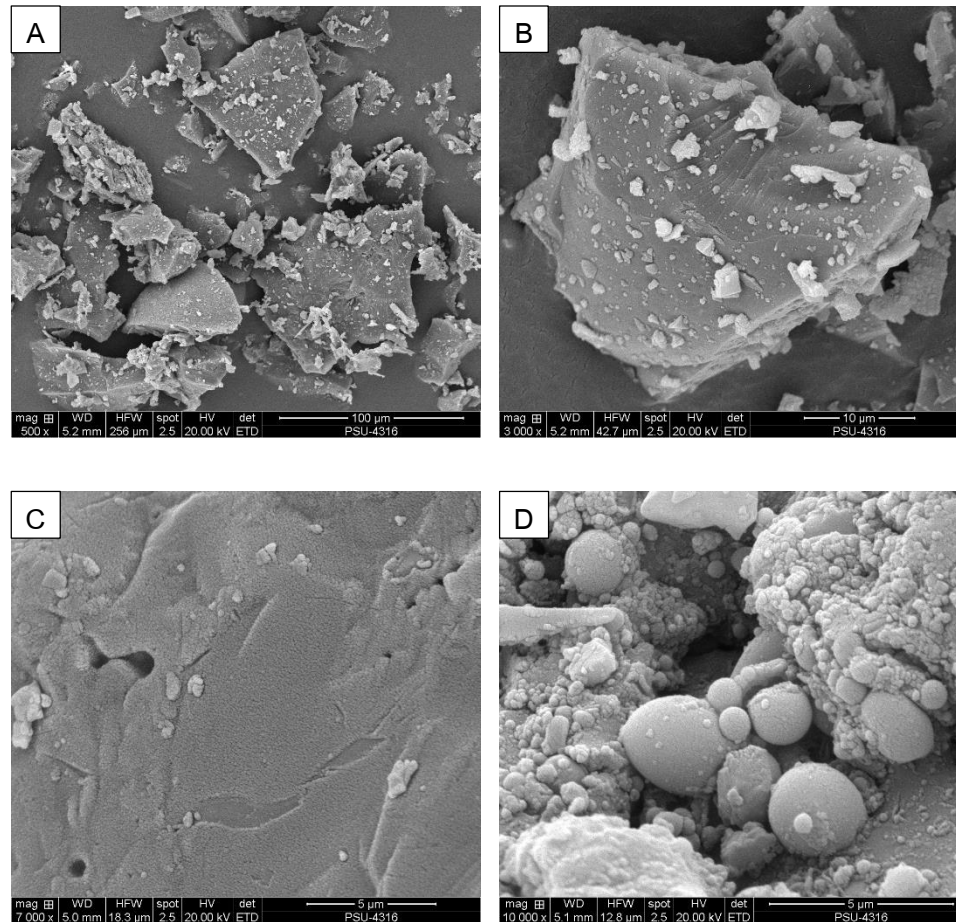
Figure 14 Morphology of POBC aggregate (A-B) and characteristics of POBC surface's texture (C-D)

The morphology of CB is illustrated in Figure 15C-D. The compactness of the sheet-like structure of a small CB particle represented to the clay mineral characteristics. The clump of sheet-like CB particle was rounded in shape and high sphericity. Besides, the sub-angular particle of OPC is shown in Figure 15E. It can be seen that the OPC contained poorly graded coarser particle sizes than those of RHA and CB. The combination of OPC, RHA, and CB particles showed well graded characteristic and dense particle packing with the different particle sizes and shapes, as demonstrated in Figure 15F.
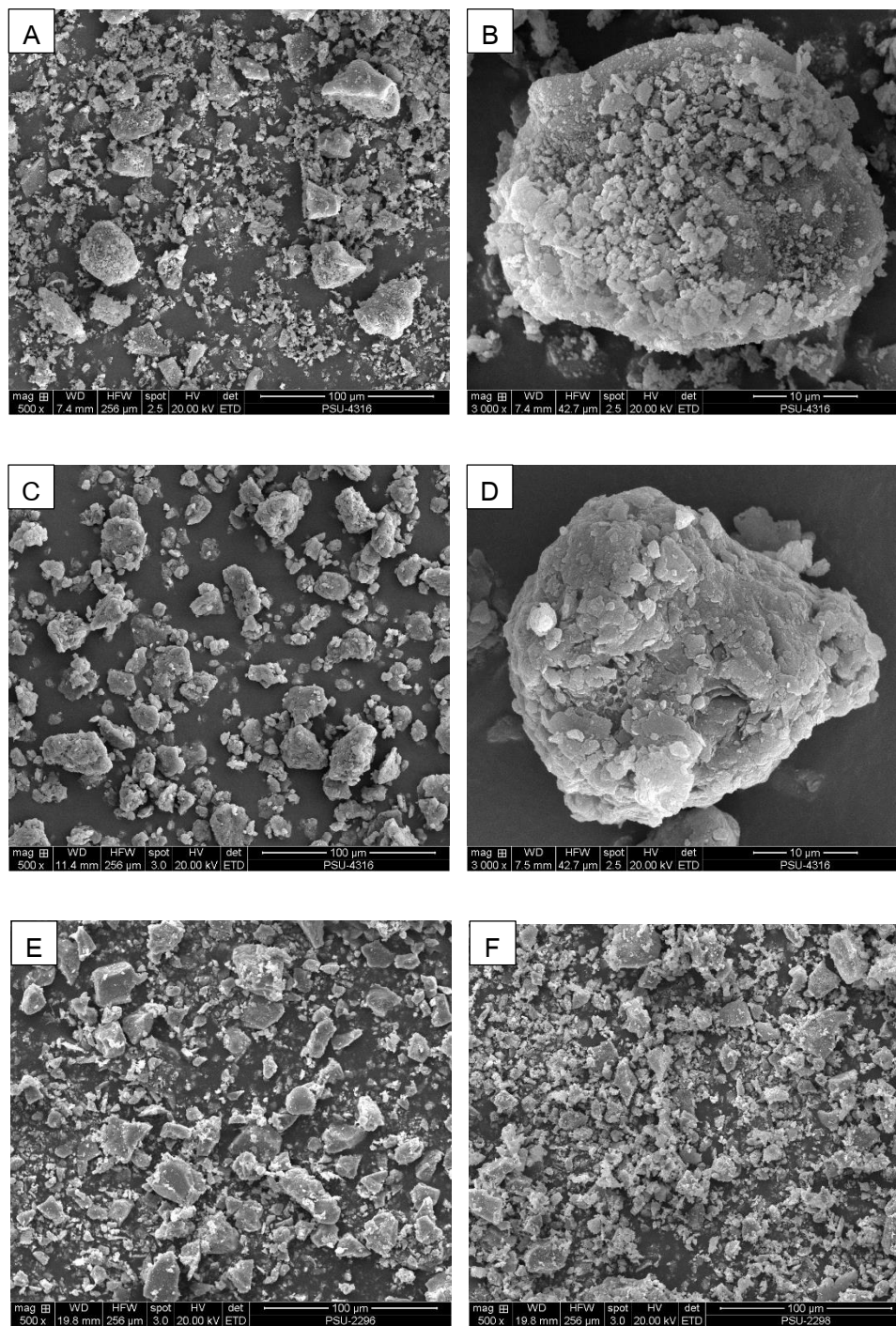
Figure 15 Morphology of RHA (A-B), CB (C-D), OPC (E), and ternary blends of OPC, RHA, and CB particles (F)

Properties of paste incorporating CB and RHA

Setting time by Vicat needle test

In this study, the test method for evaluate Vicat initial and final time of setting was adapted from ASTM C191 (2008). The Vicat initial setting time was carried out by measuring the elapsed time until the penetration depth of Vicat needle was 25 mm, while the Vicat final time of setting was determined as the Vicat needle failed to pierce the mold. The Vicat setting time of different mix designations are presented in Figure 16. It is evident that both of the Vicat initial and final setting time decreased with an increase in percentage of RHA replacement. For the ternary blends of RHA and CB, the same trend of Vicat initial and final setting time was found to be decreased with an increase in percentage of RHA replacement. Besides, the Vicat initial and final setting time of mixes containing 10% to 30% RHA ranged from 96 to 133 minutes and 240 to 285 minutes, which decreased up to 32% and 16% as up to 30% of RHA replacement, when compared to that of the control mix. These findings are in agreement with the previous studies on the effect of RHA as a cement replacement on setting time. According to Liu et al. (2020) and Venkatanarayanan & Rangaraju (2015), the RHA particle absorbed more free water, which in turn reduced the water to binder ratio of the fresh paste and setting time. Meanwhile, an increase in CB contents slightly increased either the Vicat initial and final setting time, which were in the range of 199 to 211 minutes and 300 to 320 minutes, respectively. At up to 30% CB replacement, the Vicat initial and final setting time were 50% and 12% greater than that of the control. The previous studies also found that the setting time increased with increasing the CB contents, this is due to the packing effect of CB which could hindered and delayed the hydration process (Sha et al., 2018; Zhou et al., 2020).
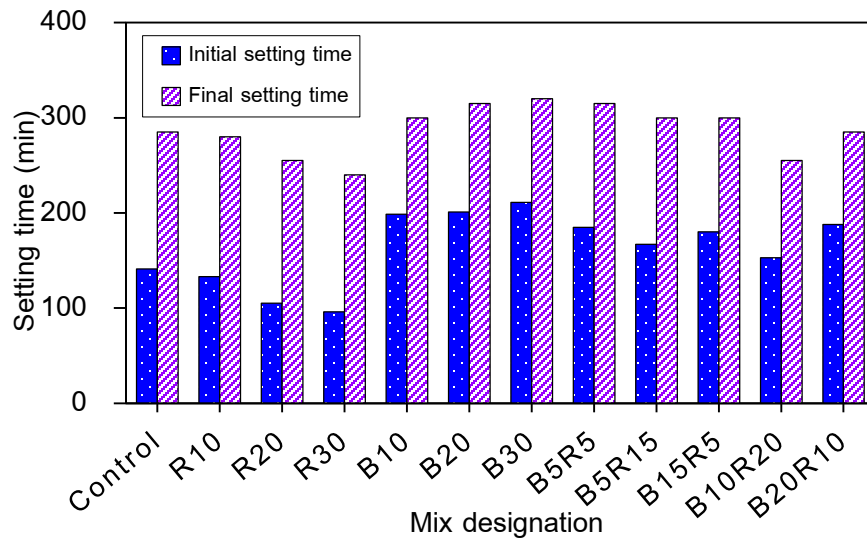
Figure 16 Vicat initial and final setting time of different binary and ternary mix designations

Temperature of hydration

The temperature of hydration was measured during the setting time had been carried out, by using Fluke Digital Multimeters (DMMs). For all mix designations, the temperature of hydration was measured every 15 minutes until the paste hardened and the results are demonstrated in Figure 17. Generally, the heat of hydration is chiefly generated from tricalcium aluminate and free lime in cement contents, hence a decrease in cement contents by using pozzolans as a cement substitution decreases the hydration temperature due to a decrement of tricalcium aluminate and free lime (Gómez & Rojas, 2013). The hydration temperature ranged from 28.4 to 31.2 °C for the mix designation containing RHA and CB, while that of control mix was 33.6 °C. Particularly, the maximum binary substitution of OPC by 30% of RHA, CB, or ternary blends of RHA and CB provided the lower hydration temperature than that of the control by 9 to 14%. Wei & Gencturk (2019) studied the hydration of blends containing bentonite and stated that the dilution effect by reducing the use of cement could decrease the heat of hydration due to lower cement take part in both of hydration reaction and tricalcium aluminate reaction.
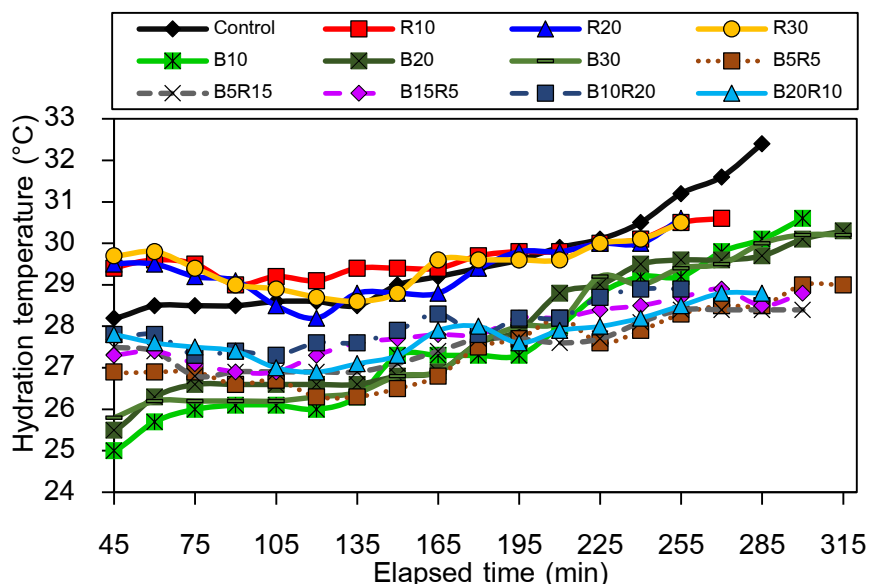
Figure 17 Temperature of hydration of different binary and ternary mix designations of pastes

Fresh properties of POBC mortar

1. Percentage of flow

        The flowability test of fresh POBC mortars was performed in accordance with (2015). The percentages flow of different binary and ternary mix designations are presented in Figure 18. Generally, an increase in RHA and CB contents decreased the flowability of POBC mortar. For the binary mix designation of R10, R20, and R30, the percentages of flow were lower than that of control mix by 19%, 31%, and 38%, respectively. Additionally, the percentage flow of the binary mix containing up to 30% CB was lesser than the control mix by 20%. Subsequently, an increase in percentages of cement substitution by the ternary blends of RHA and CB decreased the flowability. However, the mix incorporating up to 10% RHA, 20% CB, and ternary mix designation of B5R5, B5R15, and B15R5 showed the acceptable percentages of flow within the range of 98% to 119%. Laidani et al. (2020) also revealed that the flowability of concrete containing CB decreased with an increase in CB contents due to the fineness and specific surface area of CB particle were greater than that of cement, therefore, the more water was required. Subsequently, the percentage of flow

gradually decreased with an increase in RHA replacement ratios for the ternary blends of RHA and CB (Figure 18). This finding is in accordance with those of previous studies. Siddika et al. (2020) pointed out that RHA particle absorbed water on its surface and stored water in its pore, an increase in RHA contents and fineness of RHA particle decreased free water, which in turn increased the viscosity of the fresh mix and decreased the flowability. As well as, the filler effect of RHA played the important role in reducing the segregation and flowability of fresh mix (Fapohunda et al., 2017). In addition, Sua-Iam et al. (2019) and Abbas et al. (2017) suggested that more superplasticizer dosages are required to restore flowability and achieve the targeted flow of 110±5% for the mixture incorporating RHA.
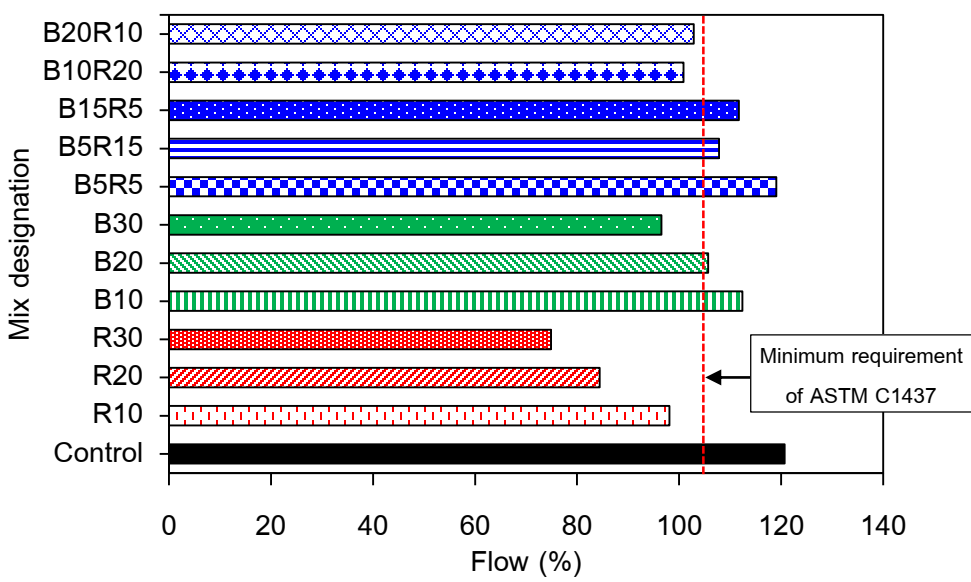
Figure 18 Percentage flow of different binary and ternary mix designations

2. Fresh density

    The fresh density of POBC mortars with different mix designations was measured according to ASTM C138 (2017) and demonstrated in Figure 19. It can be seen that the fresh density decreased with an increase in RHA and CB contents. For the mix incorporating 10%, 20%, and 30% RHA, the fresh density was 3%, 6%, and 8% lower than that of control mix. Similarly, an increase in CB partial replacement of OPC from 10% to 30% reduced the fresh density by 2% to 5% compared to the control mix. The fresh density of the ternary blends of RHA and CB ranged 2% to 6% lower than that of the control mix. It is on account of the fact that the fresh density was the function of the true density and specific gravity. The true density and specific gravity values of OPC were greater than that of RHA and CB. Consequently, the control mix had the highest fresh density compared to the rest of mix designations. This result is consistent with the previous studies. Memon et al. (2012) revealed that the fresh density of mortar containing up to 21% CB was lower than that of without CB by 7%. Furthermore, an increase in the percentage of OPC substitution by RHA up to 20% decreased the fresh density of mortar by 2.5% compared to the control mix, due to the specific gravity of RHA (2.2) was lower than that of OPC (3.2) (Sua-iam et al., 2016).
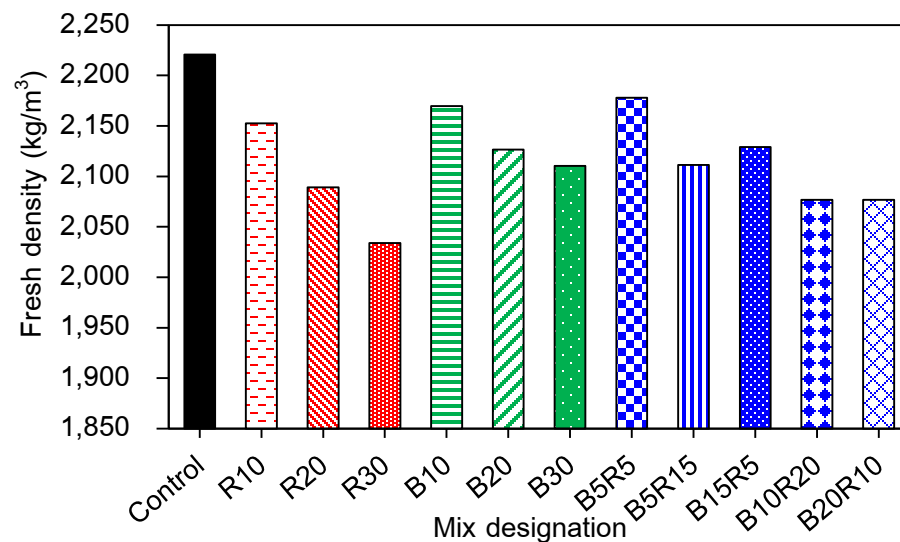
Figure 19 Fresh densities of different binary and ternary mix designations

Properties of POBC mortars

Water absorption and apparent porosity

The water absorption and apparent porosity were conducted conforming to ASTM C373-14a (2014). The water absorption and apparent porosity results of POBC mortars with different binary and ternary mix designations at the ages of 7, 28, and 56 days, as presented in Figure 20. An increase in RHA contents increased the water absorption at the early curing age (7 days), while, at the prolonged curing periods, the water absorption decreased with an increase in RHA contents. For instance, the water absorption of 56-day POBC mortars containing 10%, 20%, and 30% RHA was 21%, 28%, and 35% lesser than that of the control mix, respectively. Similar result was confirmed by Balraj et al. (2020) that the water absorption of 28-day concrete decreased with a reduction in particle size of RHA and an increase in RHA contents. The possible reason could be due to the reduction of permeable void by the pozzolanic effect of RHA, which took place at the later ages (up to 28 days of curing), whereas an increase in water absorption at the early age could be attributed to the absorption capacity of the porous RHA particle (Ganesan et al., 2008). For the mix containing CB, the water absorption decreased with prolonged curing ages and a reduction in CB content. For example, the minimum 56-day water absorption value was found in the mix containing 10% CB, which was lesser than that of the control mix by 13%, whereas the mortar containing up to 30% CB showed greater water absorption value than that of control mix by 13%.

Accordingly, the apparent porosity results were in same trend of the water absorption results, as presented in Figure 20. An increase in RHA contents and curing ages decreased the apparent porosity due to the filler effect of RHA and the secondary C-S-H formed in the pore of the mortar specimen. For example, the 56-day mortar containing 30% RHA showed the lowest apparent porosity (14%), which was 33% lower than that of the control mix. Conversely, an increase in CB contents increased the apparent porosity of the mortars, while the substitution of OPC by 10% CB reduced the 56-day apparent porosity of mortar by 14% compared to the control mix. The possible reason could be due to the absorption capacity of more CB particles that absorbed more water and swelled in the fresh

mix, when the water released, the pore size of approximately 1 μm was produced (Hu et al., 2019). Thus, the optimum substitution of OPC by 10% CB was recommended based on this study result. Moreover, a decrease in porosity was observed in the mix containing the optimum amount of 10-15% CB as an OPC substitution, which was reported by Laidani et al. (2020).This finding is in line with Man et al. (2019) and Targan et al. (2002).
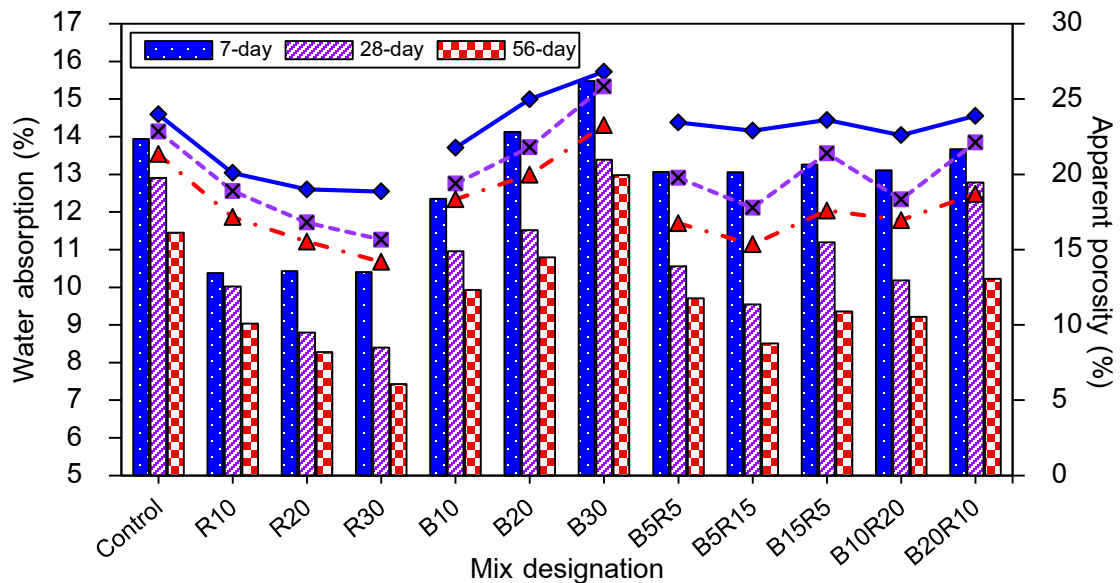
Figure 20 Water absorption and apparent porosity of different binary and ternary mix designations and curing ages

Compressive strength

The compressive strength of POBC mortars with different mix designations at 7, 28, and 56 days was determined conforming to ASTM C109 (2016). As can be clearly seen in Figure 21, the compressive strength of each mix designation increased with curing ages. The development of compressive strength for the mix incorporating RHA was observed at up to 28 days of curing period. The highest compressive strength was found in the binary mix designation of R20, which was 45 MPa and 53 MPa at the age of 28 and 56 days, respectively. However, at an early curing period of 7 days, an increase in RHA contents decreased the compressive strength. This is due to the pozzolanic effect, which is the reaction

between SiO_2 derived from RHA and $Ca(OH)_2$ from hydration process. This reaction was confirmed by Hu et al. (2020) that it took place at later age (up to 28 days) and produced calcium silicate hydrate (C-S-H), which resulted in strength development. Similar results was reported by Khan et al. (2018). Nevertheless, an increase in CB contents decreased the development of compressive strength. The highest compressive strength of the mix incorporating CB was 41 MPa at the age of 56 days, which was found in the 10% CB supplemented mix. The reduction in compressive strength of that mix was only 11% compared to the control mix. For mix designation containing the ternary blends of RHA and CB, the highest compressive strength was observed in the mix designation B5R15, which was 39 MPa and 48 MPa, respectively, at the age of 28 and 56 days. The possible reason is CB contained 57% SiO_2 in comparison with 94% SiO_2 of RHA, thus the mix designations incorporating RHA and/or more RHA contents provided more compressive strength values than those of CB. Moreover, an addition of excessive CB could hinder the hydration and pozzolanic reaction. This finding is in line with Ahmad et al. (2011) and Mesboua et al. (2018).
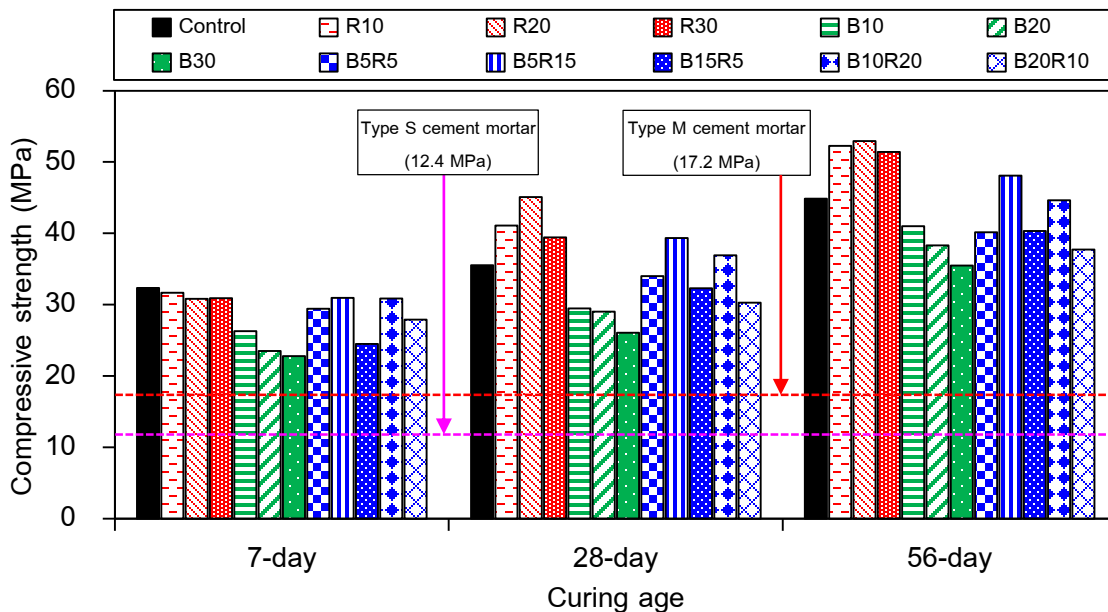
Figure 21 Compressive strength of different binary and ternary mix designations and curing ages

Strength activity index (SAI)

    The SAI is the ratio between the compressive strength of mortar containing pozzolanic materials to the compressive strength of the control mix. The SAI was calculated and tested as per ASTM C311 (2018) and C618 (2019). According to ASTM C618 (2019), the minimum standard requirement of SAI was 75% of the control mix. It can be seen that the SAI increased with prolonged curing ages, as illustrated in Figure 22. For all of the mix incorporating RHA and the ternary blends of RHA and CB at the ages of 7, 28 and 56 days, the SAI values were met the standard requirement. Regarding to the compressive strength results, the same trend was observed in the SAI. The highest SAI was found to be 127% and 107%, respectively, for the mix designation of R20 and B5R15 at the age of 28 days, whereas, the mix incorporating up to 10% CB provided the highest SAI (83% and 91%) at the ages of 28 and 56 days. However, an increase in CB contents decreased the SAI, similar results were reported by Mesboua et al. (2018) and Mirza et al. (2009). Additionally, Abbas et al. (2017) concluded that substitution of OPC by up to 30% RHA with the curing age up to 28 days could be capably in strength development due to the 28-day SAI was exceeded than 75% of the control mix.
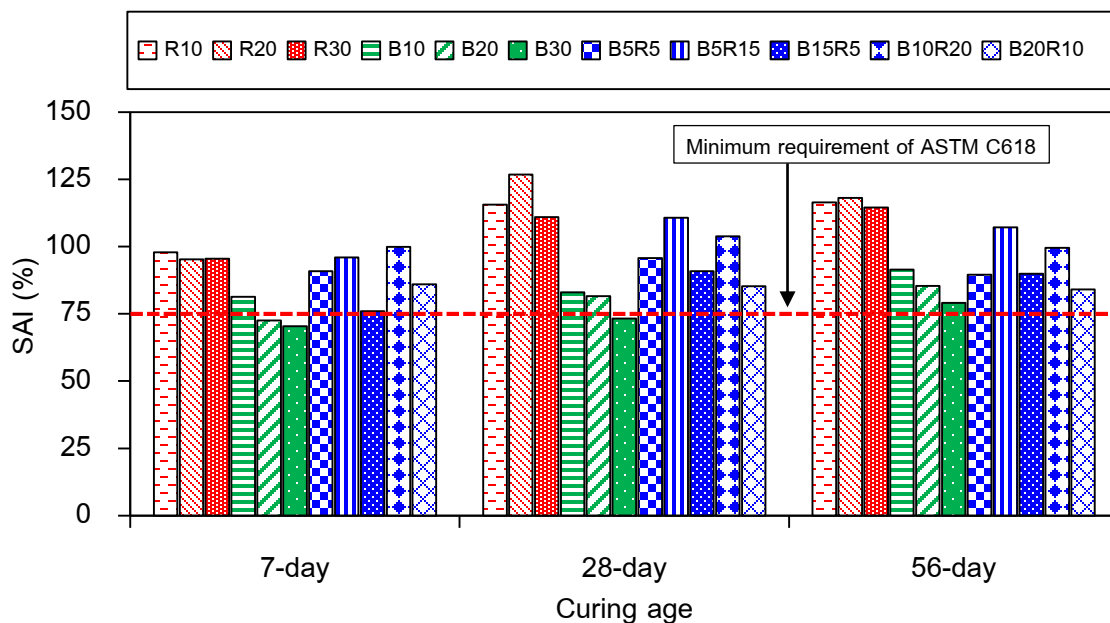
Figure 22 Strength activity index of different binary and ternary mix designations and curing ages

Sulfuric acid attack

The different mix designations of the POBC mortar specimens cured in water for 7, 28 and 56 days, were then exposed to 0.005 M (0.1% w/v, pH=2.5) sulfuric acid solution (H_2SO_4) for 6 weeks (42 days). The weight of each specimen was measured before and after exposure. The change in compressive strength was examined by comparison of the compressive strength at particular curing age of 7, 28, and 56 days before exposure with those of after exposure to sulfuric acid.

1. Loss in weight

The percentage loss in weight of different mix designations is revealed in Figure 23. It is apparent that the percentage loss in weight gradually decreased with prolonged curing age before exposure. Additionally, an increase in RHA decreased the percentage loss in weight. The 56-day percentage loss in weight was 0.81%, 0.68%, and 0.47% for the binary mix designation of R10, R20, and R30, respectively, which was 47%, 56%, and 69% lower than that of the control mix. For the binary mix designation B10, B20, and B30, the 56-day percentage loss was 0.97%, 1.54%, and 1.57%, which was 37% lower than that of the control mix; 1%, and 3% greater than that of control mix, respectively. For the ternary mix designation B5R5, B5R15, B15R5, B10R20 and B20R10, the 56-day loss in weight was 1.14%, 0.86%, 1.47%, 0.90% and 1.52%, respectively. The reaction between cement paste and sulfuric acid solution caused the dissolution of calcium and solid phases (Subashi De Silva et al., 2021). As a result, the POBC mortars exposed to sulfuric acid showed the deteriorating characteristics i.e. change in surface's color, broken rim, and loss in weight, as revealed in Figure 24. Similar result was also reported by Subashi De Silva et al. (2021) that an increase of up to 20 wt.% RHA replacement of OPC decreased the weight loss due to sulfuric acid attack by 25%. This could be due to the pozzolanic and filler effect of RHA reduced both pore-connectivity, permeability, and sorptivity by C-S-H forming in the micro-pore spaces. Thus, the weight loss was reduced by an incorporation of RHA as an OPC replacement.

2. Loss in compressive strength

The percentage loss in compressive strength of different mix designations is presented in Figure 25. The trend of percentage loss in compressive strength was in correspondence to those of loss in weight (Figure 23). The percentage loss in compressive strength decreased with age of specimens before exposure to sulfuric acid solution. The 56-day percentage loss in compressive strength for the binary mix designation of R10, R20, and R30 was 23%, 41%, and 68% lower than that of the control mix, respectively. For the mix designation, B10, the percentage loss in compressive strength was 11% lesser than that of the control mix. Conversely, the 56-day percentage loss in compressive strength for the binary mix designation of B20 and B30 was 12% and 23% greater than that of control mix. For the ternary mix designation of RHA and CB, the 56-day percentage loss in compressive strength was in the range of 4.07% to 4.93%, where the lowest percentage loss performed by in the ternary mix designation of B5R15; which was lower than that of the control mix by 18%. This result is in agreement with the research of Kumar & Prasad (2019). The compressive strength loss could be due to the loosened surface layer of mortar and micro crack; which was induced by the formation of gypsum and ettringite via the reaction between sulfuric acid and hydration products (monosulfoaluminate, C-S-H or calcium hydroxide) (Sata et al., 2012).

Based on the sulfuric acid attack mechanism, the reaction between hydration products and sulfuric acid solution is revealed as follows (Monteny et al., 2000):

$$Ca(OH)_2 + H_2SO_4 \rightarrow CaSO_4.2H_2O \tag{1}$$
$$\text{(Portlandite)} \qquad\qquad \text{(Gypsum)}$$

$$CaO.SiO_2.2H_2O + H_2SO_4 \rightarrow CaSO_4 + Si(OH)_4 + H_2O \tag{2}$$
$$\text{(C-S-H)} \qquad\qquad \text{(Gypsum)}$$

$$3CaO.Al_2O_3.12H_2O + 3(CaSO_4.2H_2O) + 14H_2O \rightarrow 3CaO.Al_2O_3.3CaSO_4.31H_2O \tag{3}$$
$$\text{(C}_3\text{A)} \qquad\qquad \text{(Gypsum)} \qquad\qquad\qquad \text{(Ettringite formed in pore solution)}$$
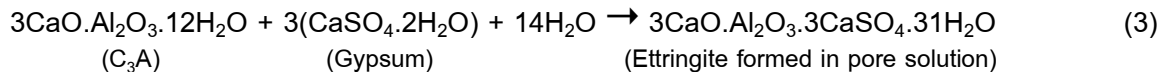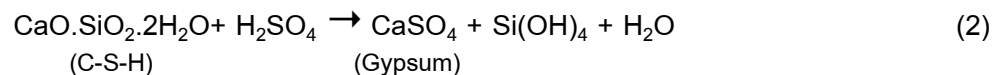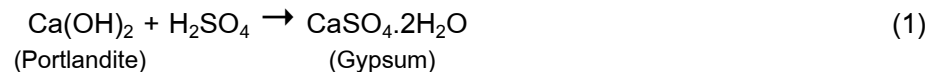
As a result, the weight loss could be explained by the dissolution of calcium of cement's paste. The mortar's structure weakened by the dissolution of that solid phase and the forming of new salt's phase. Then, the compressive strength declined consecutively.
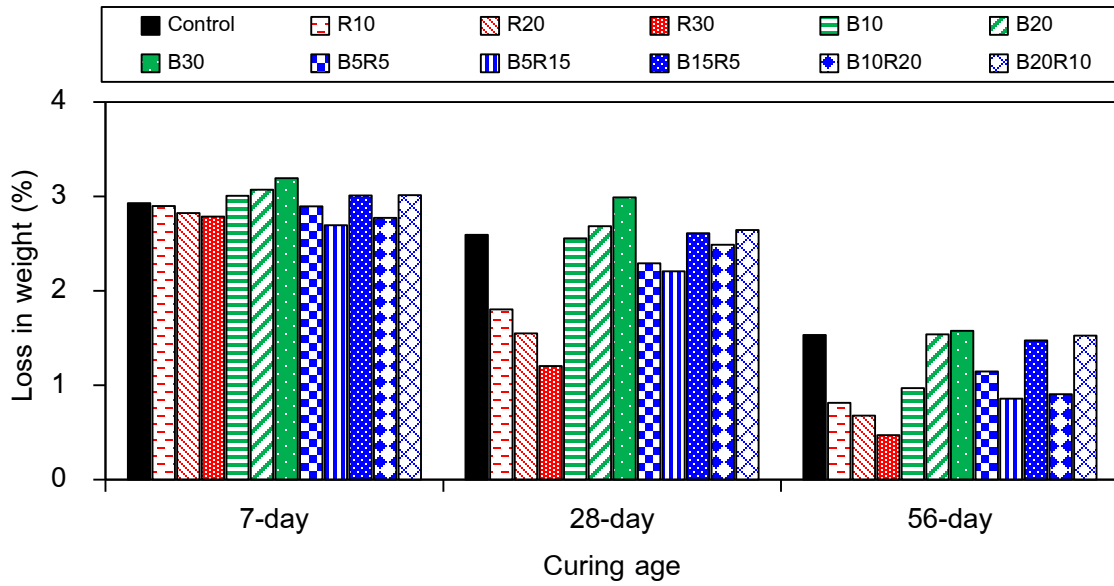
Figure 23 Percentage loss in weight of different binary and ternary mix designations and curing age after sulfuric acid attack

Figure 24 Visual observation of deteriorating characteristics of POBC mortars exposed to sulfuric acid solution for 42 days (from left to right: control mix, R10, R20, and R30)
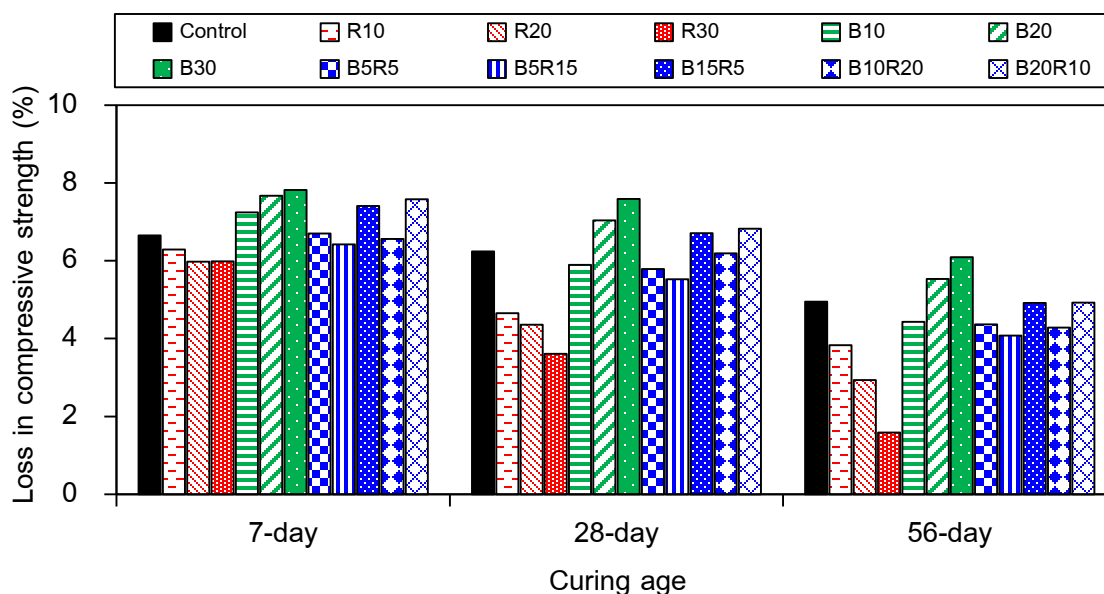
Figure 25 Percentage loss in compressive strength of different binary and ternary mix designations and curing ages after sulfuric acid attack

Sodium sulfate attack

1. Gain in weight

The POBC mortar specimens with different binary and ternary mix designations were cured in water for 7, 28 and 56 days, then were exposed to 0.5 M (8% w/v, pH=6-8) sodium sulfate solution (Na_2SO_4) for 6 weeks (42 days). Each specimen was weighed before and after exposure. The change in compressive strength was performed by comparison of the compressive strength at particular curing age of 7, 28, and 56 days before exposure with those of after exposure to sodium sulfate solution for 42 days.

It is apparent that the weight of each different mixtures slightly increased after exposure to sodium sulfate solution. However, an increase in curing age before exposure and RHA contents decreased the gain in weight. The percentage gain in weight of different mix designations was demonstrated in Figure 26. The 56-day percentage gain in weight was 0.09%, 0.07%, 0.03%, 0.12%, 0.15%, and 0.16% for the binary mix designation of R10, R20, R30, B10, B20, and B30, respectively. Additionally, the 56-day percentage gain in

weight of the ternary mix designation of B5R5, B5R15, B15R5, B10R20, and B20R10 was 0.12%, 0.09%, 0.13%, 0.10%, and 0.14%, respectively. The lowest 56-day percentage gain in weight was found in the mix designation of R30, which was 76% lesser than that of the control mix. Conversely, an increase in CB content up to 30% extended the 56- day percentage gain in weight to 23% compared to that of the control mix. Proportionately, the ternary mix designation between RHA and CB manifested lesser 56- day percentage gain in weight than the mix incorporating only CB. It could be attributed to (ⅰ) the specimen was saturated by absorption of sodium sulfate solution (ⅱ) CB was rich in alumina which could conduce more C- A- S- H and sulfate salts forming (ⅲ) the formation of sulfate salt on the surface of mortar's specimen, as depicted in Figure 27. This results are in agreement with Ma et al. (2014). Additionally, this result conformed to water absorption and apparent porosity results, where RHA had a filler effect to POBC mortar's matrix and reduced the penetrating ability of sulfate solution to the specimen.
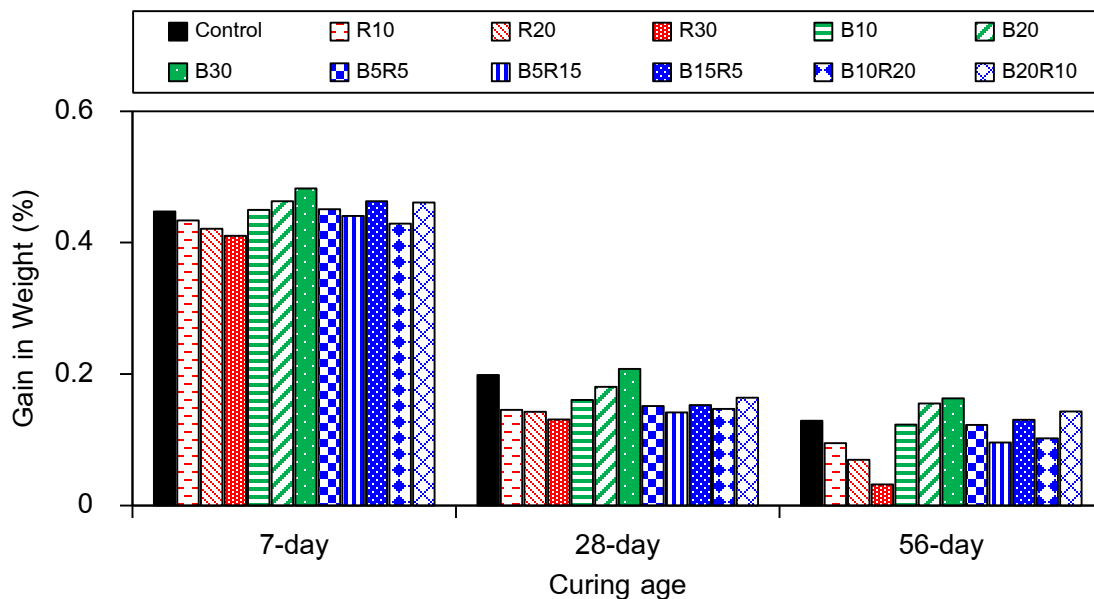
Figure 26 Percentage gain in weight of different binary and ternary mix designations and curing ages after sodium sulfate attack
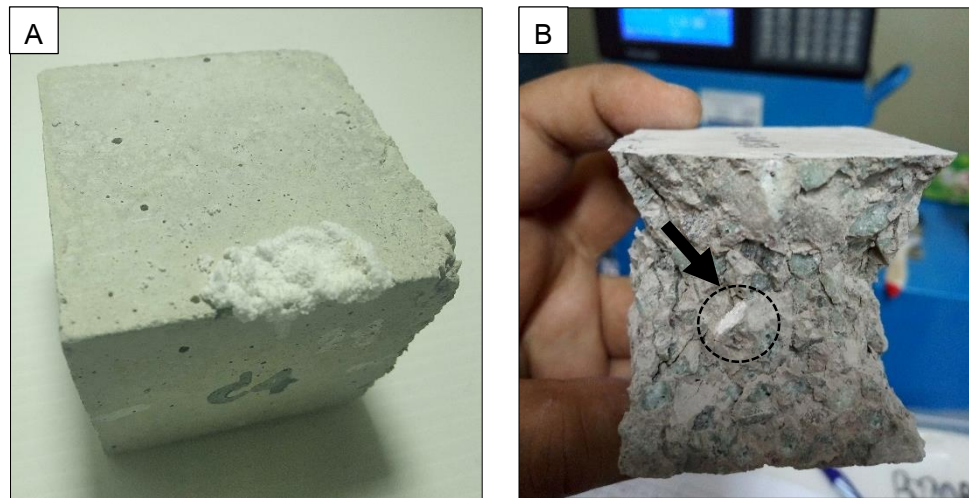
Figure 27 Visual observation of deteriorating characteristics of POBC mortars exposed to sodium sulfate solution for 42 days: sulfate salt precipitated on specimen's surface (A) and sulfate salt deposited as a plate inside cementitious material (B).

2. Loss in compressive strength

The degradation in compressive strengths after exposure to sodium sulfate solution for 42 days were monitored and represented as percentage loss in compressive strength, depicted in Figure 28. The result demonstrated the similar trend to the percentage gain in weight after exposure. In addition, an increase in curing age before exposure significantly declined the percentage loss in compressive strength. The 56-day percentage loss in compressive strength was 0.85%, 0.56%, and 0.32%, respectively, for the binary mix designation of R10, R20, and R30. For the binary mix designation of B10, B20, and B30, the 56-day percentage loss in compressive strength was 0.98%, 1.21%, and 1.32%, respectively. Consequently, the lesser values of 56-day percentage loss in compressive strength was observed in the ternary mix designation of B5R5, B5R15, B15R5, and B10R20. As compared to the control mix, an incorporating of up to 30% RHA, 10% CB, and the ternary mix of 5% CB and 15% RHA, provided the lower 56-day percentage loss in compressive strength than that of the control mix by 72%, 15%, and 27%, respectively. This result is in accordance with Hu et al. (2020). Based on the external sulfate attack mechanism that was proposed by Lv et al. (2020), the reaction between hydration products and sodium sulfate solution is demonstrated as follows:

$$Ca(OH)_2 + Na_2SO_4 + 2H_2O \rightarrow CaSO_4.2H_2O + NaOH \qquad (4)$$
$$\text{(Portlandite)} \qquad\qquad\qquad \text{(Gypsum)}$$

$$CAH + Na_2SO_4 + 2H_2O \rightarrow 3CaO.Al_2O_3.3CaSO_4.31H_2O + NaOH \qquad (5)$$
$$\text{(CAH or } 3CaO.Al_2O_3.6H_2O \qquad\qquad \text{(Ettringite)}$$
$$\text{from hydration reaction of } C_3A)$$

$$CaSO_4.2H_2O + CAH \rightarrow 3CaO.Al_2O_3.3CaSO_4.31H_2O + Ca(OH)_2 \qquad (6)$$
$$\text{(Gypsum, as formed in equation 4)} \qquad \text{(Ettringite)}$$

The hydration products, i.e., porlandite and C-A-S-H reacted with the sulfate solution to form gypsum and ettringite. As a result, the formation of gypsum and ettringite deposited nearly the specimen's surface induced microstructural alteration, expansion, strength loss, and micro cracks (Santhanam et al., 2003).

Figure 28 Percentage loss in compressive strength of different binary and ternary mix designations and curing ages after sodium sulfate attack

X-ray diffraction analysis

The crystalline phase compositions of each mix were carried out using X-ray diffractometer at 2theta between 4° to 60° with step size of 0.026° and time·step^{-1} 127.50 seconds, respectively. Table 11 demonstrates the abbreviations of mineral phases labeled on XRD spectra and their peak positions of different mixes in accordance with the ICDD database (International center for diffraction data).

The XRD patterns of the different mix designations (control, R30, B10, and B5R15) at the age of 56 days are illustrated in Figure 29. The main hydration's products were found in all mixes, which were ettringite ($Ca_6Al_2(SO_4)_3(OH)_{12}(H_2O)_{26}$), portlandite ($Ca(OH)_2$, quartz ($SiO_2$), dicalcium silicate ($Ca_2SiO_4$), and calcium silicate hydrate ($Ca_{1.5}SiO_{3.5}·_xH_2O$, C-S-H), while calcium aluminum silicate hydrate ($Ca_2Al_4Si_{14}O_{36}·14H_2O$, C-A-S-H) was found in the mix designation B10 at 2theta of 9.79° and 29.76°, respectively. However, C-S-H is an amorphous, which can be detected at low angle scattering (Hou et al., 2015), exhibited the broad and hump peak in the background intensity at 2theta of 29.36° and 50.08°, respectively.

It is evident that the peak intensies of portlandite for the mix designation R30, B10, B5R15 were lower than that of the control mix. In addition, the mix designation R30 presented the highest C-S-H and C_2S peak intensities, followed by B5R15, B10, and control mix (Figure 29). This is indicated that RHA and CB could be effectively used as a pozzolan due to (i) the lower peak intensity of portlandite and the greater peak intensity of C-S-H was observed in the mix incorporating RHA, (ii) the incorporating of CB also reduced the peak intensity of portlandite and promoted the peak of C-A-S-H, which could attributed to the more alumina composition of CB interacted with OPC (Fernandez et al., 2016). Moreover, the peak of ettringite and C_2S also indicated the primary and prolonged strength development (Jeong et al., 2016; Saghiri et al., 2017). The pozzolanic reaction could be promoted by the SiO_2 content of RHA consumed $Ca(OH)_2$ and generated more secondary C-S-H (Jamil et al., 2016).Furthermore, the incorporating of RHA in recycled aggregate concrete could promoted the 28-day compressive strength and durability against hydrochloric acid attack by pozzolanic effect that increased the C-S-H formation (Alnahhal et al., 2018).

Table 11 The mineral phases and peak positions of XRD analysis

Abbreviation	Mineral phase	Peak position at 2theta (degree)
E	Ettringite	9.72°, 15.77°, 22.90°, and 46.66°
P	Portlandite	18.01°, 28.67°, 34.10°, and 50.81°
Q	Quartz	20.84°, 21.82°, 26.62°, and 39.43°
C_2S	Dicalcium silicate (larnite)	32.02°
C-S-H	Calcium silicate hydrate	29.36° and 50.08°
C-A-S-H	Calcium aluminum silicate hydrate	9.79° and 29.93°
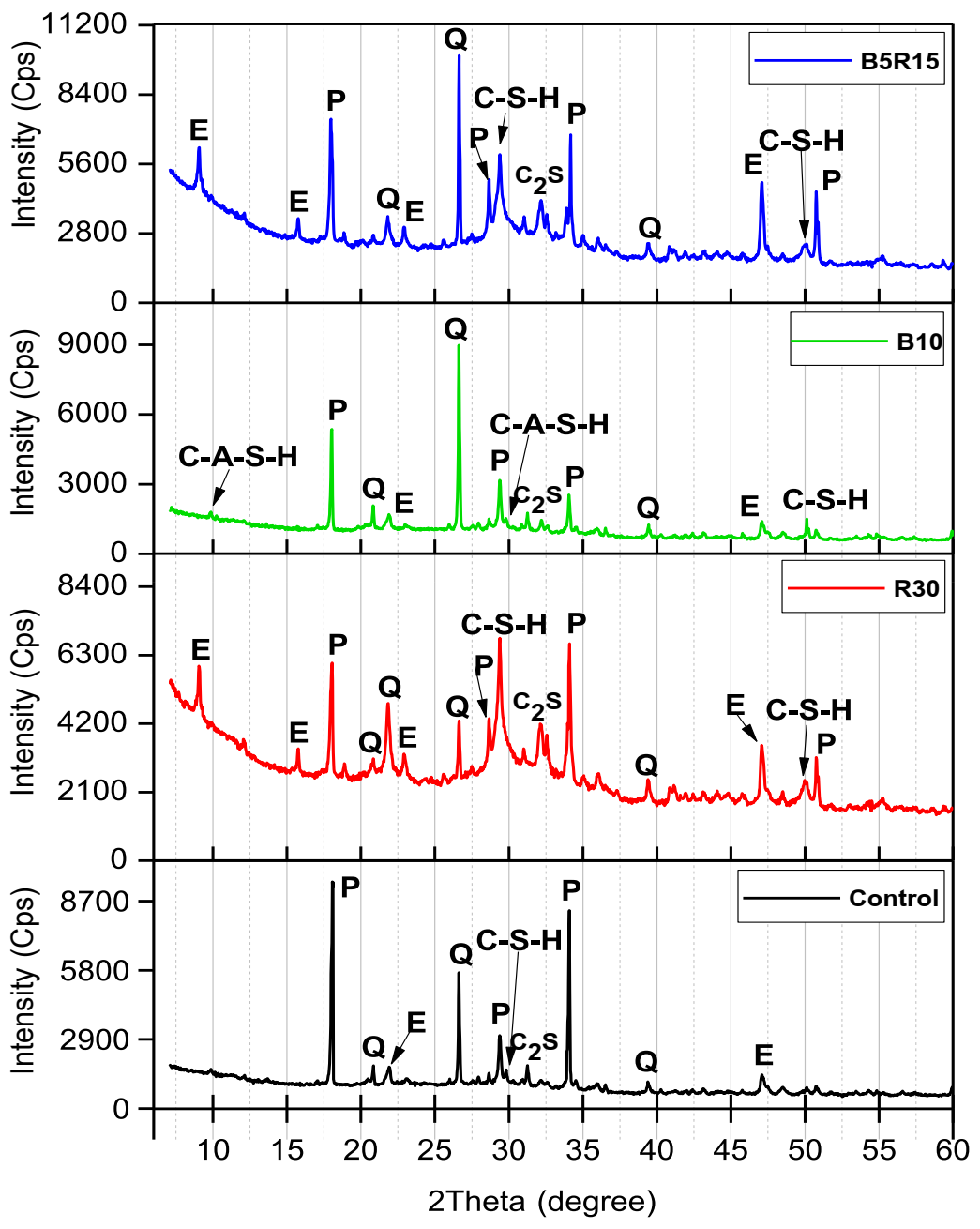
Figure 29 XRD patterns of different binary and ternary mix designations

Microstructural characterization

The SEM images of POBC specimens cured in water with different ages and mix designations are demonstrated in Figure 30. Generally, it can be seen that the hydration products of different mix designations formed in different sizes and shapes i. e. portlandite (P), ettringite (E), calcium silicate hydrate (C- S- H) in flocs- like and fibrous- like forms. The microstructural analysis was carried out based on the XRD results and crystallographic properties i. e. shapes, habits, crystal forms, crystal systems, and cleavage. Portlandite ($Ca(OH)_2$) is a hexagonal- like plate, which is classified into hexagonal crystal system and exhibited one perfect cleavage. It was formed by the hydration reaction and can generate the secondary C- S- H with the pozzolanic materials (Neville & Brooks, 2010). The negative effect of portlandite in durability properties is that it could react with the sulfate solution and gypsum. Ettringite is a hexagonal crystal form as classified into hexagonal crystal system, which often exhibits acicular or prismatic shape. The formation of ettringite could develop the strength of cement paste (Neville & Brooks, 2010). Based on this study, C-S-H is observed in two different forms: (i) flocs-like form and (ii) fibrous-like form, as shown in Figure 30A-D. Additionally, the C- S- H is an amorphous or poorly crystalline product, which widely spreads like a network on the matrix of cement paste and enhances durability (Neville & Brooks, 2010). Evidently, the microstructure of the mix designation of R10 and B5R15 showed the denser matrix occupied by C- S- H, when compared to that of the control mix and mix designation of B10. Moreover, the larger needle- like shape of ettringite was obviously found in mix designation of R10, which provided the greater compressive strength development than the control mix.

The microstructural analysis using SEM images of specimens exposed to sulfuric solution is shown in the Figure 31. The disintegration characteristics and unshaped crystals of the hydration and pozzolanic products were found in all mix, which contributed to the loss in weight and compressive strength. A monoclinic plate of gypsum (G), ettringite (E), and C- S- H was revealed in Figure 31A- D. The loosened matrix by the corrosion of sulfuric acid and formation of gypsum and ettringite could contribute to more pore spaces and some cracks. It can be seen that the microstructure of ternary mix designation of RHA and CB

showed the lesser loosed matrix than that of the control mix. This could contributed to the pozzolanic reaction, which produced more secondary C-S-H and lessening the pore spaces.

The SEM images of specimens exposed to sodium sulfate solution are demonstrated in Figure 32. Particularly, the mix designation of R10, B10, and B5R15 revealed the mild deteriorating characteristics of sodium sulfate attack, when compared to the control mix. Accordingly, the dense matrix that was observed in those mix provided the less pore spaces for the formation of gypsum (G), ettringite (E) and microcracks.

As a result, this indicated that the binary mix of RHA up to 30%, CB up to 10%, and the ternary mix of 5% CB and 15% RHA promoted the durability of the POBC mortar due to the densification of microstructure by C-S-H from pozzolanic reaction. This finding is in agreement with Hu et al. (2020), Fernandez et al. (2016), and Mohseni et al. (2017).
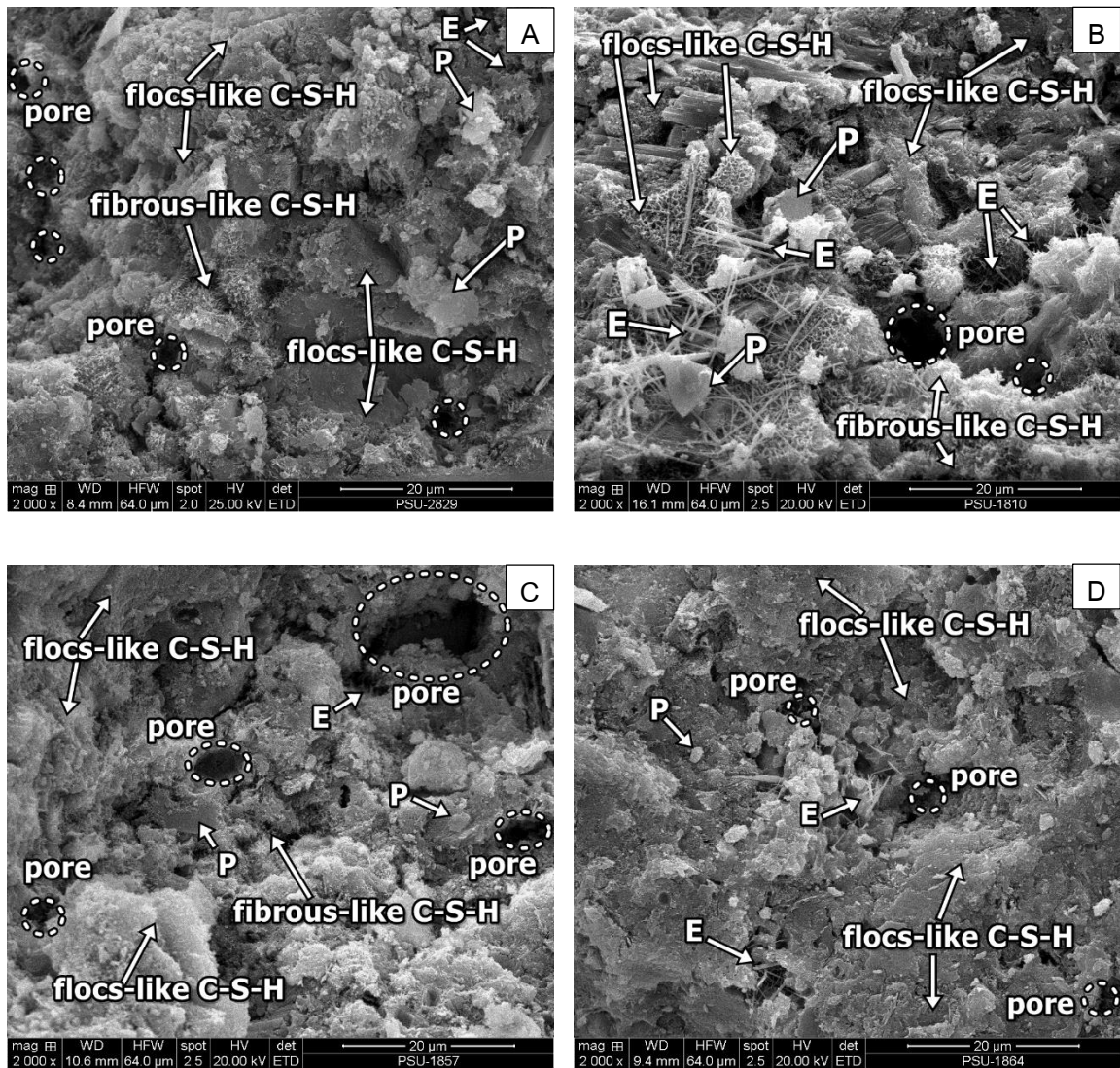
Figure 30 SEM images of control mix (A), binary mix designation of R10 (B), B10 (C), and ternary mix designation of B5R15 (D) cured in water for 56 days.
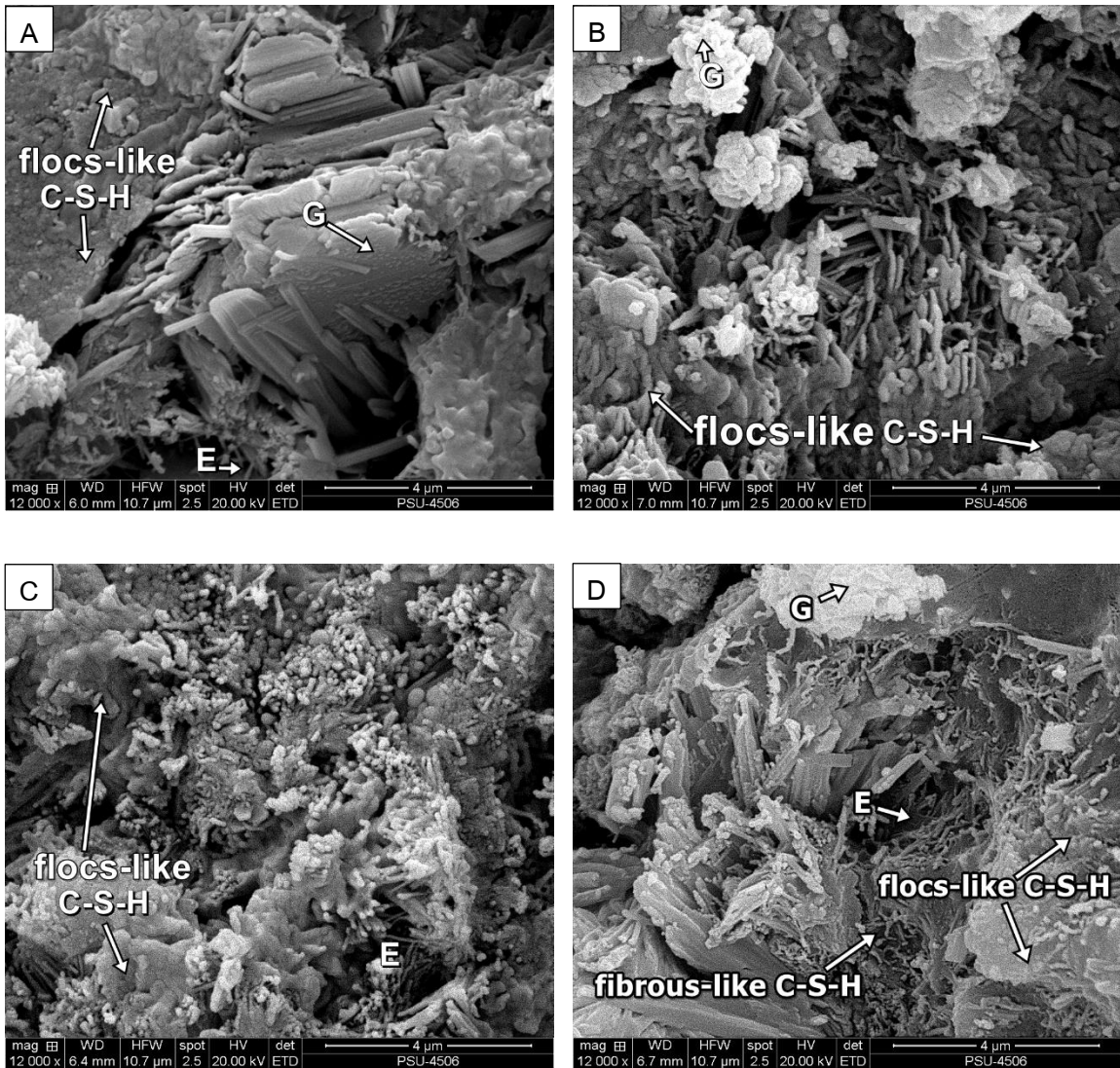
Figure 31 SEM images of control mix (A), binary mix designation of R10 (B), B10 (C), and ternary mix designation of B5R15 (D) after exposure to sulfuric acid solution
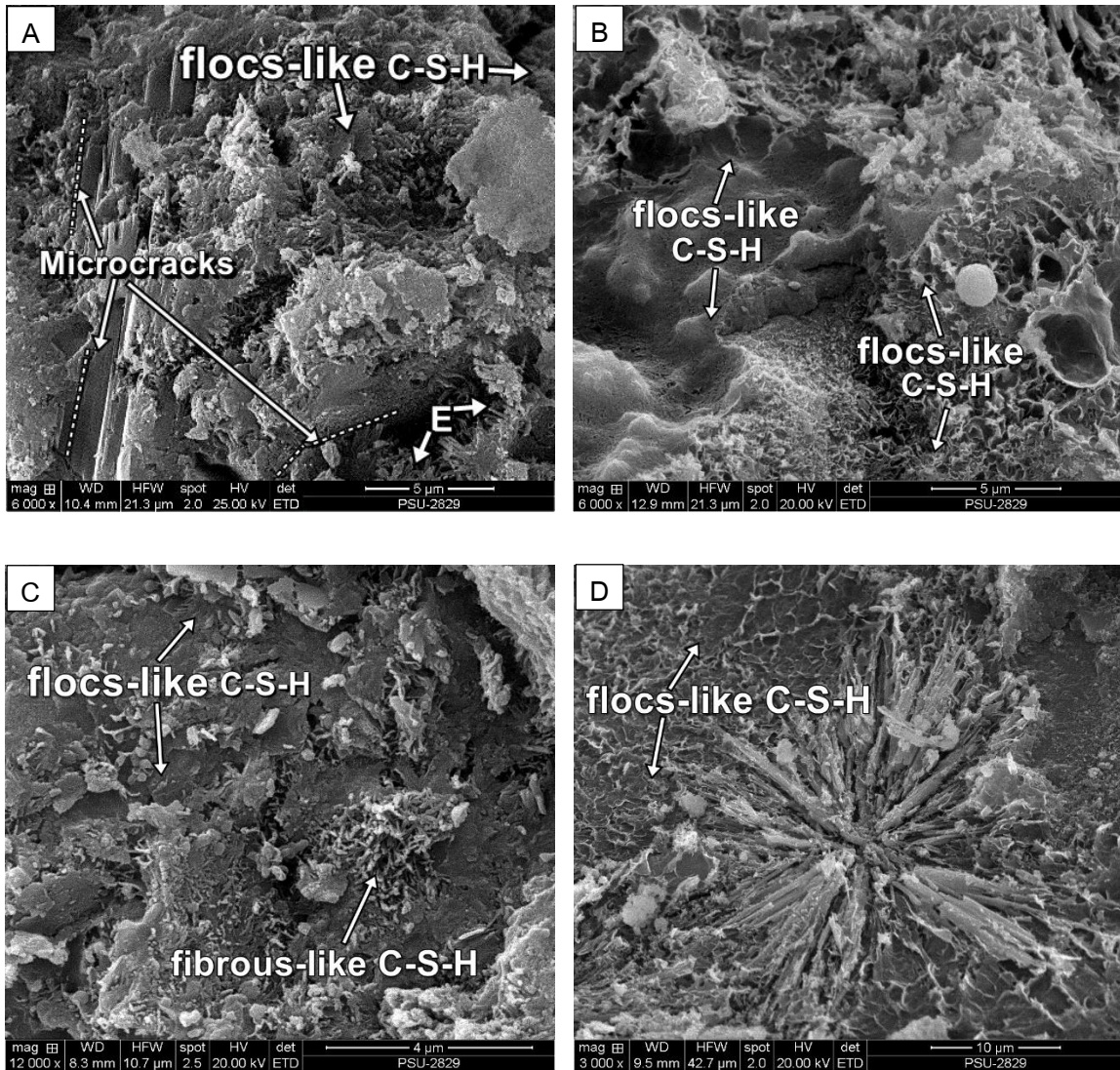
Figure 32 SEM images of control mix (A), binary mix designation of R10 (B), B10 (C), and ternary mix designation of B5R15 (D) after exposure to sodium sulfate solution

Properties of POBC concrete

Rapid chloride permeability test (RCPT)

The RCPT was carried out as per ASTM C1202 for the POBC concrete specimens with different mix designations. The apparatus for RCPT was developed by Suriyachoto & Tonnayopas (2013) in accordance with ASTM C1202. This apparatus consisted of transformer (47 VAC, 13 A), copper circuit board, bridge diode, capacitor, regulator, heat sink and fan, panel voltmeter, and ammeter, as shown in Figure 33A. The alternating current (A.C.) will be input to the apparatus, and it will be transformed to a direct current (D.C.) by full wave bridge rectifier, then the D.C. will be transferred to voltage regulator circuits. The electricity with constant voltage of 60 V was generated on the surface of tested specimen for 6 h. Then, the output of coulombs were measured by ammeter and recorded every 30 mins. The chloride ion permeability of each specimen was classified by the charge passed result. The specimen prepared for the test are shown in Figure 33B. The tested specimens were cured for 28 and 56 days before testing, the total charge passed per coulomb results are presented in Figure 34. Corresponding to ASTM C1202, the criteria for chloride ion penetrability is determined as tabulated in Table 12. The highest 28-day and 56-day chloride ion penetrability were observed in the mix containing 30% CB (7,536 and 6,083 coulombs), while the lowest 28-day and 56-day chloride ion penetrability were found in the binary mix containing 30% RHA (507 and 336 coulombs). Thus, an increase in curing age and RHA decreased the chloride ion penetrability, whereas an increase in CB increased the chloride ion penetrability. The similar trend was observed in the mix designation containing ternary blends of CB and RHA, the very low chloride ion penetrability of 28-day and 56-day specimens was 718 and 598 coulombs, respectively, for the mix designation B5R15 and B10R20, respectively. Hence, the optimum ternary blend ratios of CB and RHA could be considered as 5 to 10% CB with 15 to 20% RHA substitution by weight of OPC in the POBC concrete. Based on the investigated results in this study, a significant decrease in chloride ion penetration was prominently found in the mix supplemented with RHA. The supplementing RHA into CB reduced the chloride ion permeability by 56%, 81%, 76%, 86%, and 76%, respectively, for the ternary mixes of B5R5, B5R15, B15R5, B10R20 and B20R10, compared to the minimum incorporation of 10% CB (mix designation B10) cured for 56 days.

This is due to the greater pozzolanic activity of RHA than CB, which could improve the microstructure by producing more C‐S‐H and denser the matrix. Correspondingly, previous studies reported that the RHA excellently performed the important role in improving chloride ion penetrability over metakaolin (Gill & Siddique, 2018), sugarcane‐bagasse ash and palm oil fuel ash (Joshaghani & Moeini, 2018), and fly ash (Chindaprasirt et al., 2008).

Overall, an increase in curing age up to 56 days with an incorporation of RHA and ternary blends of CB and RHA reduced the chloride ion penetrability of POBC concrete, which were in acceptable range for low to very low chloride ion penetrability, whereas that of the control mix steadily fell in the moderate range base on ASTM C1202.
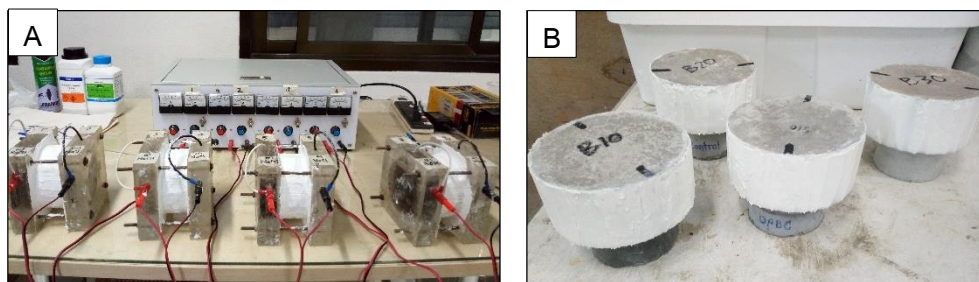
Figure 33 The apparatus for RCPT (A) and concrete specimen prepared for RCPT (B)
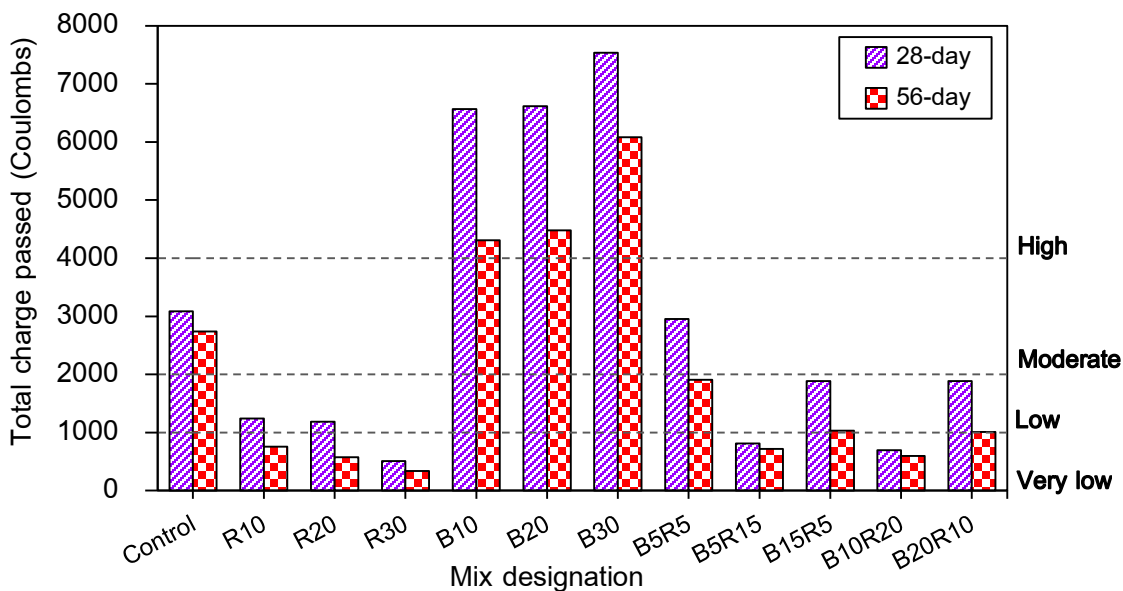
Figure 34 Total charge passed per coulomb from RCPT at different mixes and ages

Table 12 Criteria for chloride ion penetrability from RCPT according to ASTM C1202

Total charge passed (coulombs)	Penetrability
>4,000	High
2,000 to 4,000	Moderate
1,000 to 2,000	Low
<1,000	Very low

Capillary absorption coefficient

The ability of concrete's surface to absorb water by capillary suction is determined as capillary water absorption. The capillary absorption coefficient is the rate of capillary water absorption, which is a mass gain per unit area of exposed specimen's surface to water as a function of time. The capillary absorption coefficient of POBC concrete with different mix designation at the age of 28 and 56 days was measured and calculated in accordance with ASTM C1585 (2020), as shown in Figure 35. It can be clearly seen that an increase in curing age and percentage replacement of RHA decreased the capillary absorption coefficient. For example, the binary mix containing maximum 30% RHA substitution by weight of an OPC showed the lowest capillary absorption coefficient by 0.06 kg/mm^2/h$^{0.5}$ at the age of 56 days, which was 40% lower than that of the control mix. Conversely, an increase in CB increased the capillary absorption coefficient. The lowest capillary absorption coefficient of the binary mix containing 10% CB was 0.11 kg/mm^2/h$^{0.5}$ at the age of 56 days, which was 10% higher than that of the control mix. In addition, for the mix designation containing the ternary blends of CB and RHA, the lowest capillary absorption coefficient was found in the ternary mix designation B5R15 and B10R20 cured for 56 days, which were equally 0.07 kg/mm^2/h$^{0.5}$. Coincidently, the capillary absorption coefficient was in the same trend of the chloride ion permeability. This is due to the capillary pore was filled up by C-S-H, which in turn resulted in the denser matrix. Thus, the chloride ion permeability and capillary absorption coefficient reduced. Moreover, the more SiO$_2$ was provided by the more amount of micro RHA particles, which reacted with Ca(OH)$_2$ and generated more C-S-H (Balapour et al., 2017).
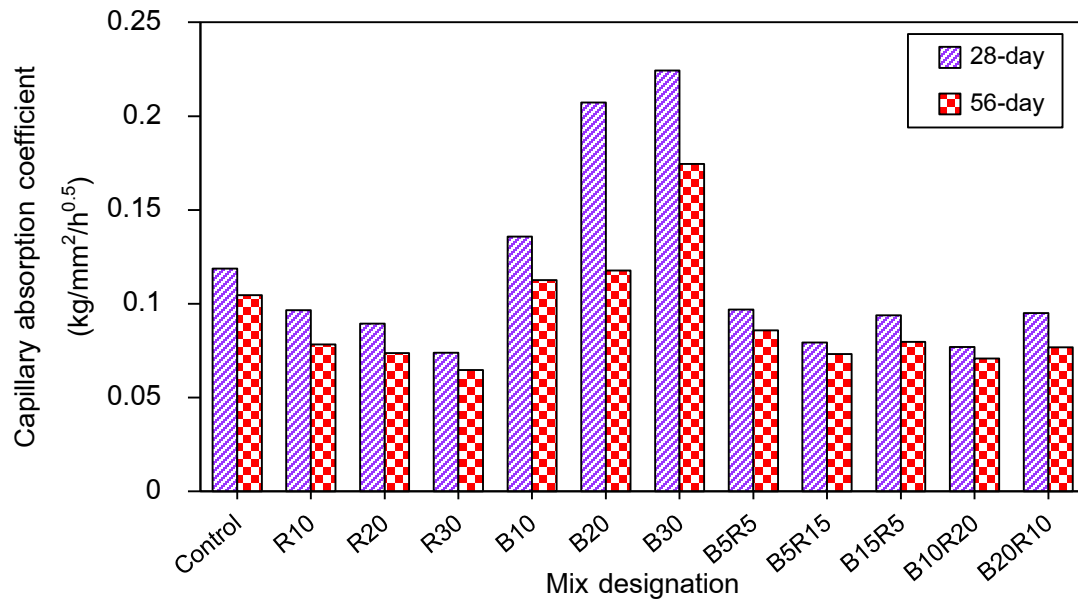
Figure 35 Capillary absorption coefficient of different binary and ternary mix designations and curing ages

Indirect tensile strength

The concrete specimens after tested for the RCPT, were then taken to determine the indirect tensile strength in compliance with Brazilian method (the test method was adapted from ASTM C496/C496M (2017)). The results of indirect tensile strength are in range of 2 to 4 MPa, as shown in Figure 36. It can be seen that the indirect tensile strength increased with prolonged curing age. The development of 56-day indirect tensile strength is clearly found in the binary and ternary mix designation of R10, R20, B10, B5R15, and B10R20, which was 23%, 3%, 3%, 14%, and 7%, respectively, greater than the control mix. On the contrary, the reduction in 56-day indirect tensile strength was observed in the mix designation of R30, B20, B30, B5R5, B15R5, and B20R10, which was 5%, 3%, 4%, 2%, 1%, and 3%, respectively, lower than the control mix. As a result, an increase in CB content decreased the indirect tensile strength as well as the incorporation of RHA content exceeded than 20% by weight of an OPC. The development in indirect tensile strength of the binary mix incorporating the optimum amount of up to 20% RHA and 10% CB could be due to the

pozzolanic reaction of the reactive micro SiO_2 particles from RHA and CB, which in turn promoted the precipitation of C-S-H and the densification of POBC concrete. The previous work reported that the maximum improvement in tensile strength of 14% was found in the binary mix containing 15% RHA as an OPC replacement, which could ascribed to the improvement of the bond between interfacial transition area of the specimen by C-S-H (Qureshi et al., 2020). This finding also in line with the previous study, that the optimum 10-15% CB improved the indirect tensile strength of concrete specimen by 5%, compared to the mix without adding CB at the age of 180 days (Masood et al., 2020).
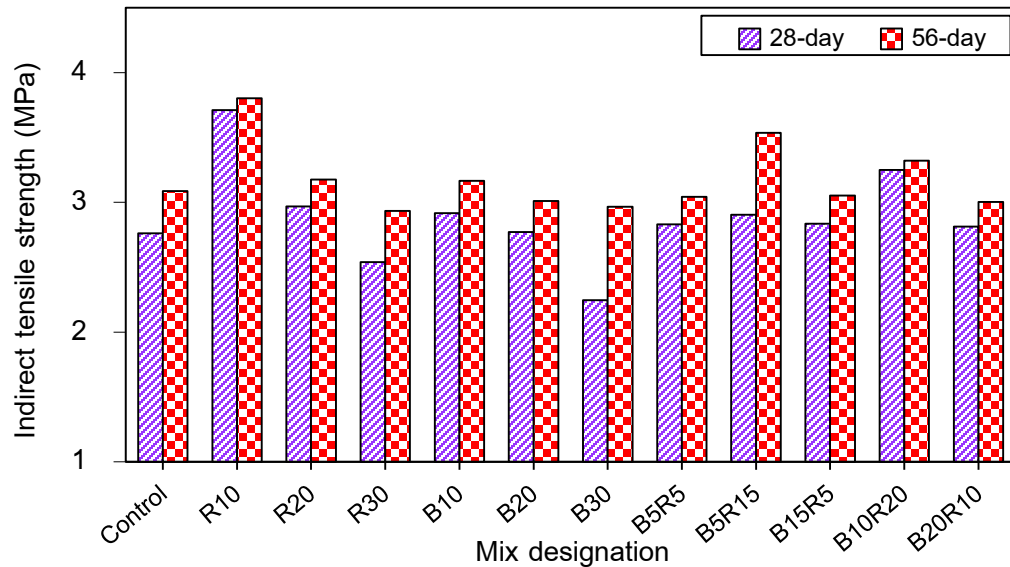
Figure 36 Indirect tensile strength of different binary and ternary mix designations and curing ages

Criteria and comprehensive properties of POBC mortars and concretes

Based on the standard requirement of ASTM C270, the maximum replacement of up to 30% of binary RHA mixture and ternary blends of RHA and CB by weight of OPC can be possibly considered as a practical implication for type S and type M cement mortars and concrete with chloride ion penetrability resistance, as tabulated in Table 13. However, the maximum replacement of 20% of CB for binary mixture is recommended for using as a natural pozzolan without restrain the compressive strength development, as per ASTM C618.

Table 13 Criteria and comprehensive properties of POBC mortars and concretes with different binary and ternary mix designations for future practical implication

Properties			Mix designations											
			Control	R10	R20	R30	B10	B20	B30	B5R5	B5R15	B15R5	B10R20	B20R10
Mortar		Flow (≥105%) (ASTM C 1437)	✓	✗	✗	✗	✓	✓	✗	✓	✓	✓	✗	✗
	28-day UCS (ASTM C270)	Type S (≥12.4 MPa)	✓	✓	✓	✓	✓	✓	✓	✓	✓	✓	✓	✓
		Type M (≥17.2 MPa)	✓	✓	✓	✓	✓	✓	✓	✓	✓	✓	✓	✓
	28-day SAI (75% of control mix) (ASTM C618)		-	✓	✓	✓	✓	✓	✗	✓	✓	✓	✓	✓
	Recommendation: According to the 28-day compressive strength and SAI results, all of the binary and ternary mix designations were met the standard requirement of type S and type M cement mortar (ASTM C270). Thus, it could be possibly applied in foundations, parapet walls, exterior walls, and traditional purpose.													
Concrete	Low to very low chloride ion penetrability (28-day) (ASTM C1202)		✗	✓	✓	✓	✗	✗	✗	✗	✓	✓	✓	✓

Conclusions and Suggestions

Conclusions

This study focused on utilization of POBC as fine and coarse aggregate substitution and incorporating binary and ternary mixes of CB and RHA as a partial OPC replacement in green mortar and concrete production. Based on the study, these following conclusions and suggestions can be stated:

1. The physical properties, chemical compositions, and morphology of POBC showed that the POBC can be used to replace natural aggregate for nonstructural mortar and concrete production.

2. The chemical compositions and physical properties of CB and RHA can be classified as type N and type C according to ASTM C618 (2019).

3. The setting times were decreased by an increase in RHA replacement level and a decrease in CB replacement level. Likewise, a decrease in cement contents by an increase in CB and/RHA replacement level reduced the heat of hydration.

4. The flowability of fresh mortars were reduced as an increase in CB and/ RHA replacement level due to the fineness of CB particles and filler effect of RHA. Subsequently, the fresh density of mortars were slightly decreased by an increase in CB and/ RHA replacement level due to the lower true density and specific gravity of CB and RHA compared to that of OPC.

5. The compressive strength increased as a function of curing age. The optimum binary replacement level of CB and RHA were 10% and 20%, respectively. The highest compressive strength was found to be 53 MPa for the mix containing 20% RHA at the age of 56 days. Accordingly, the highest compressive strength of the mix containing 10% CB cured for 56 days was 41 MPa. The optimum ternary replacement level of CB and RHA was the incorporating of 5% CB and 15% RHA, which provided the highest 56- day compressive strength of 48 MPa. However, the compressive strength values of all binary and ternary mixtures were classified into type S and type M mortars, which could be possibly used in both foundation and traditional purpose.

Subsequently, the SAI results were in accordance with the compressive strength developments. Moreover, the 28-day SAI values of binary RHA mixture and ternary blends of CB and RHA were met the standard requirement of ASTM C618 (2019). Thus, the CB and RHA could be utilized as an OPC replacement as up to 20w.% and 30wt.%, respectively, which could provided the SAI not lesser than 75% of the control mix.

6. The water absorption and apparent porosity decreased with (i) prolonged curing ages, (ii) a reduction in CB replacement level, and (iii) an increase in RHA replacement level.

7. The deteriorations due to sulfuric acid and sodium sulfate attack: compressive strength and weight variations, as investigated in this study were mitigated by an increase in RHA replacement level and curing ages.

8. According to the XRD analysis and SEM images, the mix incorporating RHA apparently revealed dense microstructure with C-S-H forming compared to control mix and mix incorporating CB.

9. The rapid chloride ion permeability and capillary absorption coefficient of concretes decreased as an increase in RHA replacement level and curing ages. The very low ranges of total charge passed were found in the binary mix incorporating up to 30% RHA, ternary mix of 5-10% CB and 10-20% RHA.

10. The indirect tensile strength decreased as an increase in CB replacement level, while the replacement level of not exceeded than 20% RHA provided the development in indirect tensile strength.

Suggestions

        1. The water reducing agents are recommended to add into the green mortars or concrete containing SCMs or other type of wastes and/ or recycle aggregates in order to develop the high performance in both strength and durability.

        2. The CB could be activated by appropriate temperature to improve the pozzolanic activity and induce the amorphousness phases.

        3. The investigations of fire resistant should be carried out to consider the suitable usages of these mortars and concretes as well as develop the mix designation and production process.

        4. To promote the sustainable construction, reduce the use of natural resources, and degrade the local wastes, the potential of developing a cementless composite containing 100% of palm oil boiler clinker as a natural aggregate substitution is possible, according to the experimental investigation of this study.

REFERENCES

Abbas, S., Kazmi, S. M. S., & Munir, M. J. (2017). Potential of rice husk ash for mitigating the alkali-silica reaction in mortar bars incorporating reactive aggregates. *Construction and Building Materials*, *132*, 61-70. https://doi.org/10.1016/j.conbuildmat.2016.11.126

Ahmad, S., Barbhuiya, S. A., Elahi, A., & Iqbal, J. (2011). Effect of Pakistani bentonite on properties of mortar and concrete. *Clay Minerals*, *46*(1), 85-92. https://doi.org/10.1180/claymin.2011.046.1.85

Alnahhal, M. F., Alengaram, U. J., Jumaat, M. Z., Alsubari, B., Alqedra, M. A., & Mo, K. H. (2018). Effect of aggressive chemicals on durability and microstructure properties of concrete containing crushed new concrete aggregate and non- traditional supplementary cementitious materials. *Construction and Building Materials*, *163*, 482-495. https://doi.org/10.1016/j.conbuildmat.2017.12.106

Abutaha, F., Abdul Razak, H., & Kanadasan, J. (2016). Effect of palm oil clinker (POC) aggregates on fresh and hardened properties of concrete. *Construction and Building Materials*, *112*, 416-423. https://doi.org/https://doi.org/10.1016/j.conbuildmat.2016.02.172

Achyutha Kumar Reddy, M., & Ranga Rao, V. (2019). Utilization of bentonite in concrete: A review. *International Journal of Recent Technology and Engineering*, 7(6C2), 541-545.

Ahmad, S., Barbhuiya, S. A., Elahi, A., & Iqbal, J. (2011). Effect of Pakistani bentonite on properties of mortar and concrete. *Clay Minerals*, *46*(1), 85-92. https://doi.org/10.1180/claymin.2011.046.1.85

Ahmmad, R., Alengaram, U. J., Jumaat, M. Z., Sulong, N. H. R., Yusuf, M. O., & Rehman, M. A. (2017). Feasibility study on the use of high volume palm oil clinker waste in environmental friendly lightweight concrete. *Construction and Building Materials*, *135*, 94-103. https://doi.org/https://doi.org/10.1016/j.conbuildmat.2016.12.098

Ahmmad, R., Jumaat, M. Z., Alengaram, U. J., Bahri, S., Rehman, M. A., & bin Hashim, H. (2016). Performance evaluation of palm oil clinker as coarse aggregate in high

strength lightweight concrete. *Journal of Cleaner Production*, *112*, 566- 574. https://doi.org/10.1016/j.jclepro.2015.08.043

Al-Hammood, A. A., Frayyeh, Q. J., & Abbas, W. A. (2021). Raw bentonite as supplementary cementitious material – a review. *Journal of Physics: Conference Series*, *1795*(1), 012018. https://doi.org/10.1088/1742-6596/1795/1/012018

Alex, J., Dhanalakshmi, J., & Ambedkar, B. (2016). Experimental investigation on rice husk ash as cement replacement on concrete production. *Construction and Building Materials*, *127*, 353-362. https://doi.org/https://doi.org/10.1016/j.conbuildmat.2016.09.150

Alqahtani, F. K., Rashid, K., Zafar, I., Khan, M. I., & Ababtain, A. A. (2021). Production of sustainable green mortar by ultrahigh utilization of fly ash: Technical, economic and environmental assessment. *Construction and Building Materials*, *281*, https://doi.org/10.1016/j.conbuildmat.2021.122617

American Society for Testing and Materials. (2001). ASTM C270-01: Standard Specification for Mortar for Unit Masonry, ASTM International, West Conshohocken, PA. In.

American Society for Testing and Materials. (2014). ASTM C373-14a: Standard Test Method for Water Absorption, Bulk Density, Apparent Porosity, and Apparent Specific Gravity of Fired Whiteware Products, Ceramic Tiles, and Glass Tiles, ASTM International, West Conshohocken, PA. In.

American Society for Testing and Materials. (2015). ASTM C1437-15: Standard Test Method for Flow of Hydraulic Cement Mortar, ASTM International, West Conshohocken, PA. In.

American Society for Testing and Materials. (2016). ASTM C109/C109M-16a: Standard Test Method for Compressive Strength of Hydraulic Cement Mortars (Using 2- in. or [50-mm] Cube Specimens), ASTM International, West Conshohocken, PA. In.

American Society for Testing and Materials. (2017). ASTM C138/C138M-17a: Standard Test Method for Density (Unit Weight), Yield, and Air Content (Gravimetric) of Concrete, ASTM International, West Conshohocken, PA. In.

American Society for Testing and Materials. (2020). ASTM C1585-20: Standard Test Method for Measurement of Rate of Absorption of Water by Hydraulic- Cement Concretes, ASTM International, West Conshohocken, PA. In.

American Society for Testing and Materials. (2018). ASTM C311/C311M: Standard Test Methods for Sampling and Testing Fly Ash or Natural Pozzolans for Use in Portland-Cement Concrete, ASTM International, West Conshohocken, PA. In.

American Society for Testing and Materials. (2019). ASTM C618-19: Standard Specification for Coal Fly Ash and Raw or Calcined Natural Pozzolan for Use in Concrete, ASTM International, West Conshohocken, PA. In.

American Society for Testing and Materials. (2017). ASTM C496 / C496M-17, Standard Test Method for Splitting Tensile Strength of Cylindrical Concrete Specimens, ASTM International, West Conshohocken, PA. In.

Asadi, I., Shafigh, P., Hashemi, M., Akhiani, A. R., Maghfouri, M., Sajadi, B., Mahyuddin, N., Esfandiari, M., Talebi, H. R., & Metselaar, H. S. C. (2021). Thermophysical properties of sustainable cement mortar containing oil palm boiler clinker (OPBC) as a fine aggregate. *Construction and Building Materials*, *268*, https://doi.org/10.1016/j.conbuildmat.2020.121091

Balapour, M., Ramezanianpour, A., & Hajibandeh, E. (2017). An investigation on mechanical and durability properties of mortars containing nano and micro RHA. *Construction and Building Materials*, *132*, 470-477. https://doi.org/10.1016/j.conbuildmat.2016.12.017

Balraj, A., Jayaraman, D., Krishnan, J., & Alex, J. (2020). Experimental investigation on water absorption capacity of RHA-added cement concrete. *Environmental Science and Pollution Research*. https://doi.org/10.1007/s11356-020-11339-1

Bheel, N., Keerio, M. A., Kumar, A., Shahzaib, J., Ali, Z., Ali, M., & Sohu, S. (2020). An investigation on fresh and hardened properties of concrete blended with rice husk ash as cementitious ingredient and coal bottom ash as sand replacement material. *Silicon*, 12. https://doi.org/10.1007/s12633-020-00906-3

Chai, L. J., Shafigh, P., & Bin Mahmud, H. (2019). Production of high-strength lightweight concrete using waste lightweight oil-palm-boiler-clinker and limestone powder. *European Journal of Environmental and Civil Engineering*, *23*(3), 325-344. https://doi.org/10.1080/19648189.2016.1277375

Chai, L. J., Shafigh, P., Mahmud, H., & Aslam, M. (2017). Effect of substitution of normal weight coarse aggregate with oil-palm-boiler clinker on properties of concrete. *Sains Malaysiana*, *46*(4), 645-653. https://doi.org/10.17576/jsm-2017-4604-18

Chen, J. J., Ng, P. L., Li, L. G., & Kwan, A. K. H. (2018). Use of superfine zeolite in conjunction with silica fume - Effects on rheology and strength of cementitious paste. *Powder Technology*, *328*, 75-83. https://doi.org/10.1016/j.powtec.2018.01.008

Chindaprasirt, P., Rukzon, S., & Sirivivatnanon, V. (2008). Resistance to chloride penetration of blended Portland cement mortar containing palm oil fuel ash, rice husk ash and fly ash. *Construction and Building Materials*, *22*(5), 932-938. https://doi.org/10.1016/j.conbuildmat.2006.12.001

Darvish, P., Alengaram, U. J., Poh, Y. S., Ibrahim, S., & Yusoff, S. (2020). Performance evaluation of palm oil clinker sand as replacement for conventional sand in geopolymer mortar. *Construction and Building Materials*, *258*, https://doi.org/10.1016/j.conbuildmat.2020.120352

Department of industrial works. (2020). *Oil palm plants in southern part of Thailand*. https://www.diw.go.th/hawk/content.php?mode=dataservice

Department of mineral resources. (2007). *Aggregate reserve for cement industry in Thailand*. http://www1.dpim.go.th/dpimdoc/ores/index.php?oresnamegroup=%CB%D4%B9%C

Di Febo, R., Casas, L., del Campo, A. A., Rius, J., Vallcorba, O., Melgarejo, J. C., & Capelli, C. (2020). Recognizing and understanding silica-polymorph microcrystals in ceramic glazes. *Journal of the European Ceramic Society*, *40*(15), 6188-6199. https://doi.org/10.1016/j.jeurceramsoc.2020.05.063

Fapohunda, C., Akinbile, B., & Shittu, A. (2017). Structure and properties of mortar and concrete with rice husk ash as partial replacement of ordinary Portland cement – A review. *International Journal of Sustainable Built Environment*, *6*(2), 675-692. https://doi.org/https://doi.org/10.1016/j.ijsbe.2017.07.004

Fernandez, R., Ruiz, A. I., & Cuevas, J. (2016). Formation of C-A-S-H phases from the interaction between concrete or cement and bentonite. *Clay Minerals*, *51*(2), 223-235. https://doi.org/10.1180/claymin.2016.051.2.09

Ganesan, K., Rajagopal, K., & Thangavel, K. (2008). Rice husk ash blended cement: Assessment of optimal level of replacement for strength and permeability properties of concrete. *Construction and Building Materials*, *22*(8), 1675-1683. https://doi.org/https://doi.org/10.1016/j.conbuildmat.2007.06.011

Gill, A. S., & Siddique, R. (2018). Durability properties of self-compacting concrete incorporating metakaolin and rice husk ash. *Construction and Building Materials*, *176*, 323-332. https://doi.org/10.1016/j.conbuildmat.2018.05.054

Gómez, M. I. S. d. R., & Rojas, M. F. (2013). 4 - Natural pozzolans in eco-efficient concrete. In F. Pacheco-Torgal, S. Jalali, J. Labrincha, & V. M. John (Eds.), *Eco-Efficient Concrete* (pp. 83-104). Woodhead Publishing. https://doi.org/https://doi.org/10.1533/9780857098993.2.83

Hamada, H. M., Jokhio, G. A., Al-Attar, A. A., Yahaya, F. M., Muthusamy, K., Humada, A. M., & Gul, Y. (2020). The use of palm oil clinker as a sustainable construction material: A review. *Cement & Concrete Composites*, *106*, 19, https://doi.org/10.1016/j.cemconcomp.2019.103447

Hamada, H. M., Yahaya, F. M., Muthusamy, K., Jokhio, G. A., & Humada, A. M. (2019). Fresh and hardened properties of palm oil clinker lightweight aggregate concrete incorporating Nano-palm oil fuel ash. *Construction and Building Materials*, *214*, 344-354. https://doi.org/10.1016/j.conbuildmat.2019.04.101

Hou, D. S., Ma, H. Y., & Li, Z. J. (2015). Morphology of calcium silicate hydrate (C-S-H) gel: a molecular dynamic study. *Advances in Cement Research*, *27*(3), 135-146. https://doi.org/10.1680/adcr.13.00079

Hu, L. L., He, Z., & Zhang, S. P. (2020). Sustainable use of rice husk ash in cement-based materials: Environmental evaluation and performance improvement. *Journal of Cleaner Production*, *264*, 14, https://doi.org/10.1016/j.jclepro.2020.121744

Hu, Y., Diao, L., Lai, Z. Y., He, Y. J., Yan, T., He, X., Wu, J., Lu, Z. Y., & Lv, S. Z. (2019). Effects of bentonite on pore structure and permeability of cement mortar. *Construction and Building Materials*, *224*, 276-283. https://doi.org/10.1016/j.conbuildmat.2019.07.073

Huda, M. N., Jumaat, M. Z., Islam, A., & Al-Kutti, W. A. (2018). Performance of high strength lightweight concrete using palm wastes. *Engineering Journal*, *19*(2), 30-42. https://doi.org/10.31436/iiumej.v19i2.919

Innovation in Raw Materials and Primary Industries Division. (2020). *Construction aggregate reserve in Thailand*. http://www.dpim.go.th/qry-stones/quarry3.php

Isberto, C. D., Labra, K. L., Landicho, J. M., & De Jesus, R. (2021). Effect of rice husk ash and crumb waste rubber tires to microstructure and strength of concrete. *International Journal of Geomate*, *20*(79), 16-21. https://doi.org/10.21660/2021.79.6196

Ismail, A. H., Kusbiantoro, A., Chin, S. C., Muthusamy, K., Islam, M., & Tee, K. F. (2020). Pozzolanic reactivity and strength activity index of mortar containing palm oil clinker pretreated with hydrochloric acid. *Journal of Cleaner Production*, *242*, 10, https://doi.org/10.1016/j.jclepro.2019.118565

Jamil, M., Khan, M. N. N., Karim, M. R., Kaish, A. B. M. A., & Zain, M. F. M. (2016). Physical and chemical contributions of rice husk ash on the properties of mortar. *Construction and Building Materials*, *128*, 185-198. https://doi.org/https://doi.org/10.1016/j.conbuildmat.2016.10.029

Jeong, Y., Park, H., Jun, Y., Jeong, J. H., & Oh, J. E. (2016). Influence of slag characteristics on strength development and reaction products in a CaO-activated slag system. *Cement & Concrete Composites*, *72*, 155-167. https://doi.org/10.1016/j.cemconcomp.2016.06.005

Joshaghani, A., & Moeini, M. A. (2018). Evaluating the effects of sugarcane-bagasse ash and rice-husk ash on the mechanical and durability properties of mortar. *Journal of Materials in Civil Engineering*, *30*(7), 14, https://doi.org/10.1061/(asce)mt.1943-5533.0002317

Kabir, S. M. A., Alengaram, U. J., Jumaat, M. Z., Yusoff, S., Sharmin, A., & Bashar, II. (2017). Performance evaluation and some durability characteristics of environmental friendly palm oil clinker based geopolymer concrete. *Journal of Cleaner Production*, *161*, 477-492. https://doi.org/10.1016/j.jclepro.2017.05.002

Kanadasan, J., Fauzi, A. F. A., Razak, H. A., Selliah, P., Subramaniam, V., & Yusoff, S. (2015). Feasibility studies of palm oil mill waste aggregates for the construction industry. *Materials*, *8*(9), 6508-6530. https://doi.org/10.3390/ma8095319

Kanadasan, J., Razak, H. A., & Subramaniam, V. (2018). Properties of high flowable mortar containing high volume palm oil clinker (POC) fine for eco-friendly construction. *Journal of Cleaner Production*, *170*, 1244-1259. https://doi.org/10.1016/j.jclepro.2017.09.068

Kannan, V., & Ganesan, K. (2016). Effect of tricalcium aluminate on durability properties of self-compacting concrete incorporating rice husk ash and metakaolin. *Journal of Materials in Civil Engineering*, *28*(1), https://doi.org/10.1061/(asce)mt.1943-5533.0001330

Karim, M. R., Chowdhury, F. I., Zabed, H., & Saidur, M. R. (2018). Effect of elevated temperatures on compressive strength and microstructure of cement paste containing palm oil clinker powder. *Construction and Building Materials*, *183*, 376-383. https://doi.org/10.1016/j.conbuildmat.2018.06.147

Karim, M. R., Hashim, H., Abdul Razak, H., & Yusoff, S. (2017). Characterization of palm oil clinker powder for utilization in cement-based applications. *Construction and Building Materials*, *135*, 21-29. https://doi.org/https://doi.org/10.1016/j.conbuildmat.2016.12.158

Khan, K., Ullah, M. F., Shahzada, K., Amin, M. N., Bibi, T., Wahab, N., & Aljaafari, A. (2020). Effective use of micro-silica extracted from rice husk ash for the production of high-performance and sustainable cement mortar. *Construction and Building Materials*, *258*, https://doi.org/10.1016/j.conbuildmat.2020.119589

Khan, W., Shehzada, K., Bibi, T., Ul Islam, S., & Wali Khan, S. (2018). Performance evaluation of Khyber Pakhtunkhwa Rice Husk Ash (RHA) in improving mechanical behavior of cement. *Construction and Building Materials*, *176*, 89-102. https://doi.org/https://doi.org/10.1016/j.conbuildmat.2018.04.213

Kueaket, K., & Tonnayopas, D. (2018). Enhanced properties of palm oil boiler clinker concrete with Sang Yod rice husk ash. *Journal of Advanced Research in Applied Mechanics* *51*(1), 10-19.

Kunchariyakun, K., Asavapisit, S., & Sombatsompop, K. (2015). Effect of fine Al-containing waste in autoclaved-aerated concrete incorporating rice-husk ash. *Journal of Materials in Civil Engineering*, *27*(8), https://doi.org/10.1061/(asce)mt.1943-5533.0001149

Kumar, V. V. P., & Prasad, D. R. (2019). Influence of supplementary cementitious materials on strength and durability characteristics of concrete. *Advances in Concrete Construction*, *7*(2), 75-85. https://doi.org/10.12989/acc.2019.7.2.075

Laidani, Z. E., Benabed, B., Abousnina, R., Gueddouda, M. K., & Kadri, E. (2020). Experimental investigation on effects of calcined bentonite on fresh, strength and

durability properties of sustainable self- compacting concrete. *Construction and Building Materials*, *230*, 11, https://doi.org/10.1016/j.conbuildmat.2019.117062

Lee, H. H., Wang, C. W., & Chung, P. Y. (2021). Experimental study on the strength and durability for slag cement mortar with bentonite. *Applied Sciences- Basel*, *11*(3), https://doi.org/10.3390/app11031176

Liu, M. L., Hu, Y., Lai, Z. Y., Yan, T., He, X., Wu, J., Lu, Z. Y., & Lv, S. Z. (2020). Influence of various bentonites on the mechanical properties and impermeability of cement mortars. *Construction and Building Materials*, *241*, 12, https://doi.org/10.1016/j.conbuildmat.2020.118015

Liu, R., Pang, B., Zhao, X., & Yang, Y. (2020). Effect of rice husk ash on early hydration behavior of magnesium phosphate cement. *Construction and Building Materials*, *263*, 120180. https://doi.org/https://doi.org/10.1016/j.conbuildmat.2020.120180

Lucas, J., de Brito, J., Veiga, R., & Farinha, C. (2016). The effect of using sanitary ware as aggregates on rendering mortars' performance. *Materials & Design*, *91*, 155- 164. https://doi.org/10.1016/j.matdes.2015.11.086

Lv, X. D., Dong, Y., Wang, R. K., Lu, C., & Wang, X. B. (2020). Resistance improvement of cement mortar containing silica fume to external sulfate attacks at normal temperature. *Construction and Building Materials*, *258*, https://doi.org/10.1016/j.conbuildmat.2020.119630

Ma, B. G., Wang, Y. B., & Fu, H. B. (2014). Effect of rice husk ash on the thaumasite form of sulfate attack of cement- based materials. *Arabian Journal for Science and Engineering*, *39*(12), 8517-8524. https://doi.org/10.1007/s13369-014-1414-y

Man, X. Y., Haque, M. A., & Chen, B. (2019). Engineering properties and microstructure analysis of magnesium phosphate cement mortar containing bentonite clay. *Construction and Building Materials*, *227*, https://doi.org/10.1016/j.conbuildmat.2019.08.037

Martínez-Lage, I., Vázquez-Burgo, P., & Velay-Lizancos, M. (2020). Sustainability evaluation of concretes with mixed recycled aggregate based on holistic approach: Technical, economic and environmental analysis. *Waste Management*, *104*, 9- 19. https://doi.org/10.1016/j.wasman.2019.12.044

Masood, B., Elahi, A., Barbhuiya, S., & Ali, B. (2020). Mechanical and durability performance of recycled aggregate concrete incorporating low calcium bentonite. *Construction and Building Materials*, *237*, 117760. https://doi.org/https://doi.org/10.1016/j.conbuildmat.2019.117760

Memon, S. A., Arsalan, R., Khan, S., & Lo, T. Y. (2012). Utilization of Pakistani bentonite as partial replacement of cement in concrete. *Construction and Building Materials*, *30*, 237-242. https://doi.org/https://doi.org/10.1016/j.conbuildmat.2011.11.021

Mesboua, N., Benyounes, K., & Benmounah, A. (2018). Study of the impact of bentonite on the physico‐mechanical and flow properties of cement grout. *Cogent Engineering*, *5*(1), https://doi.org/10.1080/23311916.2018.1446252

Ministry of commerce. (2020). *Rice mills in Thailand*. https://www.moc.go.th/index.php/rice-service-all/category/category-product007.html

Mirza, J., Riaz, M., Naseer, A., Rehman, F., Khan, A. N., & Ali, Q. (2009). Pakistani bentonite in mortars and concrete as low cost construction material. *Applied Clay Science*, *45*(4), 220-226. https://doi.org/https://doi.org/10.1016/j.clay.2009.06.011

Mohseni, E., Yazdi, M. A., Miyandehi, B. M., Zadshir, M., & Ranjbar, M. M. (2017). Combined effects of metakaolin, rice husk ash, and polypropylene fiber on the engineering properties and microstructure of mortar. *Journal of Materials in Civil Engineering*, *29*(7). https://doi.org/10.1061/(asce)mt.1943-5533.0001867

Monteny, J., Vincke, E., Beeldens, A., De Belie, N., Taerwe, L., Van Gemert, D., & Verstraete, W. (2000). Chemical, microbiological, and in situ test methods for biogenic sulfuric acid corrosion of concrete. *Cement and Concrete Research*, *30*(4), 623-634. https://doi.org/https://doi.org/10.1016/S0008-8846(00)00219-2

Muthusamy, K., Mirza, J., Zamri, N. A., Hussin, M. W., Majeed, A., Kusbiantoro, A., & Budiea, A. M. A. (2019). Properties of high strength palm oil clinker lightweight concrete containing palm oil fuel ash in tropical climate. *Construction and Building Materials*, *199*, 163-177. https://doi.org/10.1016/j.conbuildmat.2018.11.211

Nayaka, R. R., Alengaram, U. J., Jumaat, M. Z., Yusoff, S. B., & Ganasan, R. (2019). Performance evaluation of masonry grout containing high volume of palm oil industry by‐products. *Journal of Cleaner Production*, *220*, 1202-1214. https://doi.org/10.1016/j.jclepro.2019.02.134

Neville, A. M., & Brooks, J. J. (2010). *Concrete technology* (2 ed.). Pearson Education Limited.

Office of Agricultural Economics. (2020). *Agricultural economics in Thailand*. http://www.oae.go.th/view/1/%E0%B8%82%E0%B9%89%E0%B8%AD%E0%B8%A1

Ong, S. K., Mo, K. H., Alengaram, U. J., Jumaat, M. Z., & Ling, T. C. (2018). Valorization of wastes from power plant, steel-making and palm oil industries as partial sand substitute in concrete. *Waste and Biomass Valorization*, *9*(9), 1645-1654. https://doi.org/10.1007/s12649-017-9937-6

Qureshi, L. A., Ali, B., & Ali, A. (2020). Combined effects of supplementary cementitious materials (silica fume, GGBS, fly ash and rice husk ash) and steel fiber on the hardened properties of recycled aggregate concrete. *Construction and Building Materials*, *263*, https://doi.org/10.1016/j.conbuildmat.2020.120636

Raheem, A. A., & Kareem, M. A. (2017). Chemical composition and physical characteristics of rice husk ash blended cement. *International Journal of Engineering Research in Africa*, *32*, 25-35. https://doi.org/10.4028/www.scientific.net/JERA.32.25

Rehman, S. U., Kiani, U. A., Yaqub, M., & Ali, T. (2020). Controlling natural resources depletion through Montmorillonite replacement for cement-low cost construction. *Construction and Building Materials*, *232*, 9, https://doi.org/10.1016/j.conbuildmat.2019.117188

Rong, Z. D., Ding, J. Y., Cui, Z. J., & Sun, W. (2019). Mechanical properties and microstructure of ultra-high performance cement-based composite incorporating RHA. *Advances in Cement Research*, *31*(10), 472-480. https://doi.org/10.1680/jadcr.17.00209

Sandhu, R. K., & Siddique, R. (2017). Influence of rice husk ash (RHA) on the properties of self-compacting concrete: A review. *Construction and Building Materials*, *153*, 751-764. https://doi.org/10.1016/j.conbuildmat.2017.07.165

Saghiri, M. A., Orangi, J., Asatourian, A., Gutmann, J. L., Garcia-Godoy, F., Lotfi, M., & Sheibani, N. (2017). Calcium silicate-based cements and functional impacts of various constituents. *Dental Materials Journal, 36*(1), 8-18. https://doi.org/10.4012/dmj.2015-425

Santhanam, M., Cohen, M. D., & Olek, J. (2003). Mechanism of sulfate attack: a fresh look Part 2. Proposed mechanisms. *Cement and Concrete Research, 33*(3), 341-346, https://doi.org/10.1016/s0008-8846(02)00958-4

Sata, V., Sathonsaowaphak, A., & Chindaprasirt, P. (2012). Resistance of lignite bottom ash geopolymer mortar to sulfate and sulfuric acid attack. *Cement and Concrete Composites, 34*(5), 700-708. https://doi.org/https://doi.org/10.1016/j.cemconcomp.2012.01.010

Sha, F., Li, S. C., Liu, R. T., Li, Z. F., & Zhang, Q. S. (2018). Experimental study on performance of cement-based grouts admixed with fly ash, bentonite, superplasticizer and water glass. *Construction and Building Materials, 161*, 282-291. https://doi.org/10.1016/j.conbuildmat.2017.11.034

Siddika, A., Mamun, M. A. A., Alyousef, R., & Mohammadhosseini, H. (2020). State-of-the-art-review on rice husk ash: A supplementary cementitious material in concrete. *Journal of King Saud University - Engineering Sciences*. https://doi.org/https://doi.org/10.1016/j.jksues.2020.10.006

Shakir, A. A., Ibrahim, M. H. W., Othman, N. H., & Shahidan, S. (2019). The effect of palm oil clinker and oil palm shell on the compressive strength of concrete. *Iranian Journal of Science and Technology- Transactions of Civil Engineering, 43*, 1-14. https://doi.org/10.1007/s40996-018-0176-2

Sharma, K., & Kumar, A. (2021). Influence of rice husk ash, lime and cement on compaction and strength properties of copper slag. *Transportation Geotechnics, 27*, https://doi.org/10.1016/j.trgeo.2020.100464

Siddique, R., Singh, M., & Jain, M. (2020). Recycling copper slag in steel fibre concrete for sustainable construction. *Journal of Cleaner Production, 271*, 10, https://doi.org/10.1016/j.jclepro.2020.122559

Suan, J. D., Datta, A., & Salam, P. A. (2017). Effect of oil palm fly ash on soil properties and yield of sweet corn in the tropical zone of thailand. *Communications in Soil Science and Plant Analysis, 48*(2), 236-244. https://doi.org/10.1080/00103624.2016.1269791

Sua-Iam, G., Makul, N., Cheng, S. S., & Sokrai, P. (2019). Workability and compressive strength development of self-consolidating concrete incorporating rice husk ash and

foundry sand waste - A preliminary experimental study. *Construction and Building Materials*, *228*, https://doi.org/10.1016/j.conbuildmat.2019.116813

Sua-iam, G., Sokrai, P., & Makul, N. (2016). Novel ternary blends of Type 1 Portland cement, residual rice husk ash, and limestone powder to improve the properties of self-compacting concrete. *Construction and Building Materials*, *125*, 1028- 1034. https://doi.org/10.1016/j.conbuildmat.2016.09.002

Subashi De Silva, G. H. M. J., Vishvalingam, S., & Etampawala, T. (2021). Effect of waste rice husk ash from rice husk fuelled brick kilns on strength, durability and thermal performances of mortar. *Construction and Building Materials*, *268*, 121794. https://doi.org/https://doi.org/10.1016/j.conbuildmat.2020.121794

Sujivorakul, C., Jaturapitakkul, C., & Taotip, A. (2011). Utilization of fly ash, rice husk ash, and palm oil fuel ash in glass fiber- reinforced concrete. *Journal of Materials in Civil Engineering*, *23*(9), 1281-1288. https://doi.org/10.1061/(asce)mt.1943-5533.0000299

Suriyachoto, J. & Tonnayopas, D. (2013). *Development of chloride testing equipment for concrete.* [Senior project, Prince of Songkhla University].

Tafraoui, A., Escadeillas, G., & Vidal, T. (2016). Durability of the ultra high performances concrete containing metakaolin. *Construction and Building Materials*, *112*, 980- 987. https://doi.org/10.1016/j.conbuildmat.2016.02.169

Targan, S., Olgun, A., Erdogan, Y., & Sevinc, V. (2002). Effects of supplementary cementing materials on the properties of cement and concrete. *Cement and Concrete Research*, *32*(10), 1551-1558, https://doi.org/10.1016/s0008-8846(02)00831-1

Thai Rice Exporters Association. (2020). http://www.thairiceexporters.or.th/production.htm

Thailand rural roads standard. 231- 2562. (2019). Concrete pavement. In. Thailand: Department of rural roads.

Tonnayopas, D., & Jitnukul, K. (2013). Effect of sang yod rice husk ash on songkhla lake gravel gap-graded aggregate concrete. *Srinakharinwirot Engineering Journal*, *8*(2), 62-69.

Velde, B. (1992). *Introduction to clay minerals*. Chapman & Hall.

Venkatanarayanan, H. K., & Rangaraju, P. R. (2014). Evaluation of sulfate resistance of portland cement mortars containing low- carbon rice husk ash. *Journal of Materials in*

Civil Engineering, *26*(4), 582-592. https://doi.org/10.1061/(asce)mt.1943-5533.0000868

Venkatanarayanan, H. K., & Rangaraju, P. R. (2015). Effect of grinding of low-carbon rice husk ash on the microstructure and performance properties of blended cement concrete. *Cement & Concrete Composites*, *55*, 348-363. https://doi.org/10.1016/j.cemconcomp.2014.09.021

Wei, J. Q., & Gencturk, B. (2019). Hydration of ternary Portland cement blends containing metakaolin and sodium bentonite. *Cement and Concrete Research*, *123*, https://doi.org/10.1016/j.cemconres.2019.05.017

Yu, Q., Sawayama, K., Sugita, S., Shoya, M., & Isojima, Y. (1999). The reaction between rice husk ash and $Ca(OH)_2$ solution and the nature of its product. *Cement and Concrete Research*, *29*(1), 37-43. https://doi.org/https://doi.org/10.1016/S0008-8846(98)00172-0

Zhou, Y., Wang, G. H., & Yuan, Y. F. (2020). Basic properties and engineering application of bentonite-cement-water glass grouting. *KSCE Journal of Civil Engineering*, *24*(9), 2742-2750. https://doi.org/10.1007/s12205-020-1928-7

APPENDIX A

Proceeding 1

The 7th International Conference on Applied Sciences and Engineering (ICASEA, 2018),

December 8-9, 2018, TH Hotel, Kota Kinabalu, Sabah, Malaysia

(e-ISBN: 978-967-15744- 6-1)

Kueaket, K., & Tonnayopas, D. (2018). Enhanced properties of palm oil boiler clinker concrete with Sang Yod rice husk ash. *Proceeding of 7th International Conference on Applied Sciences and Engineering (ICASEA, 2018)*, Kota Kinabalu, Sabah, Malaysia, 29-38.

ENHANCED PROPERTIES OF PALM OIL BOILER CLINKER CONCRETE WITH SANG YOD RICE HUSK ASH

Kamolchanok Kueaket[1], Danupon Tonnayopas[1]

[1]Faculty of Engineering, Department of Mining and Materials Engineering, Prince of Songkla University, Thailand.

Abstract: *Laboratory experiments of this investigation are to reclaim palm oil boiler clinker (POBC) as coarse aggregate for concrete and partially replaced Portland cement type 1 with Sang Yod rice husk ash (SYRHA) in proportion of 10%, 20% and 30wt.%. Characterization of POBC aggregate was carried out on grain size distribution and shape analysis, specific gravity, loose and compacted bulk density, water absorption, organic impurity, aggregate impact value and Los Angeles abrasion. Each mixing specimen was kept water to binder ratio at 0.42 throughout this study and varied duration of curing in water for 7, 28 and 56 days. The properties of paste and harden cube concrete in size 10×10×10 cm including setting time, bulk density, water absorption and compressive strength and were determined. According to aggregate testing results indicated that POBC was met the specification of normal-weight aggregate. Addition of SYRHA decreased both setting time and hydration temperature of paste. Furthermore, concrete contained 20% SYRHA provided highest 56-day compressive strength of 53.12 MPa and increased water absorption of 5.27%.*

Keywords: Palm Oil Boiler Clinker Aggregate, Sang Yod Rice Husk Ash, Pozzolanic, Eco-friendly Concrete

Introduction

Palm Oil Boiler Clinker (POBC) was a by-product from palm oil mill and it is defined as kind of non-hazardous waste material (Ahmad & Noor, 2007). In the southern part of Thailand, The disposal of POBC has been unidentified and only used for landfill. The origin of POBC was made during the combustion and cooling down process with various condition depended on the mill. For a few decade, POBC were often used as a coarse and fine aggregate replacement in lightweight concrete produced (Mannan & Neglo, 2010; Abutaha, Rasak, & Kanadasan, 2016; Ahmmad et al, 2017; Karim et al, 2017). The mix design of concrete containing POBC was different from others normal aggregate according to their porous and rough surface texture characteristics. Thus, Mannan & Neglo (2010) were investigated the suitable mix design for POBC concrete. They were found that using POBC as coarse aggregate replacement with maximum size at 20 mm including Ordinary Portland cement (OPC), sand, and superplasticizer at w/c ratio 0.48-0.60 and cure in tap water for 28 days. Which can provide the compressive strength in range of 27-35 MPa. Perversely, Abutaha et al. (2016) was produced concrete containing POBC as partial coarse aggregate replacement at 10%, 20%, 40%, 60 and 100%. The compressive strength and hardened density of POBC concrete were obtained in the range of 33–49 MPa and 2074–2358 kg/m³ at 28 days, respectively. Moreover, it provided the compressive strength to 33 MPa with 100% coarse aggregate replacement by POBC. Thus, POBC has a good potential to replace natural aggregates, making it suitable to

be used in concrete (Mannan & Neglo, 2010; Abutaha, Rasak, & Kanadasan, 2016; Ahmmad et al, 2017; Karim et al, 2017). According to several researches have been investigated, There are some weak points of using POBC as aggregates that were reported from Abutaha et al. (2017); Ibrahim et al. (2016); Shafigh et al. (2014). The increasing of POBC in concrete as both coarse and fine aggregate reduces the slump and workability in fresh concrete. But only POBC coarse aggregate reduces strength value. Therefore, this research aims to enhance the POBC concrete properties with Song Yod rice husk ash (SYRHA) which was waste of rice husk derived from the rice products from Phattalung, Thailand. It also has a slim grain, dark red pericarp, soft and aromatic of cooked rice as well as nutritional enrich (Banchuen et al, 2009). As wildly usage of rice husk ash (RHA), which is beneficial in many way to concrete i.e. increase the compressive strength and reduce the corrosion deterioration (Gastaldini et al, 2010). In addition, SYRHA was characterized in chemical composition and strength activity index (SAI) of gravel gap-graded aggregate concrete by Tonnayopas & Jitmukul (2013) and met the specification of ASTM C618-12a and D5370-14. Thus, in this experimental investigation to evaluate into suitability of POBC coarse aggregate and SYRHA as a complement for green concrete.

Materials and experimental procedures

To carry out this experiment the concrete mix design are following material were used OPC type I according to ASTM C 150, palm oil boiler clinker coarse aggregate (POBCCA) regarded with sieving size between 4.75-12.5 mm, fine aggregate used river sand with fineness modulus of 3.15. The SYRHA powder particles was used as OPC partial replacement at mean particle size 16.7 microns according to Fritsch-Analysette 22 Nanotec laser particle analyser. The particle size distribution of all materials used are illustrated in Figure 1.
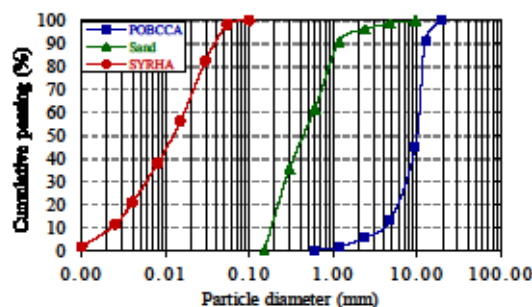
Figure 1: Particle size distribution of materials used in this study

Palm Oil Boiler Clinker Coarse Aggregate

POBC samples in this study were collected from a palm oil factory in Surat Thani, Thailand. It was obtained from the combustion of fibres, seeds and shells of palms after oil extraction process as a fuel for boiler. This combustion process will be taken time for 6-12 h at the range of temperature from 700 to 1200 °C after cooling down. The POBC is 90% greenish grey, 5-10% black and 3-1% pinkish brown color, sintered, vesicular texture with unidirectional and unconnected porous (bubble-shaped localities) because of rapid cooling down, irregular shape,

brittle edges and exposed in large lumps within 95-70 cm as shown in Figure 2(a). The POBC was washed and air-dried for one week then crushed within size less than 12.5 mm as shown in Figure 2(b).

Figure 2: POBC sample (a) lumps and (b) aggregate used

The chemical composition of POBC was also analysed via X-ray fluorescence (XRF) and tabulated on Table 1. It composed of dominant SiO_2, and moderate of CaO, K_2O, P_2O_5 and MgO contents, respectively. Particularly, loss on ignition (LOI) is very low or negligible. According to microstructure analysis, found that the evidence of POBC occurrence is similarly to "aa" lava or metal slag. The morphology of POBC- under scanning electron microscope (SEM) revealed slightly smooth concave surface with brittle fracture and thermal crack and depicted frame in Figure 3(a). It also observed clearly spherical particles cluster of silica component "Si" (Figure 3(b)).
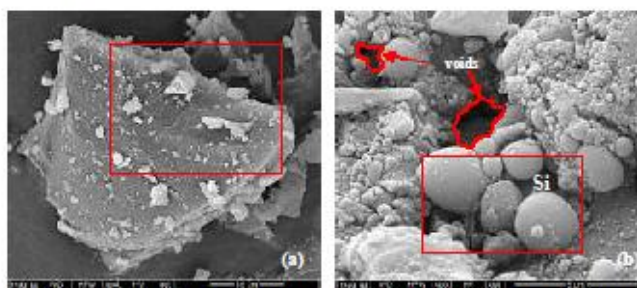
Figure 3: SEM photomicrograph of POBC (a) slightly smooth concave surface with crack trace and (b) enlargement of silica particles and small void spaces

The aggregate properties of POBC used as coarse aggregate were preliminary tests performed including grain size distribution, specific gravity and water absorption, (ASTM C127-15), loose and compacted bulk density (ASTM C29/C29M-17a), organic impurity (C40/C40M-16), aggregate impact value and Los Angeles abrasion (ASTM C535-16).

Sang Yod rice husk ash

The Sang Yod rice husk was collected from a local rice mill in Phattalung, Thailand. Then, it was burned into open-air condition by using recycled oil tank for 3-4 days (Figure 4a). Then later it was incinerated in an electrical furnace again at 700 °C for 1 h in order to reduce some

organic matter (Figure 4b). Then, grinding with jar mill for 12 h and sieved through 325 sieve mesh to obtain the final binder sample and kept in a container to prevent it from moisture. Its chemical composition result was analysed by XRF technique shown in Table 1.

Table 1: Chemical composition of POBC and SYRHA used for this study

Oxides (wt.%)	SiO_2	Al_2O_3	Fe_2O_3	MgO	P_2O_5	SO_3	K_2O	CaO	MnO	Others	LOI*
POBC	65.23	1.66	1.78	5.37	5.50	0.04	9.56	10.00	0.17	0.59	0.04
SYRHA	93.83	0.66	0.36	0.36	1.04	0.21	1.77	0.76	0.11	0.23	0.67

Figure 4: SYRHA after treatment processing of (a) open-air burned and (b) incinerated at 700 °C for 1 h

According to XRF analysis, the amount of $SiO_2+Al_2O_3+Fe_2O_3$ is greater beyond 70% and LOI is also less than 6%. In consequence, the SiO_2 contents of SYRHA is higher than Tonnayopas & Jitnukul (2013) due to the incinerated treatment process reduced unburned carbon. The XRF analysis also confirmed that SYRHA was met the threshold of artificial pozzolans in burnt materials type but cannot identify in any classes although its chemical composition was same as pozzolan definition but its evidence of occurrence was not according to ASTM C 618 and ASTM D 5370. Therefore, SYRHA was conformed to specified requirements of blended pozzolan for use in concrete and should be added to brand new type "RHA" of organic pozzolan in opportunity. The microstructure of SYRHA powder was analysed via SEM and can be noticed that the physical characteristic of SYRHA was a spherical shape and almost round (Figure 5(a)). Most particles size were in the range of 2.3-38 microns as shown in Figure 5(b), it effected on more surface area as observed on SEM image.
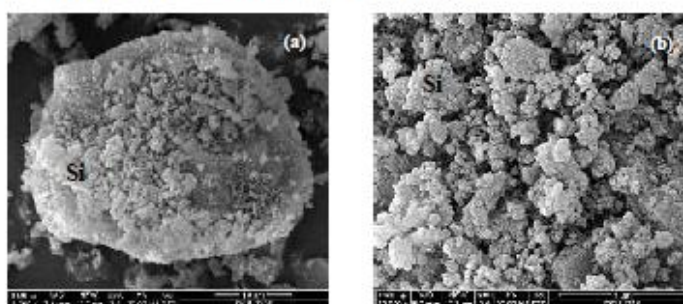
Figure 5: SEM photomicrograph of SYRHA (a) clusters and (b) spherical and rounded particle of silica

Specimen preparation and mix proportions

Whole investigated specimens were cast in cube with dimension of 100×100×100 mm. Then, the concrete mix designs were inspection on ACI 211.1-91 method to approach slump value between 35-50 mm and compressive strength at 35 MPa in 28 days as tabulated in Table 2. Mix proportions of specimens were designed by replacing OPC with SYRHA at 10, 20, 30wt.% and kept water to binder ratio at 0.42 throughout this study. The test specimens were stored in moist air for 24 h and after this period each specimens are marked and removed from the moulds then kept submerged in tap water until 7, 28, and 56 days and taken out to prior test. The various tests were carried out on paste and harden concrete specimens with standard procedures in ASTM specifications containing setting time ASTM C403/C403M-16), heat of hydration (ASTM C186-17), bulk density and water absorption according to ASTM C642-13, and compressive strength modified on ASTM C39/C39M-18.

Table 2: Mix batches of specimens

No.	Mix designation	w/b ratio	Mix containing (kg/m³)			
			OPC	Sand	POBCA	SYRHA
1	Control	0.42	500	1315	700	0
2	SYRHA10	0.42	450	1315	700	50
3	SYRHA20	0.42	400	1315	700	100
4	SYRHA30	0.42	350	1315	700	150

Results and discussions

The result of POBC coarse aggregate testing were tabulated in Table 3. It has coincided with several previous researches results even its physical appearances was not similarly i.e. color, texture but it has the highest specific gravity and lowest 24 h water absorption when compared to previous researches which are in the range of 1.67-1.8 and 2.7-5.4% respectively. (Ahmad & Noor, 2007; Abutaha, Rasak, & Kanadasan, 2016; Abutaha et al, 2017; Ahmmad et al, 2017).

Table 3: Summary of Aggregate Properties of POBC raw material used

Aggregate properties	Value
Specific gravity	2.16
Loose bulk density (kg/m³)	1013.69
Void (%)	39.66
Compacted bulk density (kg/m³)	1080.61
Void (%)	35.68
Water absorption (%)	
1 day	1.42
7 days	3.00
Organic impurity	None
Aggregate impact value (%)	37.30
Los Angeles abrasion (%)	28.30
Fineness modulus	5.42

Setting time and hydration temperature of paste

The initial and final setting times of OPC partial replacement by SYRHA at 10, 20 and 30% were tested gather with heat monitoring. The increasing SYRHA replacement effected directly on water demand due to ultrafine particles. The paste which contains high content of SYRHA signify less consistent than without SYRHA or control mix since after mixing with the same amount of water as shown in Figure 6(a). The Vicat penetration depth indicated that the increasing replacement level of SYRHA played the key role to decrease both initial and final setting time of paste due to pozzolanic reaction, high water demand and specific surface area. At 30% SYRHA replacement reduced initial and final setting time of paste down to 32% and 16% respectively when compared the result of control mix as depicted in Figure 6(b).
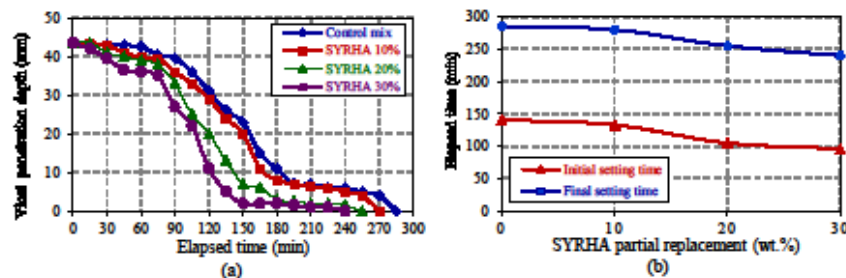
Figure 6: Effects of SYRHA partial replacement on (a) development of setting time behaviour and (b) interval duration of setting time

The hydration temperature of paste also decreased when increased replacement level of SYRHA due to reduce cement contents or tricalcium silicate (C_3S) and aluminate hydrated (C_3A) by SYRHA as shown in Figure 8. Concordantly, there are 3 factors controlled the heat of hydration including pozzolanic reaction, tricalcium silicate hydrated (C_3S) content and tricalcium aluminate hydrated content (Hewlet, 2003).
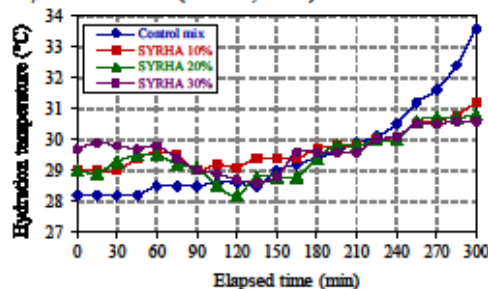
Figure 8: Effects of SYRHA on hydration temperature of paste

Bulk density

The POBC concrete at the ages of 56-day without SYRHA as a cement replacement can be achieved bulk density at 2205.81 kg/m³ (Figure 9) which is not significantly different from normal weight concrete densities owing to higher specific gravity of POBC coarse aggregate

than previous researches (Mannan & Neglo, 2010; Abutaha, Rasak, & Kanadasan, 2016; Ahmmad et al, 2017). The entire results have shown that increasing replacement level of SYRHA decreased the bulk density at all curing periods. As the result of OPC was replaced by SYRHA, bulk density of concrete also reduced. Conversely, the long term curing ages effected on increasing POBC concrete density by given more hydration process and condensation of concrete structure (Locher & Richartz, 1974).
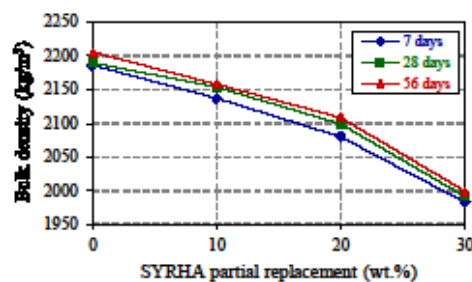
Figure 9: Effects of SYRHA on bulk density of POBC concrete at different ages

Water absorption

According to Figure 10, it can be represented that at 10% SYRHA replacement of OPC decreased water absorption of POBC concrete compared to control mix. It is represented the optimum usage for reduce porosity of POBC concrete as water absorption value calculated from the saturated water was taken place on void in concrete. Thence, further water absorption was gone beyond 10% SYRHA replacement of cement and depended on curing time in this study. In general, adding some pozzolans i.e. rice husk ask, fly ash and silica fume can be decreased pore size of concrete. In conversely on this study, due to SYRHA is particle usually absorption water, thus it may not be optimum for pozzolanic reaction and should not over grinding if using SYRHA to produce concrete for durability usage.
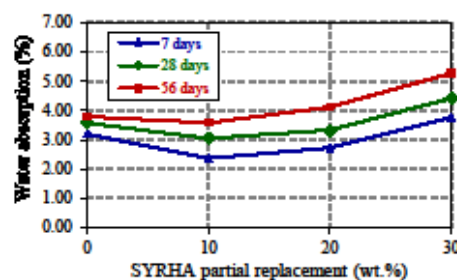
Figure 10: Effects of SYRHA on water absorption of POBC concrete at different ages

Compressive strength

Effect of OPC replacement by SYRHA on compressive strength was depicted Figure 11. All level of replacement performed higher strength at prolonger curing ages. At 20% SYRHA, the compressive strength of 56-day concrete was the highest of 53.12 MPa. The maximum strength

activity index (SAI) of 7, 28 and 56-day concrete were 116%, 113%, 109% at 10% and 20% SYRHA replacement, respectively. It can be implied that at 10% SYRHA was suitable for early strength development and at 20%SYRHA for late strength development since 28 days of curing ages. It can be noticed physical and mechanical properties of POBC concrete blended SYRHA had closely relationships.
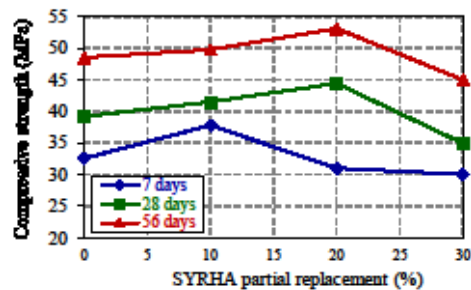
Figure 11: Effects of OPC replacement by SYRHA on compressive strength of POBC concrete at different ages

Conclusions

According to experimental results on this study can be delineated the POBC is classified into normal-weight aggregate and was available as coarse aggregate on concrete produced for other construction applications except heavy duty and pavement wearing surfaces. Chemical composition of SYRHA was met the specification of artificial pozzolans in burnt materials type. It is also reduced setting time, heat of hydration of paste and bulk density of POBC concrete. Considering as enhanced POBC concrete, 10% SYRHA replacement of OPC was significant developed the early strength and reduced water absorption of POBC concrete, benefit of 20% SYRHA replacement of OPC was provided satisfactory strength for long term of the curing ages of 28-day concrete.

Acknowledgement

References

Abutaha, F., Razak, H. A., & Ibrahim, H. A. (2017). Effect of Coating Palm Oil Clinker Aggregate on the Engineering Properties of Normal Grade Concrete. *Coatings, 7(10),* 175.

Abutaha, F., Razak, H. A., & Kanadasan, J. (2016). Effect of Palm Oil Clinker (POC) Aggregates on Fresh and Hardened Properties of concrete. *Construction and Building Materials, 112,* 416-423.

Ahmad, H. M., & Noor, M. N. (2007). *Physical properties of local palm oil clinker and fly ash.* Paper presented at the 1st Engineering Conference on Energy & Environment, Kuching, Sarawak, Malaysia.

Ahmmad, R., Alengaram, U. J., Jumaat, M. Z., Sulong, N. R., Yusuf M.O., & Rehman, M. A. (2017). Feasibility Study on the Use of High Volume Palm Oil Clinker Waste in Environmental Friendly Lightweight Concrete. *Construction and Building Materials, 135.* 94-103.

ASTM International. (2012). Standard Specification for Coal Fly Ash and Raw or Calcined Natural Pozzolan for Use in Concrete *(ASTM C618–12a).* West Conshohocken, PA: American Society for Testing and Materials.

ASTM International. (2015). Standard Test Method for Density, Relative Density (Specific Gravity), and Absorption of Coarse Aggregate *(ASTM C127-15).* West Conshohocken, PA: American Society for Testing and Materials.

ASTM International. (2016). Standard Test Method for Organic Impurities in Fine Aggregates for Concrete *(ASTM* C40/C40M-16*).* West Conshohocken, PA: American Society for Testing and Materials.

ASTM International. (2016). Standard Test Method for Resistance to Degradation of Large-Size Coarse Aggregate by Abrasion and Impact in the Los Angeles Machine *(ASTM C535-16).* West Conshohocken, PA: American Society for Testing and Materials.

ASTM International. (2016). Standard Test Method for Time of Setting of Concrete Mixtures by Penetration Resistance *(ASTM C403/C403M-16).* West Conshohocken, PA: American Society for Testing and Materials.

ASTM International. (2017). Standard Test Method for Bulk Density and Voids in Aggregate *(ASTM C29/C29M-17a).* West Conshohocken, PA: American Society for Testing and Materials.

ASTM International. (2017). Standard Test Method for Compressive Strength of Cylindrical Concrete Specimens *(ASTM C39/C39M-18).* West Conshohocken, PA: American Society for Testing and Materials.

ASTM International. (2017). Standard Test Method for Density, Absorption, and Voids in Hardened Concrete *(ASTM C642-13)*. West Conshohocken, PA: American Society for Testing and Materials.

ASTM International. (2017). Standard Test Method for Heat of Hydration of Hydraulic Cement *(ASTM C186-17)*. West Conshohocken, PA: American Society for Testing and Materials.

ASTM International. (2017). Standard Test Method for Time of Setting of Concrete Mixtures by Penetration Resistance *(ASTM C186-17)*. West Conshohocken, PA: American Society for Testing and Materials.

Banchuen, J., Thammarutwasik, P., Ooraikul, B., Wuttijumnong, P., & Sirivongpaisal, P. (2009). Effect of germinating processes on bioactive component of Sangyod Muang Phatthalung rice. *Thai J. Agric. Sci., 42*, 191-199.

Gastaldini, A. L., Isaia, G. C., Saciloto, A. P., Missau, F., & Hoppe, T. F. (2010). Influence of Curing time on the Chloride Penetration Resistance of Concrete Containing Rice Husk Ash: A technical and Economical Feasibility Study. *Cement and Concrete Composites, 32(10),* 783-793.

Givi, A. N., Rashid, S. A., Aziz, F. N. A., & Salleh, M. A. M. (2010). Assessment of the effects of rice husk ash particle size on strength, water permeability and workability of binary blended concrete. *Construction and Building Materials, 24(11),* 2145-2150.

Hewlett, P.C. (2003). *Lea's chemistry of cement and concrete.* Oxford, UK: Elsevier.

Ibrahim, A., & Razak, A. (2016). Effect of Palm Oil Clinker Incorporation on Properties of Pervious Concrete. *Construction and Building Materials, 115.* 70-77.

Karim, M. R., Hashim, H., Razak, H. A., & Yusoff, S. (2017). Characterization of palm oil clinker powder for utilization in cement-based applications. *Construction and Building Materials, 135,* 21-29.

Locher, R., & Richartz, W. (1974). Study of the hydration mechanism of cement. In Symposium on the chemistry of cement, Moscow.

Mannan, A., & Neglo, K. **(2010)** .Mix Design for Oil-Palm-Boiler Clinker (OPBC) Concrete. *Journal of Science and Technology (Ghana), .(1)30* 111-118.

Shafigh, P., Mahmud, B., Jumaat, B., Ahmmad, R., & Bahri, S. (2014). Structural Lightweight Aggregate Concrete Using two Types of Waste from the Palm Oil Industry as Aggregate. *Journal of Cleaner Production, 80,* 187-196.

Tonnayopas, D., & Jitnukul, K. (2013). Effect of Sang Yod Rice Husk Ash on Songkhla Lake Gravel Gap-Graded Aggregate Concrete. *SWU Engineering Journal, 8(2),* 73-80. (in Thai).

APPENDIX B

Proceeding 2

The 13th International Conference on Mining, Materials, and Petroleum Engineering
(CMMP 2019), June 13-14, 2019, Krabi, Thailand,

Kueaket, K., & Tonnayopas, D. (2019). Palm oil boiler clinker properties used as a green aggregate for construction. *Proceeding of the 13th International Conference on Mining, Materials, and Petroleum Engineering (CMMP 2019)*, Krabi, Thailand, 86-91.

PALM OIL BOILER CLINKER PROPERTIES USED
AS A GREEN AGGREGATE FOR CONSTRUCTION

Kamolchanok Kueaket[1] and Danupon Tonnayopas[1,*]

[1]*Department of Mining and Materials Engineering, Faculty of Engineering, Prince of Songkla University*
*Corresponding author's e-mail address: danupon.t@psu.ac.th

Abstract

This research are aimed to characterize the chemical and physical properties of POBC for construction material usage. The physical properties of POBC were tested including grading, fineness modulus, flakiness and elongate index, loosed and compacted bulk density, porosity, moisture content, water absorption, organic impurity, aggregate impact value, sodium sulfate soundness and Los Angeles abrasion. The chemical composition of POBC was analyzed by X-ray florescence technique. Moreover, microstructure of POBC was observed via scanning electron microscope. As the results found that the POBC was meant to be normal weight aggregate. The physical properties of POBC were also indicated that it can be used for concrete production. In addition, compressive strength of POBC concrete and mortar with constant 0.42 water to cement ratio were also found the 56-day POBC concrete and mortar can be provided the compressive strength up to 48.86 and 47.13 MPa.

Keywords: Palm Oil Boiler Clinker, Green Aggregate, Physical Properties

Introduction

The south part of Thailand are well-known for oil palm cultivating. The products of oil palm also have taken to process in the local mill to get palm oil. The palm oil extraction process has left many waste such as seed, shell, fiber etc. There are one part of the oil extraction process can reduce the fresh oil palm waste by turning the waste to fuel for boiler. The wastes were burned with high temperature and under pressure condition. The extensive burning and imminent cooling process of the stale shell and fibrous of palm oil inside boiler will originate the hardened and compacted materials call "Palm Oil Boiler Clinker" or POBC. Their sinter produces are greenish gray with some dark pink spot in color, unconnected vesicular texture and lightweight. The POBC was widely studied in Malaysia as a lightweight aggregate for concrete production. According to several previous studies, the POBC are often mentioned as a lightweight aggregate and only considering in term of lightweight aggregate replacement at different ratios [1]. Furthermore, the POBC properties were revealed by many Malaysian researches. Their chemical and physical properties can be varied according to the heterogeneous in compacted texture or others burning and cooling environmental conditions. The POBC samples used in this study are also different from others literature reviews in details of color, texture and their appearance. Particularly, Ahmmad et al., Ahmad et al., and Mannan and Neglo [2-4] gained the physical properties of POBC were carried out that their specific gravity was in the range of 1.7-2.2, density was in the range of 683-1,813.23 kg/cm^3 and water absorption was in the range of 1.79-2.67% Investigation using POBC as a coarse aggregate [3] were found the effective mix design for POBC concretes which were used POBC as coarse aggregate and mixed with OPC, river sand and super plasticizer at w/c ratio 0.48-0.60. Their mix design can be provided the 28-day compressive strength of POBC concrete in the range of 27-35 MPa. In addition, Abutaha et al. [1] used POBC as coarse aggregate for concrete also but their mix proportion were design by (DOE) method [1] and without adding water reducing agent. The compressive strength of 28-day POBC concrete were up to 33 MPa. Likewise, considered using POBC as fine aggregate, [6] replaced river sand with POBC in proportion of 5%, 10%, 15%, 20% and 25wt.% kept water to cement ratio at 0.45. It indicated that at beyond 20% replacement can cause the reduction in workability due to the less water absorption of POBC than normal fine aggregate. It may reduce the quality of mortar by formation of void and capillary cavity in mortar matrix due to low workability. Therefore, in Thailand, there were found POBC identically but still were not delineated for waste utilization. Meanwhile, this

research is focused on physical and chemical properties of POBC obtained from Thailand and the investigation on compressive strength of POBC concrete and mortar were contained a plain POBC coarse or fine aggregates.

Materials and methods
Palm Oil Boiler Clinker

POBC samples were collected from palm oil mill at Suratthani province, Thailand. As observation of morphological features. It is looked likely between crushed POBC and vesicular basalt collected from Buriram province (Figure 1). If considering only texture that were shown in Figure 1. In addition, the chemical composition of POBC [16] (Table 1) were mostly consist of SiO_2 65.23%, CaO 10.00% and K_2O 9.56%. Which were identically after Ahmmad et al., Ibrahim and Razak., and Karim et al. [1, 6, 7]

Table 1 Chemical Composition of POBC by XRF [16]

Oxides (wt.%)	SiO_2	Al_2O_3	Fe_2O_3	MgO	P_2O_5	SO_3	K_2O	CaO	MnO	Others	Loss on ignition
POBC	65.23	1.66	1.78	5.37	5.50	0.04	9.56	10.00	0.17	0.59	0.04
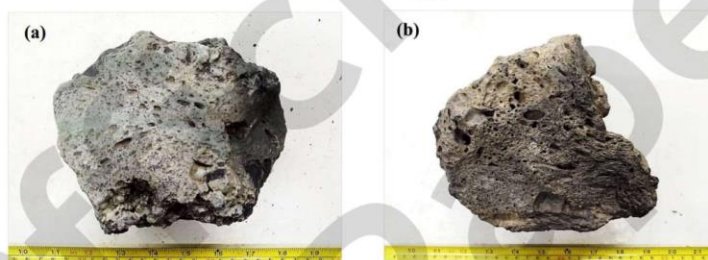
Figure 1 Comparison between (a) Large Lump of POBC and (b) Vesicular Basalt

Experimental testings

The POBC process generating might be as same as the origin of extrusive igneous rock. Aftermath palm oil extraction process was mill. The fibers and shells were left over. Then, it were taken to use as a fuel to generate the power for boiler. The combustion of remnant palm oil inside boiler will be operated under high pressure and temperature conditions for 16-18 h consecutively. After that it will be suddenly cooled down and became compacted and hardened. Before testing, the POBC were crushed into coarse aggregate (POBCCA) (> 4.75 mm) and fine aggregate (POBCFA) (< 4.75 mm) as shown in Figure 2. The aggregate properties of POBC were carried out in

Figure 2 Crushed POBC Used as (a) Coarse Aggregate (POBCCA) and (b) Fine Aggregate (POBCFA)

grading, fineness modulus, flakiness and elongate index, loosed and compacted bulk density, moisture content, water absorption, organic impurity, aggregate impact value, sodium sulfate soundness and Los Angeles abrasion were carried out according to ASTM test designation as tabulate in Table 2.

Table 2 Physical Properties Testing Designation

Characteristic	Significance	Test designation
Specific gravity	Mix design calculations	ASTM C 127 [8]
Loose and compacted bulk density	Mix design calculations; classification	ASTM C 29 [9]
Grading (sieve analysis)	Workability of fresh concrete; economy	ASTM C 136 [10]
Fineness modulus		
Flakiness and elongate index	Mix design calculations; classification	ASTM D 4791 [11]
Absorption and surface moisture	Control of concrete quality (water/cement ratio)	ASTM C 127 [8]
Organic impurity	Determine an organic of individual constituents materials	ASTM C 40 [12]
Aggregate impact value	Appropriately apply for aggregate application	ASTM C 353 [14]
Sodium sulfate soundness test		ASTM C 88 [13]
Resistance to abrasion and degradation	Index of aggregate quality	ASTM C 353 [14]

Preparation of concrete and mortar

Ordinary Portland cement, type 1 were used to mix with coarse and fine POBC. The POBC coarse aggregate concrete (POBCCA-Concrete) were investigated in the size of cube with dimension $100\times100\times100$ cm including with river sand, fineness modulus 3.15. The POBC fine aggregate mortar (POBCFA-Mortar) were investigated in the size of cube with dimension $50\times50\times50$ mm. The POBC concrete and mortar mix proportion were calculated and designed according to ACI method [15] to achieve 28-day compressive strength of 35 MPa by using constant 0.42 water to cement ratio as controlled factor, due to the compressive strength of concrete or mortar was inversely correlated with water content of mix proportion [17]. Furthermore, the water to cement ratio must be appropriate with the maximum size of POBCCA as 10 mm and fineness modulus of POBCFA as 3.74 that were conformed to ACI mix design method [15, 17]. Both POBC concrete and mortar were cured in tap water at ambient temperature (25 ± 5 °C and relative humidity 70-85%). The mix proportion of POBC concrete and mortar were tabulated in Table 3.

Table 3 POBC Concrete and Mortar Mix Design in This Study

No.	Mix designation	w/b ratio	Mix containing (kg/m³)			
			OPC	River sand	POBCA	POBCFA
1	POBCCA-Concrete	0.42	500	1,315	700	0
2	POBCFA-Mortar	0.42	250	0	0	450

Results and discussions
Microstructure of POBC

The microstructure of crushed POBC were found that it is large irregular shape Figure 3 a) and slightly smooth surface with some concave solidify fracture at the edge as was shown in Figure 3 b). Although many pores were observed when the POBC was not crushed as a bumpy surface. But literally, the photomicrograph images reveals that the POBC surface texture was smooth and rarely micro-pore with high surface area caused it contains lots of SiO_2 sintered amorphous particles. At figure 3 b) on the top right corner, there were largely conchoidal fractures similarly to quartz assumed that caused by rapid solidification process along shortly cooling down.

Gradation

Crushed POBC as a coarse aggregate or POBCCA was partially in the range between upper limit and lower limit. The fineness modulus of POBCCA is 5.58 which mean the maximum size of POBCCA is 12 mm and the

average particle size is 10 mm. Illustration shown in the red rectangle in Figure 4, The POBCCA was not well-graded and each of particle size was largely uniform grading curve. Nevertheless, using POBCCA for concrete must add sand to fill the void between poor-graded POBCCA particles and require more cement content due to poor-graded aggregate need more water to cement ratio. On the other hand, crushed POBC used as a fine aggregate or POBCFA was also fell partially into the range of upper limit and lower limit. The fineness modulus of POBCFA is 3.74 which is meant as a coarse sand. As shown in the blue line in Figure 4, the POBCCA was not well-graded and contained more coarse sand size. Which require more cement and water contents also. Additionally, both POBCCA and POBCFA are quite angular and irregular in shape.
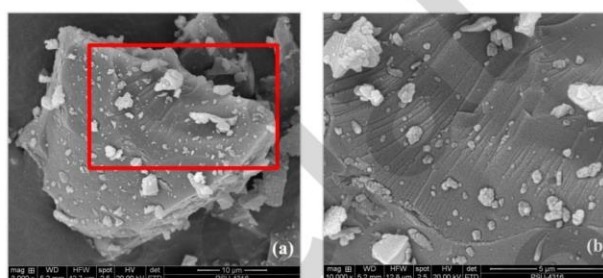
Figure 3 SEM Photograph of Crushed POBC (a) Irregular Shape [16] and (b) Magnification of Surface
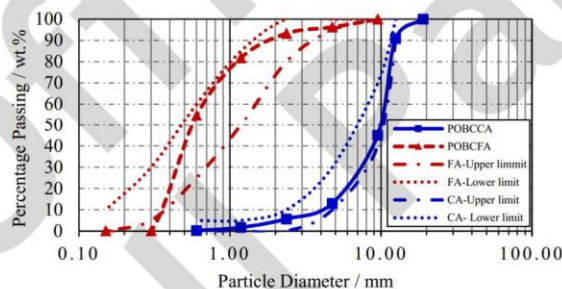
Figure 4 Grading Curve of POBCCA and POBCFA

Physical properties

Based on the testing result as tabulated in Table 4, the crushed POBC was not met in lightweight aggregate requirements specification on their specific gravity, density and weight. Moreover, porosity of crushed POBC was also low as approximately 5.59%. Percentage of voids in both loose and compacted bulk density were 39.66% and 35.68%, respectively which were represented of angular particle characteristics. The crushed POBC was rather flat after crushing process. The flakiness index of crushed POBC was in the high value as 66.62%. Which was gone beyond the requirement for 2 times. The flat or flaky particle would need more water and cement contents and caused bleeding as well. Although, the crushed POBC was satisfy in elongate index as 8.91%. The 1-and 7-day water absorption of crushed POBC were also low as 1.42% and 3.00%. Moreover, these kind of POBC was not contained harmful organic impurity. The sodium sulphate soundness test was also carried out for 5 cycles and found that it was 2.05% weight loss indicated high soundness. The aggregate impact value and loss angles abrasion were defined as the crushed POBC can be used for concrete.

Table 4 Result of Crushed POBC Coarse Aggregate Properties

Aggregate properties	Value	ASTM requirement
Specific gravity	2.16	Should be in the range of 1.8-2.9 as a normal weight aggregate [8]
Loose bulk density (kg/m³)	1,013.69	Should be equal or more than 880 kg/m³ as a
Void (%)	39.66	normal weight aggregate [9]
Compacted bulk density (kg/m³)	1,080.61	-
Void (%)	35.68	
Porosity (%)	5.59	-
Flakiness index (%)	66.62	Should not be exceeded than 35%
Elongate index (%)	8.91	for 35MPa concrete [11]
Water absorption (%)		For concrete application,
1 day	1.42	Should be less than 2% at 24-h absorption [8]
7 days	3.00	
Moisture content (%)	0.19	
Organic impurity	None	Should be none [12]
Soundness (%)	2.05	Should not be more than 12 % [13]
Aggregate impact value (%)	37.30	Suitable for subbase or other concrete work and should be avoid for structure or road surface [14]
Los Angeles abrasion (%)	37.98	Should not be exceed than 40 % Suitable for concrete [14]
Fineness modulus	5.58	For coarse aggregate, should be more than 5.5 [10]

Compressive strength

Compressive strength of both POBCCA concrete and POBCFA mortar were performed beyond the basic requirement designed by ACI method [15] at the age of 28-day which was 35 MPa. The compressive strength of 7-day POBCCA concrete and POBCFA mortar was 32.53 and 21.36 MPa, respectively. Both was increased approximately 20% and 33% after the age of 28-day and 56-day, respectively. Hence, the compressive strength of 28-and 56-day POBCCA concrete and POBCFA mortar were provided 39.50 MPa, 39.82 MPa, 48.86 MPa and 47.13 MPa, respectively. It shown that curing aging was effected to develop compressive strength of POBC specimens.
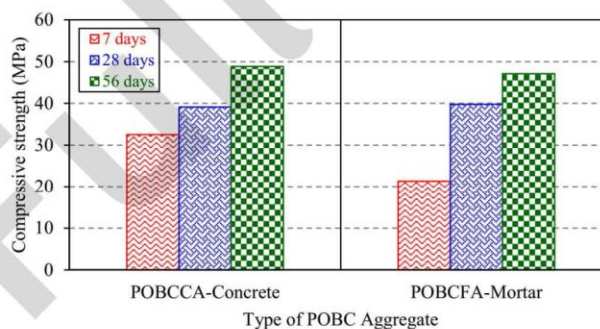
Figure 5 Compressive Strength of (a) POBCCA Concrete and (b) POBCFA Mortar at Different Curing Ages

Conclusions

According to the physical properties and morphology analysis under scanning electron microscope, it can be identified that POBC was a normal weight aggregate. The characteristics of shape and texture of POBC were angular and flaky after crushing. Thus, utilization of POBC as an aggregate must be given precedence to the suitable water and cement contents in order to get the best POBC concrete or mortar quality. Moreover, based on the tested results, the POBC aggregate is recommend for eco- or green- concrete works which is not satisfied into heavy duty, structural or surface pavement. The compressive strength of 56-day POBC concrete and mortar, obtained from this investigation, were 48.86 MPa and 47.13 MPa respectively. Hence, POBC aggregate can be the alternative green aggregate source using for eco-concrete application as well.

Acknowledgements

References

[1] Abutaha, F., Razak, H. A., & Kanadasan, J. (2016). Effect of palm oil clinker (POC) aggregates on fresh and hardened properties of concrete. *Construction and building materials, 112,* 416-423.

[2] Ahmmad, R., Jumaat, M. Z., Alengaram, U. J., Bahri, S., Rehman, M. A., & bin Hashim, H. (2016). Performance evaluation of palm oil clinker as coarse aggregate in high strength lightweight concrete. *Journal of cleaner production*, *112,* 566-574.

[3] Ahmad, M. H., Mohd, S., & Noor, N. M. (2007, December). *Mechanical properties of palm oil clinker concrete.* Paper presented at the 1st engineering conference on energy and environment, Sarawak, Malaysia

[4] Mannan, A., & Neglo, K. (2010). Mix design for oil-palm-boiler clinker (OPBC) concrete. *Journal of Science and Technology (Ghana)*, *30(1).* 111-118.

[5] Arunima, V. R., & Sreelekshmi, S. (2016). Effects on compressive strength on using palm oil clinker as partial replacement of fine aggregate in concrete. *International Journal of Science and Research*. (5)6, 815-817.

[6] Ibrahim, H. A., & Razak, H. A. (2016). Effect of palm oil clinker incorporation on properties of pervious concrete. *Construction and Building Materials, 115,* 70-77.

[7] Karim, M. R., Hashim, H., Razak, H. A., & Yusoff, S. (2017). Characterization of palm oil clinker powder for utilization in cement-based applications. *Construction and building materials*, *135,* 21-29.

[8] ASTM International. (2015). Standard Test Method for Density, Relative Density (Specific Gravity), and Absorption of Coarse Aggregate1 (ASTM C 127-15). West Conshohocken, PA: American Society for Testing and Materials.

[9] ASTM International. (2017). Standard Test Method for Bulk Density and Voids in Aggregate (ASTM C29/C29M-17a). West Conshohocken, PA: American Society for Testing and Materials.

[10] ASTM International. (2014). Standard Test Method for Sieve Analysis of Fine and Coarse Aggregates (ASTM C 136-14). West Conshohocken, PA: American Society for Testing and Materials.

[11] ASTM International. (2010). Standard Test Method for Flat Particles, Elongated Particles, or Flat and Elongated Particles in Coarse Aggregate (ASTM D 4791-10) West Conshohocken, PA: American Society for Testing and Materials.

[12] ASTM International. (2016). Standard Test Method for Organic Impurities in Fine Aggregates for Concrete (ASTM C40/C40M-16). West Conshohocken, PA: American Society for Testing and Materials.

[13] ASTM International. (2018). Standard Test Method for Soundness of Aggregates by Use of Sodium Sulfate or Magnesium Sulfate (ASTM C 88-18) West Conshohocken, PA: American Society for Testing and Materials.

[14] ASTM International. (2016). Standard Test Method for Resistance to Degradation of Large-Size Coarse Aggregate by Abrasion and Impact in the Los Angeles Machine (ASTM C535-16). West Conshohocken, PA: American Society for Testing and Materials.

[15] Day, K. W., Aldred, J., & Hudson, B. (2013). Concrete mix design, quality control and specification. CRC Press.

[16] Kueaket, K., & Tonnayopas, D. (2018). Enhanced Properties of Palm Oil Boiler Clinker Concrete with Sang Yod Rice Husk Ash. *Journal of Advanced Research in Applied Mechanics, 51(1),* 10-19.

[17] Neville, A. M., & Brooks, J. J. (2010). Concrete technology (2 ed.). England: Pearson Education Limited.

APPENDIX C

Research article 1 (Indexed by Scopus)

Kueaket, K., & Tonnayopas, D. (2021). Compressive strength and durability performance of mortar containing palm oil boiler clinker aggregate, rice husk ash, and calcium bentonite. *Journal of Applied Engineering Science*, 19(1), 193-203. doi: 10.5937/jaes0-27580

COMPRESSIVE STRENGTH AND DURABILITY PERFORMANCE OF MORTAR CONTAINING PALM OIL BOILER CLINKER AGGREGATE, RICE HUSK ASH, AND CALCIUM BENTONITE

Kamolchanok Kueaket, Danupon Tonnayopas*

Prince of Songkla University, Faculty of Engineering, Department of Mining and Materials Engineering, Hat Yai, Thailand

The utilization of local waste by-products as a building material has attracted great attention for an environmental sustainability and become a fundamental part of sustainable construction. In this experimental research, the local palm oil industrial waste and agricultural waste are utilized for the green mortar production. To examine the compressive strength and the durability performance of the green mortar mixtures, Palm oil boiler clinker (POBC) was used as a substitution material for natural fine aggregate. An ordinary Portland cement was partially replaced by rice husk ash (RHA) and calcium bentonite (CB) in the proportion of 10%, 20%, and 30% by weight of cement. The compressive strength, water absorption, porosity, durability against sulphuric acid and sodium sulphate attacks, and microstructures of the POBC mortar mixtures were evaluated at the curing age of 7, 28, and 56 days. The experimental results revealed that the compressive strength, water absorption, porosity, and durability characteristics of POBC mortar incorporating RHA and CB were improved by long-term curing. Particularly, the 56-day POBC mortar incorporating up to 30% of RHA and 10% of CB yielded the superior durability against sulphuric acid and sodium sulphate attacks.

Key words: palm oil boiler clinker, rice husk ash, calcium bentonite, compressive strength, durability against sulphuric acid and sodium sulphate attacks

INTRODUCTION

The exploitation of waste materials in mortar and concrete is studied as a means toward a sustainable, environmental-friendly construction [1]. Currently, the practice of using the industrial by-products as supplementary cementitious materials (SCMs) and as an aggregate substitution is spreading constantly. Apart from strength properties, durability is an important issue for local mortar production. Several studies reported that the introduction of the SCMs from waste by-products such as fly ash, silica fume, ceramic waste, ground granulated blast-furnace slag, and rice husk ash can improve the long-term durability of the cementitious composite. This is due to the formation of calcium silicate hydrate by the pozzolanic reaction which improves the pore structure and clogs up the cement matrix [2-6].

The palm oil boiler clinker (POBC) is a waste-by product of palm oil mill [7]. In 2019, the agricultural productivity of palm oil in Thailand was 16.8 million tons [8]. Particularly, the vast cultivation area of palm trees covers 6,765 km^2, with an approximate annual crude palm oil production of 2.4 million tons [9]. A solid wastes of crude palm oil production (such as palm fibers, empty fruit bunch, palm shells) are used as biomass fuels in boiler for sterilization process [10]. The POBC and palm oil fuel ash (POFA) are derived after the end of combustion in boiler. The POBC, POFA, and several industrial wastes derived from the palm oil industry have resulted in a significant environmental impact and landfill usage [11-12]. In an ef-

fort to mitigate this, the POBC properties were tackled by various researchers. The study on the feasibility of using the waste of palm oil mill for construction applications confirmed that the utilization of palm oil clinker as a sand replacement can reduce the cost of construction and carbon emission by 17% and 9.6% compared to that of using natural river sand [13]. In addition, the use of high replacement ratio of palm oil clinker as a sand substitution caused a 56-day mortar's strength reduction of only 22%, as compared to conventional sand mortar [14].

Rice husk ash (RHA); an agricultural by-product, is obtained after using the rice husk as a local biomass fuel. The main constituent of RHA is the reactive amorphous SiO_2 [15], therefore, several studies investigated its contribution to the properties of cementitious materials when used as an additive. It was confirmed through an XRD analysis that the addition of reactive SiO_2 derived from RHA reacted with the $Ca(OH)_2$ contents of the hydration products [16]. Thus, consuming a portion of the free $Ca(OH)_2$ and forming the additional calcium silicate hydrate (C-S-H) gel. Moreover, it was found that the pozzolanic reaction was promoted by the addition of RHA [17-18]. The promoted pozzolanic reaction contributed to the strength development and increased C-S-H content. As a reactive filler, C-S-H plays an important role in reducing the capillary pore size in the cement paste. Moreover, utilizing the RHA as supplementary cementitious material can enhance the acid resistance of recycle-aggregate concrete by decreasing calcium hydroxide $(Ca(OH)_2)$ content, while strengthening the bond between the dif-

Kamolchanok Kueaket, et al. - Compresssive strength and durability performance of mortar containing palm oil boiler clinker aggregate, rice husk ash and calcium bentonite

iipp

ferent phases within microstructure [19]. This explains the mortar's enhanced durability by the additional C-S-H, since the C-S-H forms by cement hydration and pozzolanic reaction. The deterioration reaction between the hydration product of the cement paste and sulphuric acid is the depletion of $Ca(OH)_2$ and the forming of gypsum ($CaSO_4.2H_2O$). Then, the degradation mechanisms by sulphuric acid attack occur. Subsequently, the gypsum gel can fill up the pore, intensive gypsum deposit, and the pore structure damaged [20-21].

Furthermore, calcium bentonite (CB) is a natural pozzolanic material and contains more than 60% of SiO_2 [22]. According to the assessment of the strength activity index (SAI) of concrete containing CB, the addition of up to 25% CB by weight of cement can provide a satisfactory SAI (more than 75%). Likewise, the compressive strength of concrete containing 15% CB by weight of cement is close to that of control concrete at the age of 28 days (the strength reduction was only 5% in comparison with the compressive strength of the control concrete specimen) [23]. In addition, the longer curing periods have a positive impact on improving the strength and durability characteristic of the mortar containing CB [24]. Besides, the addition of 8% CB decreased the porosity of 28-day mortar by 16.9% [25-26].

In the pursuit of promoting sustainable construction, this research focuses on the utilization of local by-products as both a fine aggregate substitution and a cement replacement. Therefore, in this study, the RHA and CB were introduced as a partial cement replacement, along with a 100% POBC fine aggregate replacement to determine the strength and durability characteristics of the mortar mixtures at different curing ages. The strength and durability characteristics; namely, the compressive strength, porosity, water absorption, and resistance to mild concentration of sulphuric acid and sodium sulphate attack were investigated together with the microstructural characterization via scanning electron microscope (SEM).

MATERIALS AND METHODS

Materials

An ordinary Portland cement (OPC) complying with ASTM C150 [27], was used in this study, while the RHA derived after raw rice husk (a local by-product from Phattalung province, Thailand) was conventionally burned in open air as a local biomass fuel. Moreover, the calcium bentonite (commercial grade) was purchased from a manufacturer in Saraburi province, Thailand. Meanwhile, the POBC was collected from the waste disposal area near the palm oil plant at Surat Thani province, Thailand.

Firstly, the obtained RHA was then exposed to a temperature of 700°C for 1 hour in a muffle furnace in order to eliminate some presence of unburned carbon and/or some organic matter contaminants. Then, it was ground with a jar mill at 70 rpm for 12 hours. The particle size distributions of the RHA and CB were analyzed by a laser particle analyzer (LPSA); model: Analysette 22 Nano tec. The mean particle size (d_{50}) of RHA and CB was 12.4 and 2.5 µm, respectively. Regarding the POBC, it was washed to remove any clay particles and organic matter. Then, it was oven-dried at 105±5°C for 24 hours, to be crushed with jaw crusher and sieved through No.4 sieve mesh (or aperture size of 4.75mm). The fresh POBC samples obtained from palm oil mill disposal area, crushed POBC, RHA, and CB powders are depicted in Figure 1. The chemical composition of the POBC, RHA, and CB were analyzed via a wavelength dispersive X-ray fluorescence spectrophotometer (WDXRF); model: Zetium, and it is expressed in Table 1. The total amount of SiO_2, Al_2O_3, and Fe_2O_3 contents of RHA and CB were higher than 70%, which met the chemical requirements of class N (raw or calcined natural pozzolans) and class F (fly ash) as per ASTM C618-19 [28]. The percentage passing results of the sieve analysis for crushed POBC, RHA, and CB were plotted against particle diameters and presented in Figure 2. Finally, the physical proper-

Table 1: Chemical composition of POBC, RHA, and CB analyzed by WDXRF

Oxides (wt.%)	SiO_2	Fe_2O_3	SO_3	K_2O	Al_2O_3	CaO	MgO	MnO	P_2O_5	LOI
POBC	65.23	1.78	0.04	9.56	1.66	10.00	5.37	0.17	5.50	0.04
RHA	93.83	0.36	0.21	1.77	0.66	0.76	0.36	0.11	1.04	0.67
CB	56.62	0.02	0.69	0.96	19.81	1.16	0.55	0.03	0.05	10.12

(a)   (b)   (c)   (d)
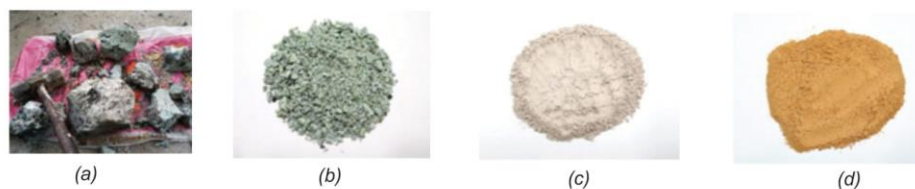
Figure 1: Lumps of POBC collected from palm oil mill disposal area (a), Crushed POBC (b), RHA powder (c), and CB powder (d)

93

Kamolchanok Kueaket, et al. - Compresssive strength and durability performance of mortar containing palm oil boiler clinker aggregate, rice husk ash and calcium bentonite

ties of POBC fine aggregate were tested and tabulated in Table 2 for convenience.

Mix proportions

Seven mortar mixtures were prepared with POBC fine aggregate and incorporating RHA and CB as an ordinary Portland cement (OPC) replacement. The OPC was partially replaced by RHA and CB at the replacement ratios of 10%, 20%, and 30% (by percent weight of OPC), respectively. The mixture proportions are 1:2.75 (Binder: POBC aggregate). Water to binder ratio of the mixture was kept constant at 0.48 in accordance with ASTM C109 [29]. The percentage of flow was carried out as following ASTM C 1437-15 [30]. The mixture series are tabulated in Table 3.

Testing methods

To determine the compressive strength, water absorption, porosity, and durability against acid and sulphate attacks, three cube specimens of 50-mm of each mixture were cast and then cured in saturated lime water at the temperature of 27±5°C for a period of 7, 28, and 56 days before testing. The compressive strength test was performed according to ASTM C109 [29] by using digital concrete compression machine model KC-150g with capacity 1,500kN. The strength activity index (SAI) was calculated as per ASTM C618-19 [28]. The water absorption and porosity measurements were conducted in accordance with the Archimedes method based on the ASTM standard C373-14a [31].

The sulphuric acid (H_2SO_4) and sodium sulphate (Na_2SO_4) resistance tests were carried out after the specimens were cured in saturated lime water for periods of 7, 28, and 56 days. During testing, the 7-day, 28-day, and 56-day specimens of each mixture were weighted by digital precision balance (0.001g), and then exposed to 0.005M (pH≈2.5) sulphuric acid solution (H_2SO_4) and 0.5M (pH≈8) sodium sulphate solution (Na_2SO_4) for a period of 42 days. The

Table 2: Physical properties of crushed POBC (fine aggregate)

Crushed POBC properties	Value
Loose bulk density (kg/m³)	1,145.71
Void (%)	32.59
Compacted bulk density (kg/m³)	1,310.71
Void (%)	22.88
Fineness modulus	3.74
Specific gravity	2.20
Soundness (%)	2.05
Water absorption (%)	
1 day	3.13
7 days	3.94
Moisture content (%)	0.80
Organic impurity (ASTM C40-20)	None
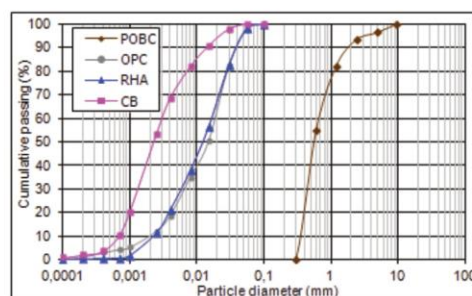
Figure 2: Grading analysis of raw materials

acid and sulphate solutions were refreshed every week, in order to maintain the pH value and reduce the effect of pH gaining by excessive lime due to the cement hydration. After 42 days of exposure to each acid and sulphate solutions, the weights and compressive strengths of each specimen were examined. Subsequently, through comparing the weight before and after exposure to the acid and sulphate solutions, the weight loss was estimated. Moreover, the change in compressive strengths after exposure to acid and sulphate solutions was investigated in comparison to the compressive strength of the specimen before exposure, as to assess the compressive strength loss.

For the microstructural analysis of the POBC mortar's cement paste, the scanning electron micrographs were carried out by using Thermo Fisher Scientific scanning electron microscope, model Quanta 400 (SEM-Quanta) at the accelerating voltage of 20 kV.

Table 3: Mix proportions of POBC mortar (kg/m³)

No.	Nomenclature	Binder (kg/m³)			Fine aggregate (kg/m³)	Flow (%)
		OPC	CB	RHA	POBC	
1	Control	500	0	0	1,375	121
2	R10	450	0	50	1,375	98
3	R20	400	0	100	1,375	83
4	R30	350	0	150	1,375	75
5	B10	450	50	0	1,375	111
6	B20	400	100	0	1,375	106
7	B30	350	150	0	1,375	97

Kamolchanok Kueaket, et al. - Compresssive strength and durability performance of mortar containing palm oil boiler clinker aggregate, rice husk ash and calcium bentonite

iipp

RESULTS AND DISCUSSIONS

Compressive strength

The compressive strength results of the POBC mortars incorporating the RHA and CB at different ages are presented in Figure 3. Generally, it is evident that the 7-day compressive strengths of the RHA and CB specimens were lower than the control specimen. However, it can be noticed that the compressive strength of all mix types increased through a prolonged period of curing.

Particularly, it was observed that the mortar incorporating the RHA developed strength gradually in the long term. At the curing age of 56 days, an increase in the compressive strength and strength activity index (SAI) was 16%, 18%, and 15% for the mortar specimens incorporating 10%, 20%, and 30% RHA, respectively, as compared to that of the control mortar; This is shown in Figure 3(a) and 4. This increase in the compressive strength of RHA mixtures with age could be due to the high pozzolanic reaction that is gradually promoted by the reactive amorphous SiO_2 contents of the RHA [32-33].

On the other hand, the compressive strength decreased with the increase in the CB replacement ratio. At the age of 56 days, a decrease in the compressive strength of the CB mixtures was observed to be 9%, 15%, and 20%, for the mortars incorporating CB content of 10%, 20%, and 30%, respectively; as shown in Figure 3(b). However, the

(a)

(b)
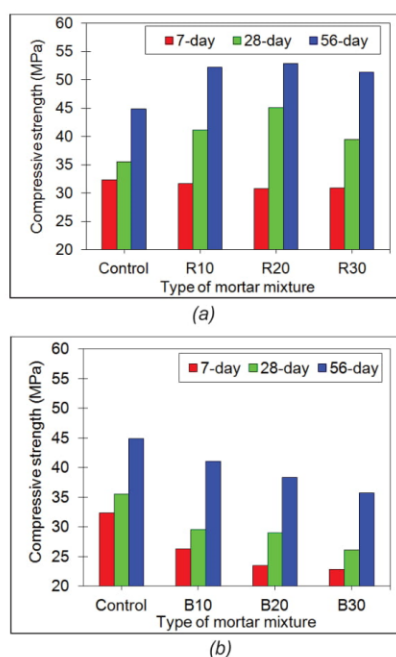
Figure 3: Compressive strength of POBC mortar containing RHA (a) and CB (b) at different ages
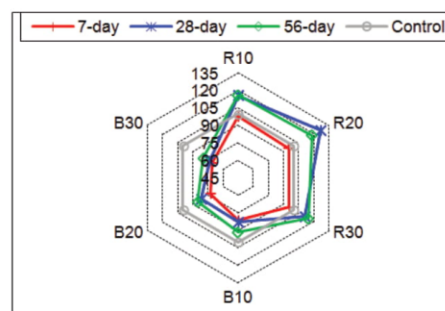
Figure 4: Strength activity index of POBC mortar containing RHA and CB at different ages

percentage of the strength development from the age of 28 days to 56 days for the specimens incorporating 0% and 10% CB was 26% and 39%, respectively. Besides, the strength activity indexes (SAI) of the mixture containing 10% CB content were 81%, 83%, and 91% at the ages of 7, 28, and 56 days, respectively; as shown in Figure 4.

Thus, it is observed that the replacement by weight of OPC by 10% CB provided the lowest strength reduction and the most desirable SAI, as per the standard requirement of ASTM C618-19 [28]. This finding is in good agreement with the previous studies [24, 34].

Water absorption and porosity

Figure 5 shows the water absorption and porosity of the POBC mortars incorporating RHA and CB at the age of 7, 28, and 56 days. In general, the water absorption and porosity of all mixtures decrease as the curing age increases.

An increase in the replacement ratio of the RHA significantly reduced the water absorption and porosity of the RHA specimens, compared to that of the control specimen; as shown in Figure 5(a). At the age of 56 days, both the water absorption and porosity of the specimen incorporating 30% RHA were lower than the control specimen by 36% and 33%, respectively. The decrease in porosity could be due to the high pozzolanic reaction and the filler effect of RHA [35].

On the other hand, it was observed that incorporating 10% CB content reduced the water absorption and porosity by 9% and 14%, respectively, compared to that of the control specimen at the curing age of 56 days; as shown in Figure 5(b). However, an increase in CB replacement of OPC above 10% (by weight) showed a negative impact on the water absorption and porosity characteristics of the mortar. This finding is consistent with previous researches [25-26], where it was shown that incorporating 8-15% CB content can decrease the porosity of mortar. Conversely, they pointed out that the water absorption and porosity of the mortar incorporating

high replacement ratio of CB (more than 15%) increased owing to the high CB content, which could hinder the hydration reaction. Thus, it could lead to aggravating the more heterogeneous matrix structure of mortar. In addition, an excess CB replacement absorbs additional water content. Consequently, the water absorption of the mortar incorporating a high amount of CB increases [23].

Effects of sulphuric acid attack

Weight loss

The weight loss of the specimens containing RHA and CB at different ages was assessed after 42 days of exposure to 0.005M (pH=2.5) sulphuric acid solution, as shown in Figure 6. The overall trend shows a decrease in weight loss with prolonged curing before exposure to sulphuric acid.

The examination of the RHA specimens, clearly demonstrates that an increase in the RHA replacement ratio significantly reduced the weight loss of the RHA specimens compared to that of the control specimen. For instance, the weight loss was 1.53%, 0.81%, 0.68% and 0.47% for the 56-day specimens containing 0%, 10%, 20% and 30% RHA content; as shown in Figure 6(a).
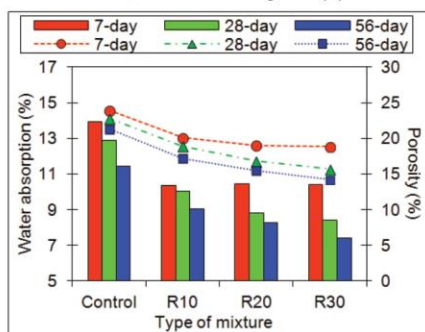
(a)
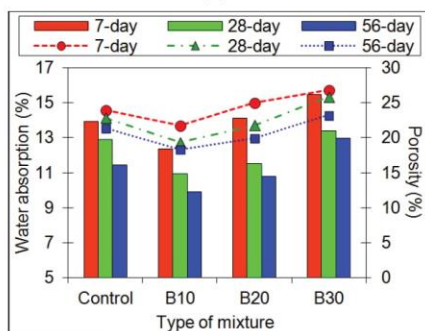
(b)

Figure 5: Water absorption and porosity of POBC mortar containing RHA (a) and CB (b) at different ages
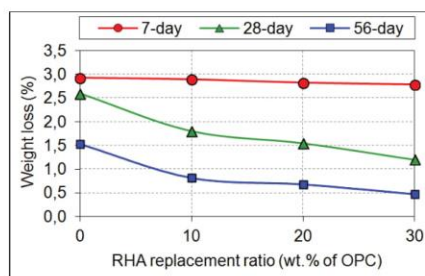
(a)
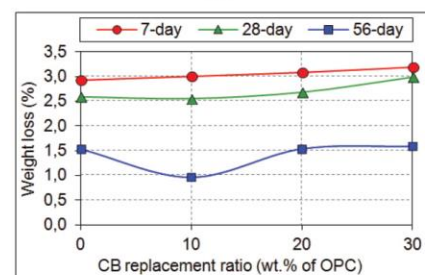
(b)

Figure 6: Weight loss of POBC mortar containing RHA (a) and CB (b) after exposure to sulphuric acid solution

Likewise, it was found that the 56-day specimen containing 10% CB content, provided 0.97% of weight loss, which was lower than that of the control specimen and the specimens containing 20% and 30% CB content; as per Figure 6(b). On the contrary, an increase in the CB replacement ratio of more than 10% performed greater weight loss and has a negative effect on the resistance to sulphuric acid exposure.

Strength loss

The compressive strength loss values of different mixtures at the curing ages of 7, 28, and 56 days are revealed in Figure 7. Generally, a decrease in the strength loss is noted with an increase in the curing age before the exposure to sulphuric acid. For instance, the strength loss was recorded to be 4.93%, 3.84%, 2.90% and 1.59% for the 56-day specimens incorporating 0%, 10%, 20% and 30% RHA, respectively, as depicted in Figure 7(a). In addition, the 56-day specimen containing CB content of 10% provided the lower strength loss (4.43%), in comparison with the specimen containing 20% and 30% CB content; with a strength loss of 5.54% and 6.08% (Figure 7(b)).

Consequently, an increase in RHA replacement ratio of RHA showed a decrease in the strength loss and has a positive effect on sulphuric acid resistance, while the specimen incorporating more than 10% CB content provided an increase in strength loss and has an adverse

iipp

effect on the resistance of POBC mortar to sulphuric acid attack.

Effects of sodium sulphate attack

Weight gain

An increase in weight was observed in all specimens after 42 days of exposure to 0.5 M (pH=8) sodium sulphate solution, as demonstrated in Figure 8. Generally, there is a mild decrease in the weight gain with exposure to sodium sulphate solution after prolonged curing. For example, the weight gain was 0.13%, 0.09%, 0.07% and 0.03% for the 56-day specimens incorporating 0%, 10%, 20% and 30% of RHA, respectively, as presented in Figure 8(a). Additionally, it is found that the 56-day specimen incorporating 10% CB provided the lowest weight gain by 0.12%, whereas the weight gains of the control specimen and the specimens with 20%, and 30% CB content were 0.13%, 0.15%, and 0.16%, respectively, as illustrated in Figure 8(b). Hence, the increase in proportions of RHA replacement of OPC and the specimen incorporating 10% CB yielded a better performance to sulphate resistance by demonstrating the lower weight gain when compared to that of the control specimen. This result is in agreement with that of [36], who explained that

the weight gain after early exposure to sodium sulphate solution (up to 90 days) could be due to the sulphate salt and hydration products were formed.

Strength loss

Figure 9 presents the compressive strength loss of the RHA and CB mixtures at different curing ages before exposure to the sodium sulphate solution. The overall trend shows a decrease in the strength loss with prolonged curing age for all mixtures.

As for the RHA specimens (Figure 9(a)), it is constantly observed that the strength loss gradually diminishes as the RHA replacement ratio increases. For example, the loss in compressive strength of the 56-day control specimen was 1.15% while the strength loss of the 56-day specimens incorporating 10%, 20%, and 30% RHA content was found to be 0.85%, 0.55%, and 0.32%, respectively. Furthermore, the strength loss of the 56-day specimen containing 10% CB content was 0.98% in which was lower than that of the control specimen by 14.78% (Figure 9(b)). However, an increase in the CB replacement ratio up to 30% slightly extended the strength loss by 34.69% compared to that of specimen containing 10% CB content.
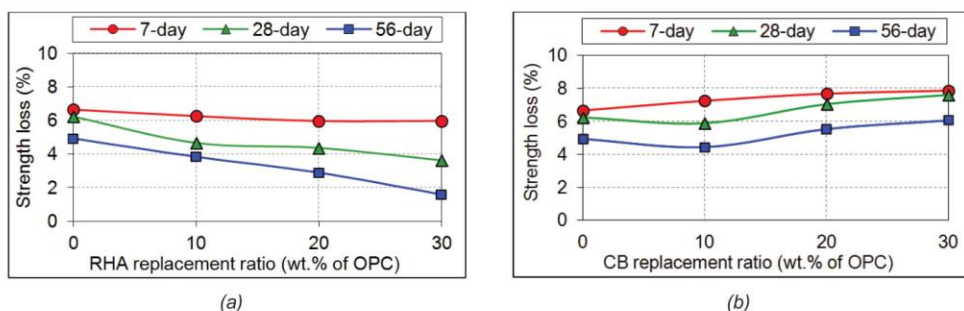
Figure 7: Strength loss of POBC mortar containing RHA (a) and CB (b) after exposure to sulphuric acid solution
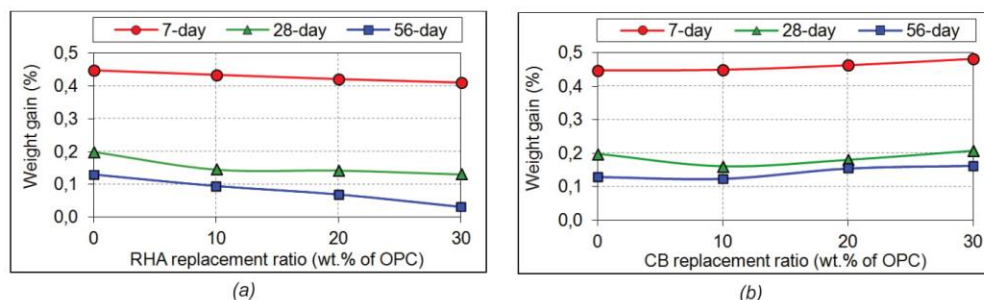
Figure 8: Weight gain of POBC mortar containing RHA (a) and CB (b) after exposure to sodium sulphate solution

(a)

(b)
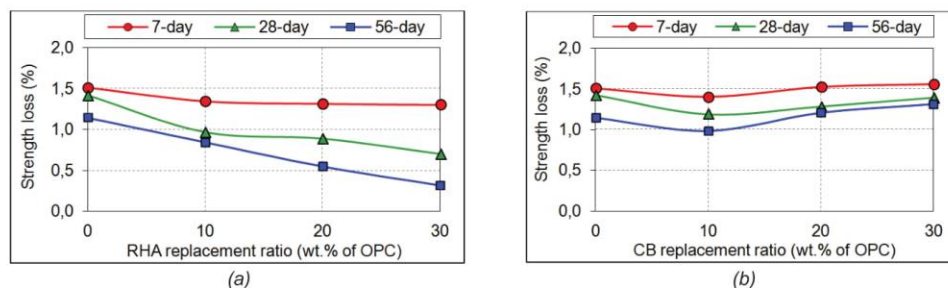
Figure 9: Strength loss of POBC mortar containing RHA (a) and CB (b) after exposure to sodium sulphate solution

Microstructural analysis

The scanning electron micrographs of the control specimen, specimen incorporating 10% RHA, and 10% CB at the ages of 56 days (before exposure to sulphuric acid and sodium sulphate solutions) are demonstrated in Figure 10. It can be observed that the microstructure of each POBC mortar mixtures consisted of 3 components, including POBC fine aggregate fragment, cement matrix, and interfacial transition zone (ITZ) located between the POBC fine aggregate and the cement matrix. As depicted in Figure 10(a)-10(c), the POBC fine aggregate had an angular shape and smooth surface with subconchoid-

al fracture. In addition, the mixture containing RHA also provided a denser ITZ structure when compared to those of control specimen and CB specimen. The denser ITZ could contributed to the compressive strength improvement of the POBC mortar.

After 42 days of exposure to the sulphuric acid solution (pH≈2.5), alterations of the hydration products were observed under the scanning electron microscope. The photomicrographs of 56-day OPC specimen, specimens incorporating 10% RHA, and 10% CB are presented in Figure 11. It can be seen that the acid attack promoted some disintegration features within the microstructures, which accounted for both a weight loss and a strength reduction.
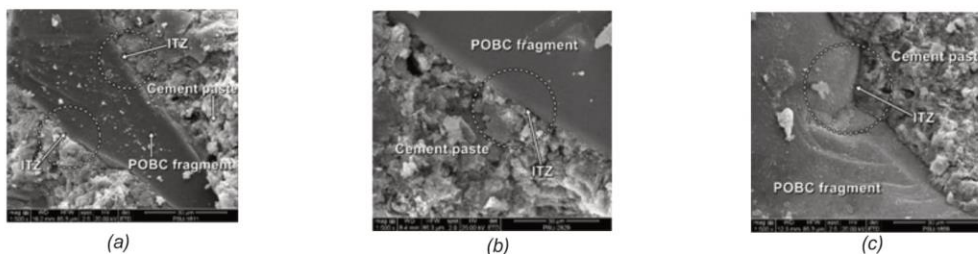
Figure 10: Scanning electron micrographs of the 56-day OPC specimen (a), specimen incorporating 10% RHA (b), and 10% CB (c) before exposure to sulphuric acid and sodium sulphate solutions

Figure 11: Scanning electron micrographs of the 56-day OPC specimen (a), specimen incorporating 10% RHA (b), and 10% CB (c) after exposure to sulphuric acid solution for 42 days

Kamolchanok Kueaket, et al. - Compresssive strength and durability performance of mortar containing palm oil boiler clinker aggregate, rice husk ash and calcium bentonite

iipp

The deleterious mechanism of acid attack is the dissolution of calcium hydroxide (a hydration product of cement paste) and the formation of gypsum ($Ca_2SO_4.2H_2O$) and ettringite ($Ca_6Al_2(SO_4)_3(OH)_{12}.26H_2O$) [37-38]. As a result, the softening of cement paste and the propagating of some microcracks could lead to the weakening of the mortar specimen. The gypsum (a light monoclinic shape with one direction cleavage) and the ettringite (needle-like or elongate prismatic shape) crystals embedded in the matrix of the control specimen, as depicted in Figure 11(a). While a small amount of gypsum and ettringite crystals were observed in the specimens incorporating the RHA and CB supplements, as shown in Figure 11(b) and 11(c). In addition, the control specimen revealed less compactness, high porosity, and loosed matrix. Contrastingly, the specimens incorporating either the RHA or CB supplements displayed a denser matrix occupied by the C-S-H framework.

The SEM micrographs of the 56-day OPC specimen, specimen incorporating 10% RHA, and 10% CB exposed to sodium sulphate solution (pH=8) for 42 days, are illustrated in Figure 12. It is apparent that the specimens incorporating the RHA and CB exhibited lesser pore space and denser matrix (clogged up by C-S-H), compared to that of the control specimen. Moreover, the less ettringite and microcracks were observed in the specimens incorporating the RHA and CB supplements, as shown in Figure 12(b) and 12(c), when compared to that of the control specimen (Figure 12(a)).

In general, the external sodium sulphate attack mechanism is the penetration of dissolute sulphate salt into the cement matrix which resulted in weight gain at the early sulphate exposure [39]. Such an attack can provide the deleterious effects on the cement matrix by inducing in the precipitation of sulfoaluminate phase ettringite (E) and gypsum (G) due to the destabilized calcium hydroxide in cement paste reacts with dissoluble sulphate salt. Additionally, the formation of ettringite causes an increase in the volume of the cementitious matrix and induces some micro cracks. Subsequently, the expansion and microcracks could lead to the strength reduction [40-41]. An increase in the densification of the matrix within the POBC mortar incorporating the RHA and CB supplements could contributed to the pore refinements

and reduction of the connectivity of pores, which in turn mitigates the deterioration from the penetration of the dissoluble sulphate salt into the matrix.

CONCLUSIONS

This study investigated the performance of mortar containing waste materials namely, palm oil boiler clinker as a fine aggregate substitution, the rice husk ash and calcium bentonite as a partial cement replacement. The compressive strength, water absorption, porosity, durability against sulphuric acid and sodium sulphate attacks at the age of 7, 28, and 56 days were examined. Based on the experimental results, the following conclusions are drawn:

- The compressive strengths of the POBC mortar incorporating the rice husk ash (RHA) and calcium bentonite (CB) were enhanced by a prolonged period of curing up to 28 days. The highest SAI of the RHA and CB mixtures at the age of 28 and 56 days was obtained in the mixtures containing RHA content of up to 20% and CB content of 10%.

- The increase in the RHA replacement ratio and the curing ages of POBC mortar have a positive impact on reducing both the water absorption and porosity. Additionally, the POBC mortar incorporating up to 10% CB provided lower water absorption and porosity compared to the control mixture. However, any increase in the CB replacement ratio of more than 10% significantly increases the water absorption and porosity.

- The weight variation and strength loss due to sulphuric acid and sodium sulphate attacks of each POBC mortar mixtures were mitigated by increasing the curing duration before such exposure. Evidently, the POBC mortars incorporating the RHA supplement of up to 30%, and 10% of CB yielded the optimum durability against sulphuric acid and sodium sulphate attack.

- The SEM micrographs revealed that the interfacial transition zones were found to be denser in the mixture incorporating RHA. After exposure to sulphuric acid and the sodium sulphate solutions, the POBC mortars incorporating the RHA and CB provided less

(a)   (b)   (c)
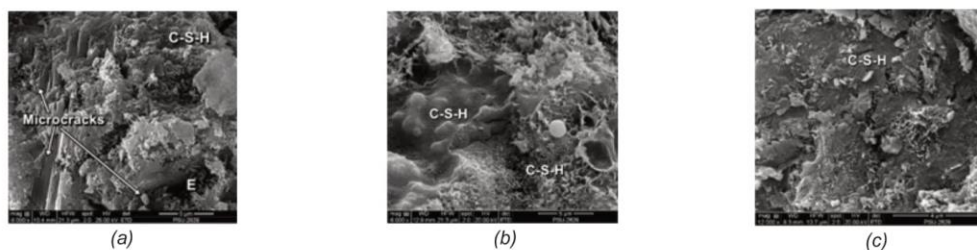
Figure 12: Scanning electron micrographs of the 56-day OPC specimen (a), specimen incorporating 10% RHA (b), and 10% CB (c) after exposure to sodium sulphate solution for 42 days

disintegration combined with a dense matrix occupied by C-S-H.

The POBC mortar in this study can be served as the non-heavy duty construction materials, eco-brick, and eco-mortar block productions. Besides, the supplement of up to 30% RHA and 10% CB can be possibly added as an OPC replacement to alleviate the cement consumption and promote the performance of the POBC mortar against the non-aggressive environment.

ACKNOWLEDGEMENTS

REFERENCES

1. Martínez-Lage, I., Vázquez-Burgo, P., Velay-Lizancos, M. (2020). Sustainability evaluation of concretes with mixed recycled aggregate based on holistic approach: Technical, economic and environmental analysis. Waste Management, vol. 104, 9-19, DOI: 10.1016/j.wasman.2019.12.044.

2. Liu, K.W., Sun, D.S., Wang, A.G., Zhang, G.Z., Tang, J.H. (2018). Long-term performance of blended cement paste containing fly ash against sodium sulfate attack. Journal of Materials in Civil Engineering, vol. 30, no. 12, 10, DOI: 10.1061/(asce)mt.1943-5533.0002516.

3. Kumar, V.R.P., Gunasekaran, K., Shyamala, T. (2019). Characterization study on coconut shell concrete with partial replacement of cement by GGBS. Journal of Building Engineering, vol. 26, 9, DOI: 10.1016/j.jobe.2019.100830.

4. Chopra, D., Siddique, R., Kunal. (2015). Strength, permeability and microstructure of self-compacting concrete containing rice husk ash. Biosystems Engineering, vol. 130, 72-80, DOI: 10.1016/j.biosystemseng.2014.12.005.

5. Lim, N., Mohammadhosseini, H., Tahir, M.M., Samadi, M., Sam, A.R.M. (2018). Microstructure and strength properties of mortar containing waste ceramic nanoparticles. Arabian Journal for Science and Engineering, vol. 43, no. 10, 5305-5313, DOI: 10.1007/s13369-018-3154-x.

6. He, Z., Chang, J., Liu, C., Du, S., Huang, M.A.N., Chen, D. (2018). Compressive strengths of concrete containing rice husk ash without processing. Revista Romana de Materiale/ Romanian Journal of Materials, vol. 48, no. 4, 499-506

7. Kueaket, K., Tonnayopas, D. (2018). Enhanced properties of palm oil boiler clinker concrete with Sang Yod rice husk ash. Journal of Advanced Research in Applied Mechanics, vol. 51, no. 1, 10-19

8. Economics. (2019). Palm oil agricultural statistics of thailand. Ministry of Agriculture and Cooperatives Thailand

9. Nutongkaew, P., Waewsak, J., Riansut, W., Kongruang, C., Gagnon, Y. (2019). The potential of palm oil production as a pathway to energy security in Thailand. Sustainable Energy Technologies and Assessments, vol. 35, 189-203, DOI: 10.1016/j.seta.2019.07.002.

10. Saswattecha, K., Kroeze, C., Jawjit, W., Hein, L. (2016). Options to reduce environmental impacts of palm oil production in Thailand. Journal of Cleaner Production, vol. 137, 370-393, DOI: 10.1016/j.jclepro.2016.07.002.

11. Karim, M.R., Hashim, H., Abdul Razak, H., Yusoff, S. (2017). Characterization of palm oil clinker powder for utilization in cement-based applications. Construction and Building Materials, vol. 135, 21-29, DOI: 10.1016/j.conbuildmat.2016.12.158.

12. Saswattecha, K., Kroeze, C., Jawjit, W., Hein, L. (2015). Assessing the environmental impact of palm oil produced in Thailand. Journal of Cleaner Production, vol. 100, 150-169, DOI: 10.1016/j.jclepro.2015.03.037.

13. Kanadasan, J., Fauzi, A.F.A., Razak, H.A., Selliah, P., Subramaniam, V., Yusoff, S. (2015). Feasibility studies of palm oil mill waste aggregates for the construction industry. Materials, vol. 8, no. 9, 6508-6530, DOI: 10.3390/ma8095319.

14. Kanadasan, J., Razak, H.A., Subramaniam, V. (2018). Properties of high flowable mortar containing high volume palm oil clinker (POC) fine for eco-friendly construction. Journal of Cleaner Production, vol. 170, 1244-1259, DOI: 10.1016/j.jclepro.2017.09.068.

15. Sandhu, R.K., Siddique, R. (2017). Influence of rice husk ash (RHA) on the properties of self-compacting concrete: A review. Construction and Building Materials, vol. 153, 751-764, DOI: https://doi.org/10.1016/j.conbuildmat.2017.07.165.

16. Prameetthaa, J., Bharatkumar, B.H., Iyer, N.R. (2015). Investigation on micronized biomass silica as a sustainable material. Cement & Concrete Composites, vol. 60, 25-33, DOI: 10.1016/j.cemconcomp.2015.04.004.

17. Kang, S.-H., Hong, S.-G., Moon, J. (2019). The use of rice husk ash as reactive filler in ultra-high performance concrete. Cement and Concrete Research, vol. 115, 389-400, DOI: 10.1016/j.cemconres.2018.09.004.

18. Gill, A.S., Siddique, R. (2018). Durability properties of self-compacting concrete incorporating metaka-olin and rice husk ash. Construction and Building Materials, vol. 176, 323-332, DOI: 10.1016/j.conbuildmat.2018.05.054.

19. Koushkbaghi, M., Kazemi, M.J., Mosavi, H., Mohse-ni, E. (2019). Acid resistance and durability properties of steel fiber-reinforced concrete incorporating rice husk ash and recycled aggregate. Construction and Building Materials, vol. 202, 266-275, DOI: 10.1016/j.conbuildmat.2018.12.224.

20. Monteny, J., Vincke, E., Beeldens, A., De Belie, N., Taerwe, L., Van Gemert, D., Verstraete, W. (2000). Chemical, microbiological, and in situ test methods for biogenic sulfuric acid corrosion of concrete. Cement and Concrete Research, vol. 30, no. 4, 623-634, DOI: 10.1016/S0008-8846(00)00219-2.

21. Yuan, H., Dangla, P., Chatellier, P., Chaussadent, T. (2013). Degradation modelling of concrete submitted to sulfuric acid attack. Cement and Concrete Research, vol. 53, 267-277, DOI: 10.1016/j.cemconres.2013.08.002.

22. Memon, S.A., Arsalan, R., Khan, S., Lo, T.Y. (2012). Utilization of Pakistani bentonite as partial replacement of cement in concrete. Construction and Building Materials, vol. 30, 237-242, DOI: 10.1016/j.conbuildmat.2011.11.021.

23. Laidani, Z.E., Benabed, B., Abousnina, R., Gueddouda, M.K., Kadri, E. (2020). Experimental investigation on effects of calcined bentonite on fresh, strength and durability properties of sustainable self-compacting concrete. Construction and Building Materials, vol. 230, 11, DOI: 10.1016/j.conbuildmat.2019.117062.

24. Mirza, J., Riaz, M., Naseer, A., Rehman, F., Khan, A.N., Ali, Q. (2009). Pakistani bentonite in mortars and concrete as low cost construction material. Applied Clay Science, vol. 45, no. 4, 220-226, DOI: 10.1016/j.clay.2009.06.011.

25. Hu, Y., Diao, L., Lai, Z.Y., He, Y.J., Yan, T., He, X., Wu, J., Lu, Z.Y., Lv, S.Z. (2019). Effects of bentonite on pore structure and permeability of cement mortar. Construction and Building Materials, vol. 224, 276-283, DOI: 10.1016/j.conbuildmat.2019.07.073.

26. Man, X.Y., Haque, M.A., Chen, B. (2019). Engineering properties and microstructure analysis of magnesium phosphate cement mortar containing bentonite clay. Construction and Building Materials, vol. 227, DOI: 10.1016/j.conbuildmat.2019.08.037.

27. ASTM C150 / C150M-19a, Standard Specification for Portland Cement, ASTM International, West Conshohocken, PA, 2019.

28. ASTM C618-19, Standard Specification for Coal Fly Ash and Raw or Calcined Natural Pozzolan for Use in Concrete, ASTM International, West Conshohocken, PA, 2019.

29. ASTM C109 / C109M-16a, Standard Test Method for Compressive Strength of Hydraulic Cement Mortars (Using 2-in. or [50-mm] Cube Specimens), ASTM International, West Conshohocken, PA, 2016.

30. ASTM C1437-15, Standard Test Method for Flow of Hydraulic Cement Mortar, ASTM International, West Conshohocken, PA, 2015.

31. ASTM C373-14a, Standard Test Method for Water Absorption, Bulk Density, Apparent Porosity, and Apparent Specific Gravity of Fired Whiteware Products, Ceramic Tiles, and Glass Tiles, ASTM International, West Conshohocken, PA, 2014.

32. Alex, J., Dhanalakshmi, J., Ambedkar, B. (2016). Experimental investigation on rice husk ash as cement replacement on concrete production. Construction and Building Materials, vol. 127, 353-362, DOI: 10.1016/j.conbuildmat.2016.09.150.

33. Muthukrishnan, S., Gupta, S., Kua, H.W. (2019). Application of rice husk biochar and thermally treated low silica rice husk ash to improve physical properties of cement mortar. Theoretical and Applied Fracture Mechanics, vol. 104, 12, DOI: 10.1016/j.tafmec.2019.102376.

34. Mesboua, N., Benyounes, K., Benmounah, A. (2018). Study of the impact of bentonite on the physico-mechanical and flow properties of cement grout. Cogent Engineering, vol. 5, no. 1, DOI: 10.1080/23311916.2018.1446252.

35. Rong, Z.D., Ding, J.Y., Cui, Z.J., Sun, W. (2019). Mechanical properties and microstructure of ultra-high performance cement-based composite incorporating RHA. Advances in Cement Research, vol. 31, no. 10, 472-480, DOI: 10.1680/jadcr.17.00209.

36. Gopalakrishnan, R., Jeyalakshmi, R. (2020). The effects on durability and mechanical properties of multiple nano and micro additive OPC mortar exposed to combined chloride and sulfate attack. Materials Science in Semiconductor Processing, vol. 106, DOI: https://doi.org/10.1016/j.mssp.2019.104772

37. Izzat, A.M., Al Bakri, A.M.M., Kamarudin, H., Sandu, A.V., Ruzaidi, G.C.M., Faheem, M.T.M., Moga, L.M. (2013). Sulfuric acid attack on ordinary portland cement and geopolymer material. Revista De Chimie, vol. 64, no. 9, 1011-1014

38. T Nijland, T.G., Larbi, J.A. (2010). Microscopic examination of deteriorated concrete. Maierhofer, C., Reinhardt, H.-W., Dobmann, G. (Eds.), Non-Destructive Evaluation of Reinforced Concrete Structures, Woodhead Publishing, vol. 1, 137-179.

39. Feng, P., Garboczi, E.J., Miao, C.W., Bullard, J.W. (2015). Microstructural origins of cement paste degradation by external sulfate attack. Construction and Building Materials, vol. 96, 391-403, DOI: 10.1016/j.conbuildmat.2015.07.186.

40. Panesar, D.K. (2019). Supplementary cementing materials. Mindess, S. (Eds.), Developments in the Formulation and Reinforcement of Concrete (Second Edition), Woodhead Publishing, 55-85.

41. Boudache, S., Roziere, E., Loukili, A., Colina, H. (2018). Influence of thermal preconditioning on the mechanism of external sulphate attack. Men é ndez, E., Baroghel-Bouny, V.e.r. (Eds.), External Sulphate Attack - Field Aspects and Lab Tests, vol. 21, Springer, Spain

APPENDIX D

Research article 2 (Indexed by TCI, tier 1)

Kueaket, K., & Tonnayopas, D. (2021). Sustainable mortar and concrete made from palm oil boiler clinker aggregate comprising rice husk ash and calcium bentonite: Compressive strength and durability assessment. *Journal of Applied Science*, 20(1), 39-55. doi: 10.14416/j.appsci.2021.01.004

Research Article

Sustainable mortar and concrete made from palm oil boiler clinker aggregate comprising rice husk ash and calcium bentonite: Compressive strength and durability assessment

Kamolchanok Kueaket [1] and Danupon Tonnayopas[1*]

[1]Department of Mining and Materials Engineering, Faculty of Engineering, Prince of Songkla University, Songkhla 90112, Thailand
*E-mail: danupon.t@psu.ac.th

Abstract

This research was conducted to assess the performances of mortars and concretes made from palm oil boiler clinker aggregate (POBC) blending with rice husk ash (RHA) and calcium bentonite (CB). These blends were used to substitute of ordinary Portland cement (OPC) in the combined proportions of 5wt%CB+5wt%RHA, 5wt%CB+15wt%RHA, 15wt%CB+5wt%RHA, 10wt%CB+20wt%RHA, and 20wt%B+10wt%RHA. The POBC mortars were examined for compressive strength, water absorption, sulfuric acid resistance, and microstructural characterization at the age of 7, 28, and 56 days. Subsequently, the POBC concretes were tested for rapid chloride ion permeability and capillary absorption at 28 and 56 days of curing ages. As a result, the 56-day POBC mortar with the optimum blending of 5% CB and 15% RHA provided the greatest compressive strength of 48 MPa as well as revealed denser microstructure observed under scanning electron microscope (SEM) and greater durability against sulfuric acid attack which surpassed those of the POBC mortar without CB and RHA. Proportionately, the incorporation of 5-10% CB with 15-20% RHA to POBC concrete cured up to 56 days possessed greater durability performances by reducing the chloride ion permeability from moderate to very low ranges as well as lessening capillary absorption. The practical implications of this study are that the POBC could be potentially used in the building sector as a substitute to the conventional aggregates. In addition, the use of CB and RHA could be possibly replaced cement in the optimum proportions without compromising the strength and durability to produce efficiently sustainable POBC mortar and concrete.

Keywords: palm oil boiler clinker, rice husk ash, calcium bentonite, compressive strength, sulfuric acid resistance, chloride ion permeability

Introduction

In 2021 to 2022, the prediction of construction aggregate demand in Asia-Pacific region would be reached to approximately 45,000 million of tonnes (Wiwattananukul et al., 2019). Specifically, the estimate construction aggregate demand in Thailand was 50 million of tonnes annually, and it was predicted to be increased by 20% of each year (Material resources management division, 2019). Conversely, the construction aggregate reserve was approximately 8,010 million of tonnes in Thailand (Innovation in Raw Materials and Primary Industries Division, 2020). Thus, it is apparent that the construction aggregate demand has been inversely

proportional to the nonrenewable aggregate reserve. Therefore, the alternative construction aggregate sources should be essentially studied and further brought to use. The demolition waste of construction and industrial waste have been widely applied in the sustainable construction material sectors.

Utilization of local waste materials in construction applications has a great impact on reducing the waste itself, land-fill used, environmental pollutions, and consumption of natural construction materials (Halahla et al., 2019). These impacts also promote sustainable construction towards waste manipulation. To reduce the consumption of the natural construction material and increase the exploitations of waste by-products, the natural aggregate and the cement can be efficiently replaced by the waste by-products such as copper slag (Siddique et al., 2020), granulated blast-furnace slag (Maghool et al., 2020), brick waste (Dang & Zhao, 2019), and fly ash (Chindaprasirt et al., 2020; Klimek et al., 2020; Shakir et al., 2020; Siddique et al., 2020).

Palm oil boiler clinker (POBC) was considered as a rigid solid waste which obtained from local crude palm oil plant. This waste was generated after the combustion of solid palm oil wastes inside boiler and caused the disposal area used and environmental pollutants (Hamada et al., 2020). In regard to the rigid properties and chemical compositions of POBC, the feasibility usages had been studied in term of sustainable construction application as a building material replacements (Shakir et al., 2019). According to Chai et al (2017), POBC can be potentially used as up to 50% of coarse aggregate substitution in size of 4.75-9 mm. Besides, at 100% of POBC coarse aggregate replacement for concrete with w/b ratio of 0.53, the 28-day compressive strength was up to 33 MPa which was only 30% lower than the reference mix made of granite aggregate (Abutaha et al., 2016). Moreover, natural sand can be completely substituted by POBC fine aggregate for eco-mortar production with a minor effect on compressive strength (Kanadasan et al., 2018). The percentage replacement of natural sand by POBC was recommended between 40 to 60% to maintain the mechanical properties (Babalghaith et al., 2020). Although, the studies of using POBC as an aggregate substitution in concrete, asphalt, and geopolymer productions and its mechanical properties have been reported by several researchers , the durability of those composites have not yet been clearly characterized in order to determine the suitability usage and application of POBC. Besides, the study of using 100% of POBC as coarse and fine aggregate with other type of waste as a binder and its durability characteristics have not been reported elsewhere.

Additionally, rice husk ash (RHA) is one of the most useful materials in cement industry. Several important roles of RHA as a pozzolan in cementitious material had been revealed, it could reduce the capillary pore and promote long term compressive strength of concrete, especially, for the low carbon RHA (Kang et al., 2019; Sandhu & Siddique, 2017). The pozzolanic activity was promoted by the addition of RHA which resulted in the micro-filler effect that filled up the capillary pore of cement matrix by the production of calcium silicate hydrate gels (C-S-H gels) (Gill & Siddique, 2018). Besides, the efficiency of using RHA as a cement replacement on acid resistance was also found that concrete incorporating RHA performed the superior resistance due to the pozzolanic activity consumed calcium hydroxide (CH) content and strengthened the bond between different phases in microstructure by producing more C-S-H (Koushkbaghi et al., 2019). Conversely, the large amount of RHA replacement in concrete can be decreased the compressive strength (Umasabor & Okovido, 2018).

Furthermore, calcium bentonite (CB) was addressed for a natural pozzolan (Memon et al., 2012). The Pakistani bentonite or CB was partially replaced by weight of cement and found that the compressive strength of 56-day mortar containing 12-15% CB as a cement replacement can reach approximately 30 MPa, which was significantly 2.7% higher than that of without adding

CB. The pore filling effect of using up to 10% CB replaced by weight of cement was achieved in mortar cured up to 28 days. This effect established the particle packing improvement and a decrease in water absorption due to the very-fine grain particles of CB (Ahmad et al., 2011).

This research aims to utilize the local waste by-products and evaluate the performances of mortars and concretes containing POBC aggregate with the combination of RHA and CB as a cement replacements. The compressive strength, water absorption, and sulfuric acid (H_2SO_4) resistance of POBC mortars were carried out at the age of 7, 28, and 56 days. In addition, the POBC concretes cured at 28 and 56 days were determined for rapid chloride ion permeability and 72-hour capillary absorption. Accordingly, the microstructures of POBC mortar containing CB and RHA blends were characterized via scanning electron microscope (SEM).

Materials and methods

Ordinary Portland cement (OPC) as per ASTM C150 was used in this study. POBC was collected from disposal area of oil palm plant at Surat Thani province, as received POBC was displayed in Figure 1a. The POBC was washed, dried, and crushed with jaw crusher to achieve the POBC coarse aggregate (POBCCA) and gyratory crusher to achieve the POBC fine aggregate (POBCFA), as depicted in Figure 1b-c. The enlargement of the POBC mortar's cross-section obtained from stereo microscope is shown in Figure 1d. The mineralogical characteristics of POBC were characterized via X-ray diffraction (XRD) analysis, as shown in Figure 2. The mineral compositions of POBC consisted of whitlockite, diopside, and three polymorphs of SiO_2, which were quartz, tridymite, and crystobalite. The green color of POBC can be accounted for the mineral composition of diopside. The properties of POBC aggregates were listed in Table 1. Conforming to ASTM C131 (2020) and BS 182-112 (1990), the POBCCA is not recommended for using in road surfacing, structural works, or heavy duty constructions due to the lower resistance to crushing and abrasion. In addition, CB was purchased from supplier (product of Thailand), as seen in Figure 1b.

RHA was obtained after the open air burning of using rice husk as a biomass fuel in Phatthalung province. Then, it was calcined with an electrical furnace at 700 °C for 1 hour (HR: 5 °C/min) in order to reduce the contaminated organic matters or unburned carbon. After calcining process, RHA was ground with jar mill at rotation speed of 65 revolution per minute for 12 hours to meet the requirement of ASTM C618 (2019). The chemical compositions and particle size of CB and RHA were analyzed via wavelength dispersive X-ray fluorescence spectrophotometer (WDXRF) and laser particle size analyzer (LPSA), as tabulated in Table 2. The XRD pattern of RHA is depicted in Figure 3. The RHA composed of few crystalline phase of crystobalite and quartz, mostly contained amorphous silica, which confirmed by the broad hump peak between 2Θ of 15° to 25° and other wide range of low intensity peaks, as presented in the dashed line circle. The particle size distributions of the binders and aggregates used are shown in Figure 4.
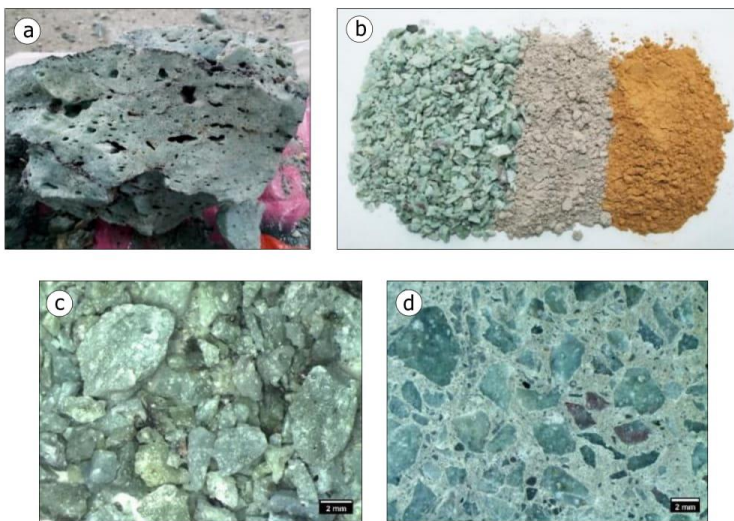
Figure 1 As received POBC (a), from left to right: crushed POBC as a fine aggregate, rice husk ash, and calcium bentonite (b), enlargement of POBC fine aggregate (c), and cross-section of mortar made of POBC fine aggregate (d)
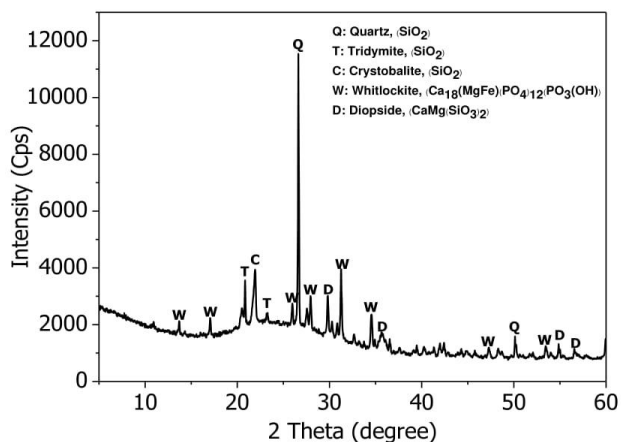
Figure 2 XRD pattern and phase compositions of POBC

Table 1 The physical properties of POBC aggregates

Properties	POBCCA	POBCFA
Organic impurity (ASTM C40, 2020)	None	
24-hour water absorption (%)	2.80	3.10
Specific gravity	2.28	2.40
Unit weight (kg/m^3)	1,182	1,350
Fineness modulus	5.30	3.70
Aggregate impact value (%)	36	-
Los Angles abrasion (%)	38	-

Table 2. The chemical and physical properties of CB and RHA

	CB	RHA
Chemical compositions		
SiO_2 (%)	56.62	93.93
Fe_2O_3 (%)	0.02	0.36
Al_2O_3 (%)	19.81	0.33
SO_3 (%)	0.69	0.21
$SiO_2 + Fe_2O_3 + Al_2O_3$ (%)	76.45	94.62
Loss on ignition (%)	10.12	0.67
Physical properties		
D_{10} (μm)	0.6	2.3
D_{50} (μm)	2.3	12.5
D_{90} (μm)	14.2	38.6
$D[4,3]$ (μm)	5.5	16.5
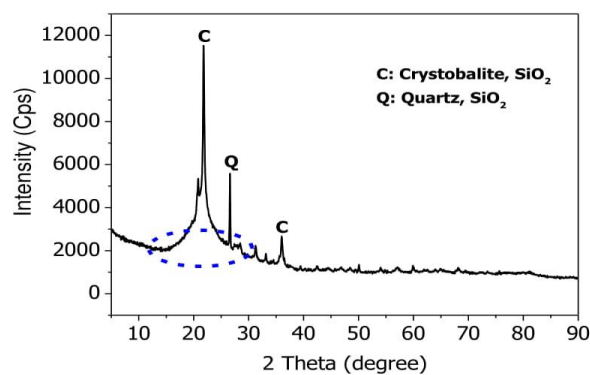
Figure 3 XRD pattern and phase compositions of RHA
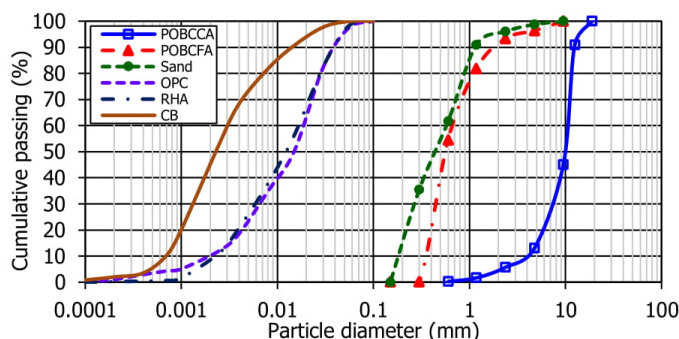
Figure 4 Particle size distribution of POBC aggregates and binders

Mix designation

      Mix designations of POBC mortar and concrete were done complying with ASTM C109 (2016), ASTM C192 (2019), and ACI 211.1 (1991). For both of POBC mortar and concrete, the blending of RHA and CB partially replaced by weight of OPC, as followed in Table 3. For example, the mix designation B5R5 was the combination between 5% CB and 5% RHA replaced by weight of OPC. The POBC mortar specimen was taken for determine the compressive strength, water absorption, and resistance to sulfuric acid (H_2SO_4) attack. The POBC concrete specimen was taken for determine the rapid chloride permeability and capillary absorption. For the POBC mortar mix designations, 50-mm cube specimens were casted with the binder to aggregate ratio of 1:2.75 and water to binder ratio of 0.48. The percentage flow of fresh mortar was determined as per ASTM C1437 (2015). Then, the hardened mortar specimens were cured in saturated lime water at ambient temperature (25±5°C) with 80-85% relative humidity for 7, 28, and 56 days. For the POBC concrete mix designations, 100 mm diameter with 50 mm length concrete discs were prepared by using natural sand (F.M 3.15), POBCCA with maximum size of 10 mm (F.M. 5.31), and taken water to binder ratio of 0.48. The concrete specimens were cured in the same condition of POBC mortar for 28 and 56 days.

Table 3 The mix designations of POBC mortar for various combination ratios of RHA and CB

Mix designations	Mix proportions									
	POBC mortar					POBC concrete				
	Binder (kg/m^3)			POBCFA (kg/m^3)	Flow (%)	Binder (kg/m^3)			Sand (kg/m^3)	POBCCA (kg/m^3)
	OPC	CB	RHA			OPC	CB	RHA		
Control	500	0	0	1,375	121	500	0	0	1,175	765
B5R5	450	25	25	1,375	119	450	25	25	1,175	765
B5R15	400	25	75	1,375	108	400	25	75	1,175	765
B15R5	400	75	25	1,375	112	400	75	25	1,175	765
B10R20	350	50	100	1,375	101	350	50	100	1,175	765
B20R10	350	100	50	1,375	103	350	100	50	1,175	765

Test procedures

The compressive strength and water absorption of POBC mortar were prepared and tested in accordance with ASTM C109 (2019) and ASTM C373 (2014). The strength activity index was determined according to ASTM C618 (2019). Resistance to 0.005 M sulfuric acid attack (pH=2.5) was measured by the comparison between the weight and compressive strength of POBC mortars before exposure and after exposure to sulfuric acid solution at particular curing ages. The sulfuric acid was renewed every week in order to maintain the pH value of the solution. The sulfuric acid resistance test was conducted for 6 weeks. The rapid chloride permeability test and capillary absorption test of POBC concretes were performed conforming to ASTM C1202 (2019) and ASTM C1585 (2020). The tests set up of the rapid chloride ion permeability and the capillary absorption are presented in Figure 5. For the microstructural characterization, the POBC mortars cured at 56 days were investigated using scanning electron microscope (SEM) at the accelerate voltage of 20 kV.
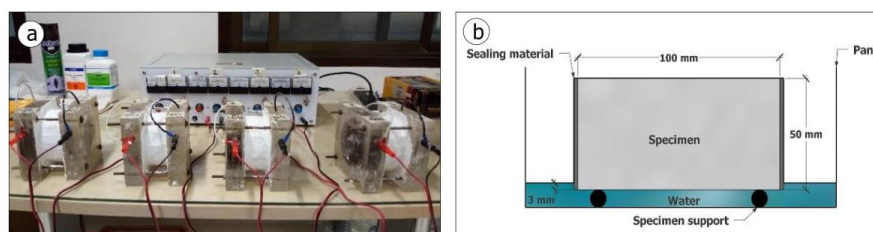
Figure 5 Schematics of rapid chloride permeability (a) and capillary absorption test (b) configurations

Results and discussion
1. Compressive strength

The compressive strength of mortar specimens cured in saturated lime water for a period of 7, 28, and 56 days are shown in Figure 6. Overall, the compressive strength of all mix designations was increased with curing ages. It can be observed that the compressive strength of mix designations B10R20 and B5R15 were equivalent to or higher than that of the control mix at the age of 28 and 56 days. Particularly, the highest 56-day compressive strength of 48 MPa was found in the mix B5R15, which was greater than that of the control mix by 7%. However, a reduction in 56-day compressive strength was found in the mix B5R5, B15R5, and B20R10. Which was lesser than that of the control mix by 11%, 16%, and 15%, respectively. According to these results, it can be seen that the mix designations containing more RHA/CB ratios (B5R15 and B10R20) and taken up to 28-day curing ages could be maintained and provided the development of the compressive strength in comparison to the control mix, B5R5, B15R5, and B20R10. These compressive strength results comply with those of (Joshaghani & Moeini, 2018). Who reported that the compressive strength of 90-day mortar containing 15% RHA was 6% greater than that of the mixture without RHA. Additionally, the compressive strength of 28-day mortar specimen containing 6% bentonite was higher than that of the control specimen by 3% (Memon et al., 2012). However, the effects of hybrid mixes between RHA and CB have not been studied and reported elsewhere. Therefore, according to the compressive strength results of this study, the mix designation B5R15 and B10R20 can be recommended as the optimum CB/RHA ratios for using as an OPC replacement without detrimental to the compressive strength.
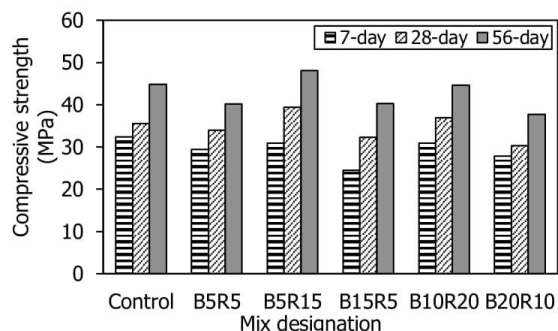
Figure 6 Compressive strengths of POBC mortars with different mix designations at the age of 7, 28, 56 days

2. Strength activity index

The strength activity index (SAI) of all mix designations is demonstrated in Figure 7. The determination of SAI is to indicate that the SCMs or any tested materials have the pozzolanic properties. According to ASTM C618 (2019), the requirement of SAI is considered as more than 75%. For the mixture containing the hybrid mixes of RHA and CB, the SAI values of those mix designations were in the range of 76-111%. In addition, the SAI of those mixes were meet the standard requirement and significantly increased with ages. In addition, the highest SAI was found in the mix B5R15 at the age of 28 days. This finding is in line with Man et al. (2019) and Rehman et al. (2020). The development of SAI and compressive strength could be due to the chemical compositions of RHA and CB. Which mainly consisted of silica (SiO_2). Moreover, the amount of SiO_2+ Fe_2O_3+ Al_2O_3 contents were more than 70%. Thus, the active silica could be reacted with $Ca(OH)_2$ and promote and pozzolanic reaction's products caused the improvement in compressive strength (Man et al., 2019; Rehman et al., 2020).
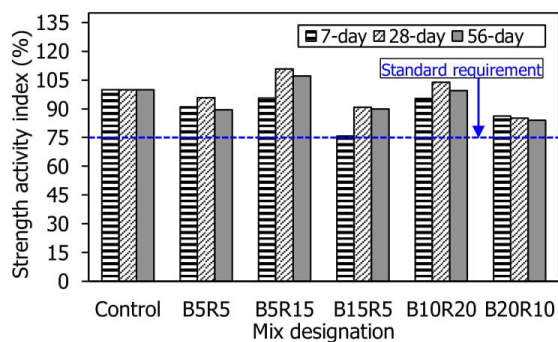
Figure 7 Strength activity index of POBC mortars with different mix designations at the age of 7, 28, 56 days

3. Water absorption

The water absorption of different mix designations at the ages of 7, 28, and 56 days is shown in Figure 8. The water absorption of all mix designations was decreased with prolonged curing ages. Meanwhile, at the early age of curing, the water absorption of the hybrid mix designations was similar to the control mix. At the age of 28 and 56 days, the percentage of water absorption was decreased by 15 to 26% for the mix B5R5, B5R15, and B10R20, when compared to that of the control mix. The lowest percentage of water absorption was found in the mix B5R15 at the age of 28 and 56 days, which was 26% lesser than the control mix. Jamil et al. (2016) pointed out that the filler effect and secondary C-S-H products from pozzolanic reaction of RHA filled up the pore space in the cement matrix and caused the reduction in the water absorption. Furthermore, the reduction in the water absorption was also found in the specimen containing up to 10% bentonite. This is due to the micro-filling effect of very fine-grain bentonite that can improve the particle packing of binder and reduce the water to binder ratio (Ahmad et al., 2011; Mesboua et al., 2018). However, an adverse effect of more bentonite contents could be attributed to the unreacted bentonite particles within the cement matrix absorbed more water, thus the water absorption of specimen containing more bentonite increased (Ahmad et al., 2011).

Although, the control mix revealed the highest 56-day water absorption while provided the greater compressive strength than the mix designation B5R5, B15R5, and B20R10. This could be due to the complex mechanism between RHA and CB, which contributed greatly to both of the pozzolanic reaction and filler effect. For the mechanism of RHA, the very-fine grain particle substantially improved pore size, reduced water absorption, and was ineffective to the strength development due to the pozzolanic reaction takes place in prolonged curing period. Moreover, this mechanism was confirmed by Bheel et al. (2020) that an increase in dosage of RHA replacement decreased the water absorption, whereas only the optimized 5% of RHA increased the compressive strength at the age of 28 days. Correspondingly, the significance mechanism of CB is pore refinement and improving the impermeability of cement matrix (Masood et al., 2020; Rehman et al., 2019). Liu et al. (2020) also concluded that the incorporating 10% CB developed the durability by filling effect and only the C-S-H gel formed on the surface of the specimen, whereas the strength development index need to be included (i) the forming of ettringite and (ii) the overlapping of hydration product on the specimen's surface.
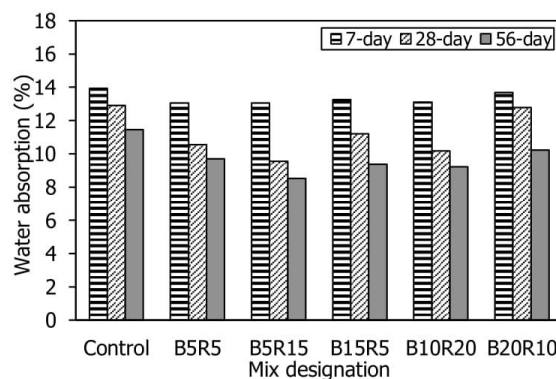
Figure 8 Water absorption of POBC mortars with different mix designations at the age of 7, 28, 56 days

4. Resistance to sulfuric acid attack
Weight loss
The weight loss of mortars at different curing ages exposed to 0.005 M sulfuric acid solution for 42 days is shown in Figure 9. It can be observed that the weight loss of all mix designations was decreased with curing age before exposure to sulfuric acid solution. At the later age, 56 days of curing, the ranges of weight loss for all hybrid mix designations were lesser than the control mix. Which were in the range of 1 to 44%. Especially, for the mix containing more combination ratio of RHA/CB (B10R20 and B5R15), the weight loss was up to 41 and 44% lower than that of the control mix. This is mainly attributed to (i) the less water absorption and (ii) the pozzolanic activity from the silica compositions of RHA (94% SiO_2) was greater than CB (57% SiO_2) which contributed to an increase in C-S-H forming and resulted in more impermeable matrix. Thus, the more durability was obtained in the mix containing more RHA contents (Ahmad et al., 2011). Correspondingly, the mix designation B5R15 showed a lesser surface erosion than that of the control mix, as shown in Figure 10. Min & Song (2018) also reported that the crucial corrosion can be indicated in the yellow color area that appeared on the exposed surface of the cement composite to sulfuric acid solution.

Compressive strength loss
The compressive strength loss of mortars exposed to 0.005 M sulfuric acid solution is shown in Figure 11. After 42 days of exposure, the compressive strength loss is seen in all mix designations. In accordance with the weight loss results, a similar trend was observed in the compressive strength loss. An increase in curing ages before sulfuric acid attack and the more RHA/CB ratios decreased the loss in compressive strength. The lowest compressive strength loss was found in the mix B5R15 at the age of 56 days. Which was 18 % lower than that of the control mix. This finding suggests that up to 20% of OPC can be replaced by the combination blend of CB and RHA at the optimum CB/RHA ratio as in the mix designation B5R15, which produced the development both in the compressive strength and durability.
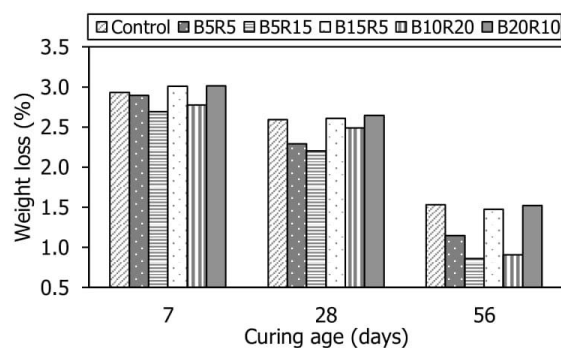
Figure 9 Weight loss of POBC mortars with different mix designations cured at 7, 28, and 56 days exposed to 0.005 M sulfuric acid solution for 42 days
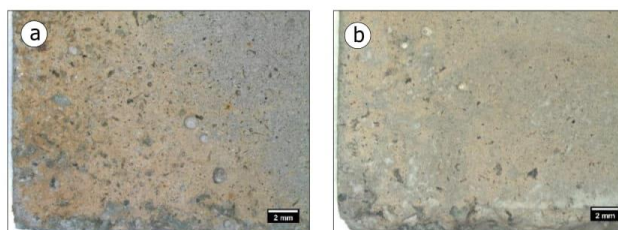
Figure 10 Enlargement of the surface of 56-day mortars: control mix (a) and mix designation B5R15 (b) after exposed to 0.005 M sulfuric acid solution for 42 days
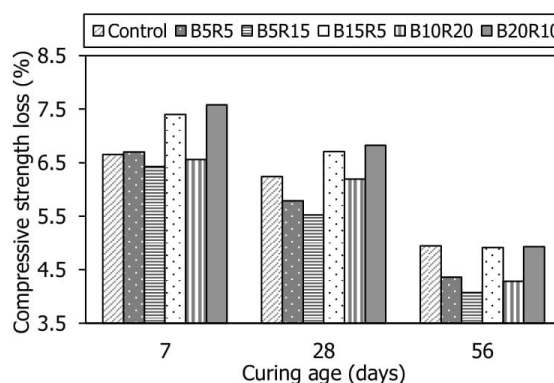
Figure 11 Compressive strength loss of POBC mortars with different mix designations cured at 7, 28, and 56 days exposed to 0.005 M sulfuric acid solution for 42 days

5. Rapid chloride permeability and capillary absorption

The total charge passed and capillary absorption of different mix designations and curing ages are given in Figure 12. According to ASTM C1202 (2019), the qualitative indication of chloride ion permeability of any concrete specimen was determined as followed: the total charges passed of concrete specimens that fall in the range of (i) >4,000 coulombs, (ii) 2,000-4,000 coulombs, (iii) 1,000-2,000 coulombs, and (iv) 100-1,000 coulombs were considered as high permeability, moderate permeability, low permeability, and very low permeability, respectively. A decrease in chloride ion permeability was observed in all hybrid mixes with prolonged curing ages. As compared to the control mix, the decrease was in the range of 4-77% and 30-78% at the age of 28 and 56 days, respectively. At the age of 56 days, the chloride ion permeability of the mix designations B5R15 and B10R20 was in very low ranges. For the mix designations B5R5, B15R5, and B20R10 cured at 56 days, the chloride ion permeability was in the low range, whereas the chloride ion permeability of the control mix was in the moderate range. Consequently, the capillary absorption results corresponded to the chloride ion permeability. An increase in curing ages decrease capillary absorption. The significant reduction in the 72-hour capillary absorption

was found in the mix designations B5R15 and B10R20 at the age of 56 days, which were lower than the control mix by 44% and 56%, respectively. It can be seen that the chloride permeability and the capillary absorption decreased with an increase in curing ages and RHA/CB ratios, as was found in mixture designations B5R15 and B10R20. Ganesan et al. (2008) also found that the chloride permeability and rate of capillary absorption had a good relationship due to the reduction of permeable voids in matrix by the pozzolanic activity of RHA as an additive and the prolonged curing ages. This finding also in agreement with those of Huang et al. (2017), Laidani et al. (2020), and Zareei et al. (2017) that the capillary absorption and chloride ion penetration of concrete specimen containing RHA were reduced by an increase in the RHA content, while only adding up to 10% bentonite could reduce the capillary absorption. Moreover, an increase in RHA content up to 20% reduced the 72-hour capillary absorption by 15%, compared to the specimen without RHA (Zahedi et al., 2015).
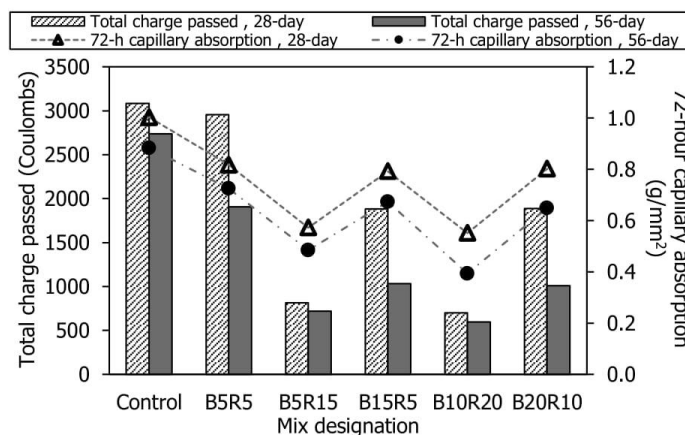
Figure 12 The chloride ion permeability and 72-hour capillary absorption of POBC concrete with different mix designations at the age of 28 and 56 days

6. Microstructural characterization

The SEM images are demonstrated the comparison between OPC particles and combination blends of OPC, RHA, and CB particles of the mix designation B5R15 as shown in Figure 13a-b. It can be seen that the different in particle sizes among OPC, RHA, and CB played the important role in increasing the particle packing of the binder. An increase in particle packing was observed in the binder of the mix designation B5R15 in comparison to the pure OPC particles. Accordingly, the very fine micro-particles of CB and rounded agglomerate RHA particles also contributed to the reduction in water content of the binder due to RHA and CB absorbed more water (Ahmad et al., 2011; Mesboua et al., 2018). The SEM images of the hardened pastes of the control mix and mix designation B5R15 are illustrated in Figure 13c-d. It can be clearly seen that the hydration's products were found in both mix designations. Particularly, the mix designation B5R15 manifested denser matrix and lower micro-pore spaces when compared to the control mix. The dense flocs-like C-S-H was obviously found in the groundmass of the mix

designation B5R15 and the micro-pore spaces were reduced by the spreading of the dense C-S-H framework. For the matrix of the control mix, the loosely fibrous-like and flocs-like C-S-H were found. The more C-S-H embedded in the mix containing RHA and CB could be due to the pozzolanic activity that consumed free $Ca(OH)_2$ from both of hydration and pozzolanic reaction's products, then produced more C-S-H (Chopra et al., 2015; Masood et al., 2020). Besides, the denser microstructure could be attributed to the development in compressive strength, the reduction in water absorption, and the durability improvement of the mix designation B5R15 in comparison to the control mix. The morphology of C-S-H observed from SEM images of this study was characterized and compared to the flocs-like C-S-H found by Yu et al. (1999), Cizer et al. (2007), and the fibrous-like C-S-H found by El-gama et al. (2018). However, the characteristics of C-S-H can be shown in various forms depended on the curing condition, additive used, water to binder ratios, and designation of mixture (Cizer et al., 2007; Shen et al., 2019).
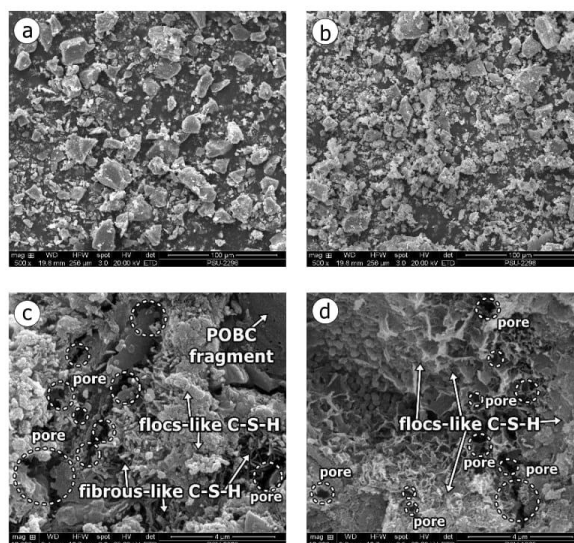
Figure 13 SEM images of OPC particles (a), blends consisted of OPC, CB, and RHA particles of mix designation B5R15 (b), the hardened paste cured at 56 days of the control mix (c), and the mix designation B5R15 (d)

Conclusion

Based on this study results, the conclusions can be provided as following:

(1) The POBC mortar with the optimum combination of 5% of CB and 15% of RHA replaced by weight of OPC (mix designation B5R15) developed the superior performance at the curing age up to 56 days when compared to the control and the others mix designations. Moreover, the mix designation B5R15 provided the highest compressive strength, the lowest water absorption, and the lowest weight and compressive strength loss due to sulfuric acid attack.

(2) The chloride ion permeability and capillary absorption decreased with an increase in RHA combination ratios and curing ages. The very low range of chloride ion permeability belonged

to the mix designation B5R15 and B10R20 cured at 56 days. However, the chloride ion permeability of the others mix designations were fallen into the low range except for the control mix that was continually fallen in the moderate range when the curing ages increased. The optimum combination of 5-10% of CB and 15-20% of RHA replaced by weight of OPC would be recommended for the chloride ion permeability resistance of the POBC concrete.

(3) According to the microstructure characterization using SEM images, the denser matrix occupied by C-S-H framework and lower pore spaces of the mix designation B5R15 in comparison to the control mix contributed to the compressive strength and durability improvement.

(4) Regarding to this investigation, the POBC can be used as an aggregate substitution for producing conventional mortars and concretes in non-structural construction work. The optimum combinations of CB and RHA for POBC mortars and concretes could help diminishing the cement used and promoting the durability performance.

Acknowledgements

References

Abutaha, F., Abdul Razak, H., & Kanadasan, J. (2016). Effect of palm oil clinker (POC) aggregates on fresh and hardened properties of concrete. *Construction and Building Materials, 112*, 416-423. doi:https://doi.org/10.1016/j.conbuildmat.2016.02.172

Ahmad, S., Barbhuiya, S. A., Elahi, A., & Iqbal, J. (2011). Effect of Pakistani bentonite on properties of mortar and concrete. *Clay Minerals, 46*(1), 85-92. doi:10.1180/claymin.2011.046.1.85

American Concrete Institute. (1991). *ACI 211.1-91: Standard Practice for Selecting Proportions for Normal, Heavyweight, and Mass Concrete* . Detroit, MI.

American Society for Testing and Materials. (2014). *ASTM C373-14a: Standard Test Method for Water Absorption, Bulk Density, Apparent Porosity, and Apparent Specific Gravity of Fired Whiteware Products, Ceramic Tiles, and Glass Tiles*, ASTM International, West Conshohocken, PA.

American Society for Testing and Materials. (2015). *ASTM C1437-15: Standard Test Method for Flow of Hydraulic Cement Mortar*, ASTM International, West Conshohocken, PA.

American Society for Testing and Materials. (2016). *ASTM C109/C109M-16a: Standard Test Method for Compressive Strength of Hydraulic Cement Mortars (Using 2-in. or [50-mm] Cube Specimens)*, ASTM International, West Conshohocken, PA.

American Society for Testing and Materials. (2019). *ASTM C150/C150M-19a: Standard Specification for Portland Cement*, ASTM International, West Conshohocken, PA.

American Society for Testing and Materials. (2019). *ASTM C192/C192M-19: Standard Practice for Making and Curing Concrete Test Specimens in the Laboratory*, ASTM International, West Conshohocken, PA.

American Society for Testing and Materials. (2019). *ASTM C618-19: Standard Specification for Coal Fly Ash and Raw or Calcined Natural Pozzolan for Use in Concrete*, ASTM International, West Conshohocken, PA.

American Society for Testing and Materials. (2019). *ASTM C1202-19: Standard Test Method for Electrical Indication of Concrete's Ability to Resist Chloride Ion Penetration*, ASTM International, West Conshohocken, PA.

American Society for Testing and Materials. (2020). *ASTM C40/C40M-20: Standard Test Method for Organic Impurities in Fine Aggregates for Concrete*, ASTM International, West Conshohocken, PA..

American Society for Testing and Materials. (2020). *ASTM C1585-20: Standard Test Method for Measurement of Rate of Absorption of Water by Hydraulic-Cement Concretes*, ASTM International, West Conshohocken, PA.

American Society for Testing and Materials. (2020). *ASTM C131/C131M-20: Standard Test Method for Resistance to Degradation of Small-Size Coarse Aggregate by Abrasion and Impact in the Los Angeles Machine*, ASTM International, West Conshohocken, PA.

Babalghaith, A. M., Koting, S., Sulong, N. H. R., Karim, M. R., & AlMashjary, B. M. (2020). Performance evaluation of stone mastic asphalt (SMA) mixtures with palm oil clinker (POC) as fine aggregate replacement. *Construction and Building Materials, 262*, 11. doi:10.1016/j.conbuildmat.2020.120546

Bheel, N., Keerio, M. A., Kumar, A., Shahzaib, J., Ali, Z., Ali, M., & Sohu, S. (2020). An investigation on fresh and hardened properties of concrete blended with rice husk ash as cementitious ingredient and coal bottom ash as sand replacement material. *Silicon*, 12. doi:10.1007/s12633-020-00906-3

British Standards Institute. (1990). *BS 812-112: Methods for determination of aggregate impact value (AIV)*. London.

Chai, L. J., Shafigh, P., Mahmud, H., & Aslam, M. (2017). Effect of substitution of normal weight coarse aggregate with oil-palm-boiler clinker on properties of concrete. *Sains Malaysiana, 46*(4), 645-653. doi:10.17576/jsm-2017-4604-18

Chindaprasirt, P., Kasemsiri, P., Leekongbub, S., & Posi, P. (2020). Durability of concrete containing recycled asphaltic concrete aggregate and high calcium fly ash. *International Journal of Geomate, 19*(74), 8-14. doi:10.21660/2020.74.5541

Chopra, D., Siddique, R., & Kunal. (2015). Strength, permeability and microstructure of self-compacting concrete containing rice husk ash. *Biosystems Engineering, 130*, 72-80. doi:10.1016/j.biosystemseng.2014.12.005

Cizer, O., Van Balen, K., Van Gemert, D., & Elsen, J. (2007). Carbonation and hydration of mortars with calcium hydroxide and calcium silicate binders. Paper presented at the Sustainable Construction Materials and Technologies - International Conference on Sustainable Construction Materials and Technologies.

Dang, J. T., & Zhao, J. (2019). Influence of waste clay bricks as fine aggregate on the mechanical and microstructural properties of concrete. Construction and Building Materials, 228, 9. doi:10.1016/j.conbuildmat.2019.116757

El-Gamal, S. M. A., Abo-El-Enein, S. A., El-Hosiny, F. I., Amin, M. S., & Ramadan, M. (2018). Thermal resistance, microstructure and mechanical properties of type I Portland cement pastes containing low-cost nanoparticles. Journal of Thermal Analysis and Calorimetry, 131(2), 949-968. doi:10.1007/s10973-017-6629-1

Ganesan, K., Rajagopal, K., & Thangavel, K. (2008). Rice husk ash blended cement: Assessment of optimal level of replacement for strength and permeability properties of concrete. *Construction and Building Materials, 22*(8), 1675-1683. doi:https://doi.org/10.1016/j.conbuildmat.2007.06.011

Gill, A. S., & Siddique, R. (2018). Durability properties of self-compacting concrete incorporating metakaolin and rice husk ash. *Construction and Building Materials, 176*, 323-332. doi:https://doi.org/10.1016/j.conbuildmat.2018.05.054

Halahla, A. M., Akhtar, M., & Almasri, A. H. (2019). Utilization of Demolished Waste as Coarse Aggregate in Concrete. *Civil Engineering Journal-Tehran, 5*(3), 540-551. doi:10.28991/cej-2019-03091266

Hamada, H. M., Jokhio, G. A., Al-Attar, A. A., Yahaya, F. M., Muthusamy, K., Humada, A. M., & Gul, Y. (2020). The use of palm oil clinker as a sustainable construction material: A review. *Cement & Concrete Composites, 106*, 19. doi:10.1016/j.cemconcomp.2019.103447

Huang, H., Gao, X., Wang, H., & Ye, H. (2017). Influence of rice husk ash on strength and permeability of ultra-high performance concrete. *Construction and Building Materials, 149*, 621-628. doi:https://doi.org/10.1016/j.conbuildmat.2017.05.155

Innovation in Raw Materials and Primary Industries Division. (2020). Construction aggregate reserve in Thailand. Retrieved from http://www.dpim.go.th/qry-stones/quarry3.php

Jamil, M., Khan, M. N. N., Karim, M. R., Kaish, A. B. M. A., & Zain, M. F. M. (2016). Physical and chemical contributions of rice husk ash on the properties of mortar. *Construction and Building Materials, 128*, 185-198. doi:https://doi.org/10.1016/j.conbuildmat.2016.10.029

Joshaghani, A., & Moeini, M. A. (2018). Evaluating the effects of sugarcane-bagasse ash and rice-husk ash on the mechanical and durability properties of mortar. *Journal of Materials in Civil Engineering, 30*(7), 14. doi:10.1061/(asce)mt.1943-5533.0002317

Kanadasan, J., Razak, H. A., & Subramaniam, V. (2018). Properties of high flowable mortar containing high volume palm oil clinker (POC) fine for eco-friendly construction. *Journal of Cleaner Production, 170*, 1244-1259. doi:https://doi.org/10.1016/j.jclepro.2017.09.068

Kang, S.-H., Hong, S.-G., & Moon, J. (2019). The use of rice husk ash as reactive filler in ultra-high performance concrete. *Cement and Concrete Research, 115*, 389-400. doi:https://doi.org/10.1016/j.cemconres.2018.09.004

Koushkbaghi, M., Kazemi, M. J., Mosavi, H., & Mohseni, E. (2019). Acid resistance and durability properties of steel fiber-reinforced concrete incorporating rice husk ash and recycled aggregate. *Construction and Building Materials, 202*, 266-275. doi:10.1016/j.conbuildmat.2018.12.224

Laidani, Z. E., Benabed, B., Abousnina, R., Gueddouda, M. K., & Khatib, M. J. (2020). Potential pozzolanicity of Algerian calcined bentonite used as cement replacement: optimisation of calcination temperature and effect on strength of self-compacting mortars. *European Journal of Environmental and Civil Engineering*, 23. doi:10.1080/19648189.2020.1713898

Liu, M. L., Hu, Y., Lai, Z. Y., Yan, T., He, X., Wu, J., Lv, S. Z. (2020). Influence of various bentonites on the mechanical properties and impermeability of cement mortars. *Construction and Building Materials, 241*, 12. doi:10.1016/j.conbuildmat.2020.118015

Maghool, F., Arulrajah, A., Horpibulsuk, S., & Mohajerani, A. (2020). Engineering and leachate characteristics of granulated blast-furnace slag as a construction material. Journal of Materials in Civil Engineering, 32(7), 10. doi:10.1061/(asce)mt.1943-5533.0003212

Man, X. Y., Haque, M. A., & Chen, B. (2019). Engineering properties and microstructure analysis of magnesium phosphate cement mortar containing bentonite clay. *Construction and Building Materials, 227*. doi:10.1016/j.conbuildmat.2019.08.037

Masood, B., Elahi, A., Barbhuiya, S., & Ali, B. (2020). Mechanical and durability performance of recycled aggregate concrete incorporating low calcium bentonite. *Construction and Building Materials, 237*, 117760. doi:https://doi.org/10.1016/j.conbuildmat.2019.117760

Material resources management division. (2019). 100 million of tonnes construction aggregate for EEC construction project (5 years). Retrieved from https://www.bangkokbiznews.com/news/detail/844687

Memon, S. A., Arsalan, R., Khan, S., & Lo, T. Y. (2012). Utilization of Pakistani bentonite as partial replacement of cement in concrete. *Construction and Building Materials, 30*, 237-242. doi:https://doi.org/10.1016/j.conbuildmat.2011.11.021

Mesboua, N., Benyounes, K., & Benmounah, A. (2018). Study of the impact of bentonite on the physico-mechanical and flow properties of cement grout. *Cogent Engineering, 5*(1). doi:10.1080/23311916.2018.1446252

Min, H. G., & Song, Z. G. (2018). Investigation on the sulfuric acid corrosion mechanism for concrete in soaking environment. *Advances in Materials Science and Engineering*. doi:10.1155/2018/3258123

Rehman, S. U., Kiani, U. A., Yaqub, M., & Ali, T. (2020). Controlling natural resources depletion through Montmorillonite replacement for cement-low cost construction. *Construction and Building Materials, 232*, 9. doi:10.1016/j.conbuildmat.2019.117188

Rehman, S. U., Yaqub, M., Noman, M., Ali, B., Khan, M. N. A., Fahad, M., Gul, A. (2019). The influence of thermo-mechanical activation of bentonite on the mechanical and durability performance of concrete. *Applied Sciences-Basel, 9*(24). doi:10.3390/app9245549

Sandhu, R. K., & Siddique, R. (2017). Influence of rice husk ash (RHA) on the properties of self-compacting concrete: A review. *Construction and Building Materials, 153*, 751-764. doi:https://doi.org/10.1016/j.conbuildmat.2017.07.165

Shakir, A. A., Ibrahim, M. H. W., Othman, N. H., & Shahidan, S. (2019). The Effect of palm oil clinker and oil palm shell on the compressive strength of concrete. *Iranian Journal of Science and Technology-Transactions of Civil Engineering, 43*, 1-14. doi:10.1007/s40996-018-0176-2

Shen, W. G., Zhang, W. S., Wang, J., Han, C. Z., Zhang, B. L., Li, J. W., & Xu, G. L. (2019). The microstructure formation of C-S-H in the HPC paste from nano-scale feature. Journal of Sustainable Cement-Based Materials, 8(4), 199-213. doi:10.1080/21650373.2018.1564397

Siddique, R., Singh, M., & Jain, M. (2020). Recycling copper slag in steel fibre concrete for sustainable construction. *Journal of Cleaner Production, 271*, 10. doi:10.1016/j.jclepro.2020.122559

Umasabor, R. I., & Okovido, J. O. (2018). Fire resistance evaluation of rice husk ash concrete. *Heliyon, 4*(12), e01035. doi:https://doi.org/10.1016/j.heliyon.2018.e01035

Wiwattananukul, J., Sontamino, P., Masniyom, M., Rachpech, V., & Pantaweesak, P. (2019). *The Influence of the Population on the Use of Construction Aggregate in Songkhla Lake Basin*. Paper presented at the The 13th International Conference on Mining, Materials and Petroleum Engineering (CMMP2019), Krabi, Thailand.

Yu, Q., Sawayama, K., Sugita, S., Shoya, M., & Isojima, Y. (1999). The reaction between rice husk ash and $Ca(OH)_2$ solution and the nature of its product. Cement and Concrete Research, 29(1), 37-43. doi:https://doi.org/10.1016/S0008-8846(98)00172-0

Zahedi, M., Ramezanianpour, A. A., & Ramezanianpour, A. M. (2015). Evaluation of the mechanical properties and durability of cement mortars containing nanosilica and rice husk ash under chloride ion penetration. *Construction and Building Materials, 78*, 354-361. doi:https://doi.org/10.1016/j.conbuildmat.2015.01.045

Zareei, S. A., Ameri, F., Dorostkar, F., & Ahmadi, M. (2017). Rice husk ash as a partial replacement of cement in high strength concrete containing micro silica: Evaluating durability and mechanical properties. *Case Studies in Construction Materials, 7*, 73-81. doi:https://doi.org/10.1016/j.cscm.2017.05.001

APPENDIX E

Experimental materials preparation and mix designation

Experimental materials preparation and mix designation

1. Preparing POBC aggregates

The POBC raw samples were washed with tap water, scrubbed with brush and towel to diminish access clay minerals and organic matters from the waste disposal areas, then sun drying. After that, the POBC will be break into smaller size by sledge Hammer, crushed with jaw crusher for coarse aggregate and gyratory crusher for fine aggregate. The preparation process of POBC aggregate is illustrated in Figure 37.
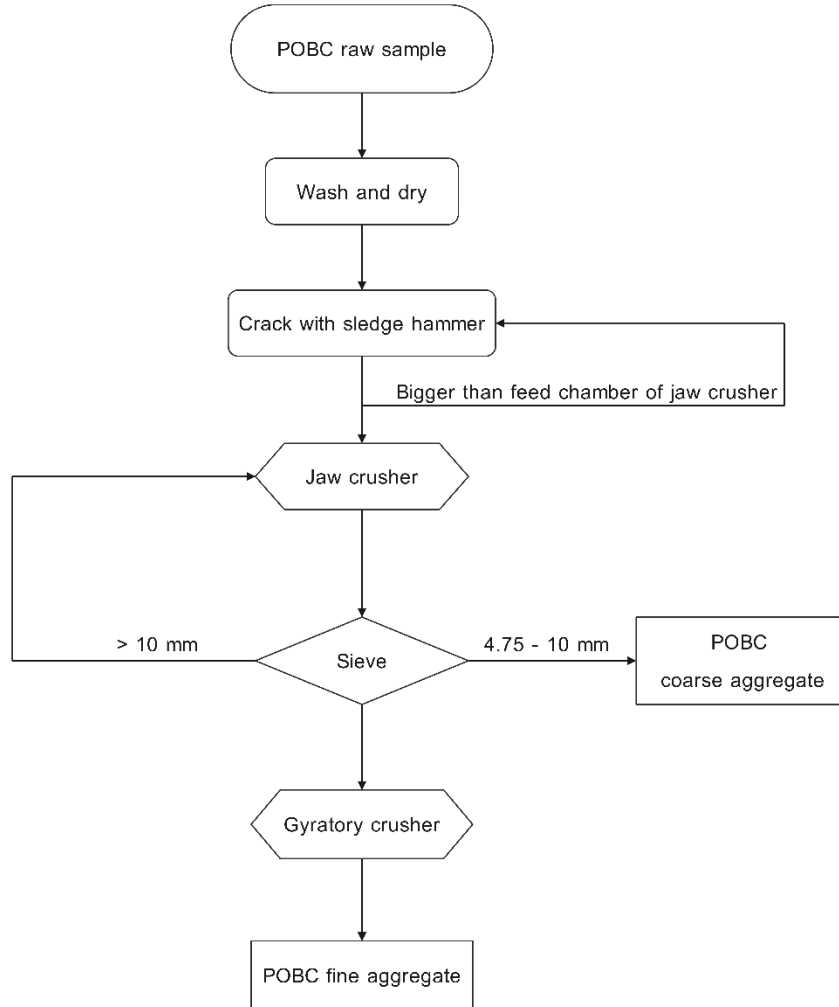
Figure 37 Flow chart of preparing POBC aggregate

2. Preparing RHA

The RHA obtained from the open-air burning of the rice husk for 72-84 hours until the RHA was cooled down. Then, the RHA was incinerated at 700 ºC by an electrical furnace and ground with jar mill for 12 hours (60-65 rpm). After that, the RHA was sampling and tested for laser particle size analysis. According to the test results (see in the results and discussions section), the particle size of RHA was lesser than 45 microns. The preparation process of RHA is presented in Figure 38.
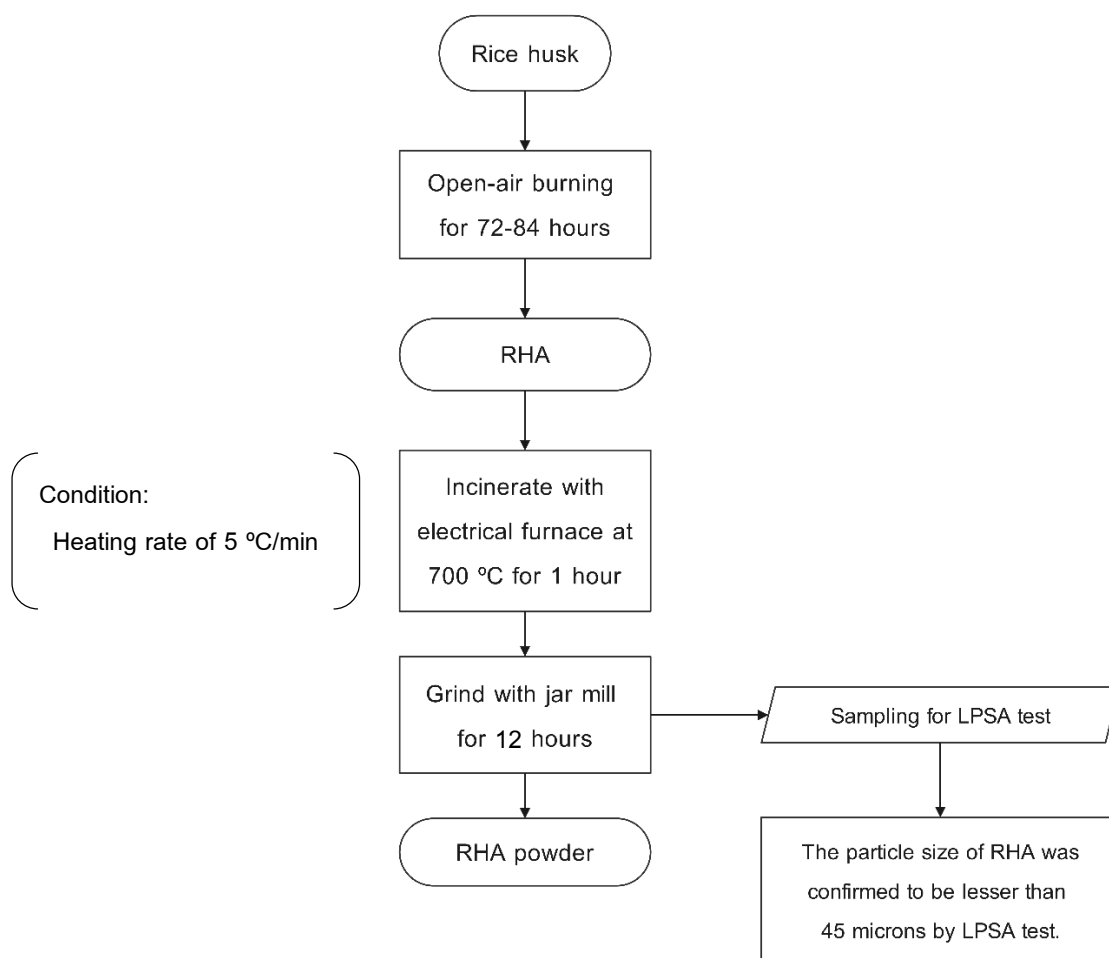
Figure 38 Flow chart of preparing RHA

3. Mix designation

The mixtures were designed in 3 levels for an OPC replacement. The RHA and CB were partially replaced an OPC, type 1 by weight of 10%, 20%, and 30%. The mixtures named R10, R20, and R30 were the mixes containing RHA as an OPC replacement for 10%, 20%, and 30%, respectively. The binary mixtures named B10, B20, and B30 were the mixes containing CB as an OPC replacement for 10%, 20%, and 30%, respectively. The ternary mixtures of CB and RHA named B5R5, B5R15, B15R5, B10R20, and B20R10. The proportions of these mixes for mortars and concretes were tabulated in Table 13. The mortar and concrete specimen will be cured in saturated-lime water at 29±3 ºC for 7, 28, 56 days and 28, 56 days, respectively. The mortar was designed as in accordance with ASTM C109 (2020). In addition, the concrete mix designs were based on ACI 211.1 (1991) for achieve compressive strength at 35 MPa in 28 days. The mortar and concrete specimens are shown in Figure 39.

Table 14 Mix proportions of POBC mortars and concretes

No.	Mix designation	w/b ratio	Mix proportion (kg/m^3)					
			OPC	Sand	POBCA	POBCFA	CB	RHA
POBC mortar								
1	Control	0.48	500	-	-	1,375	-	-
2	R10	0.48	450	-	-	1,375	-	50
3	R20	0.48	400	-	-	1,375	-	100
4	R30	0.48	350	-	-	1,375	-	150
5	B10	0.48	450	-	-	1,375	50	-
6	B20	0.48	400	-	-	1,375	100	-
7	B30	0.48	350	-	-	1,375	150	-
8	B5R5	0.48	450	-	-	1,375	25	25
9	B5R15	0.48	400	-	-	1,375	25	75
10	B15R5	0.48	400	-	-	1,375	75	25
11	B10R20	0.48	350	-	-	1,375	50	100
12	B20R10	0.48	350	-	-	1,375	100	50

Table 14 Mix proportions of POBC mortars and concretes (Continue)

No.	Mix designation	w/b ratio	Mix proportion (kg/m^3)					
			OPC	Sand	POBCA	POBCFA	CB	RHA
13	Control	0.48	500	1,175	765	-	-	-
14	R10	0.48	450	1,175	765	-	-	50
15	R20	0.48	400	1,175	765	-	-	100
16	R30	0.48	350	1,175	765	-	-	150
17	B10	0.48	450	1,175	765	-	50	-
18	B20	0.48	400	1,175	765	-	100	-
19	B30	0.48	350	1,175	765	-	150	-
20	B5R5	0.48	450	1,175	765	-	25	25
21	B5R15	0.48	400	1,175	765	-	25	75
22	B15R5	0.48	400	1,175	765	-	75	25
23	B10R20	0.48	350	1,175	765	-	50	100
24	B20R10	0.48	350	1,175	765	-	100	50
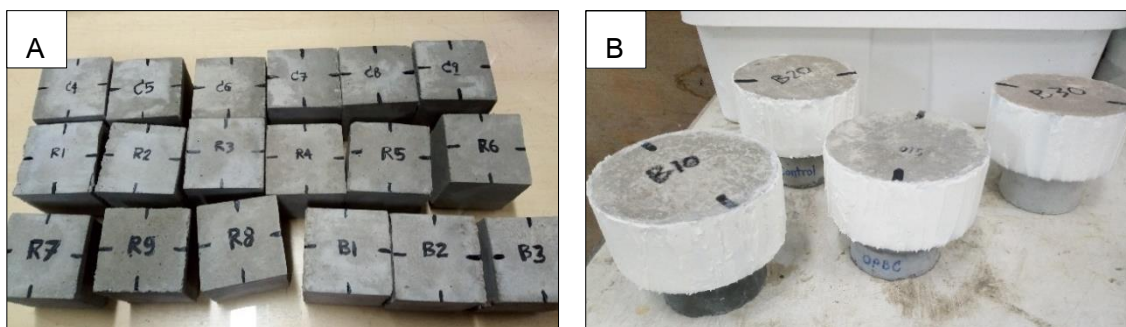
Figure 39 The POBC mortar specimens (A) and the POBC concrete prepared for RCPT test (B)

APPENDIX F

Properties of POBC mortars

Table 15 Compressive strength, apparent porosity, and water absorption of POBC mortars with different curing ages

Mix	Age (days)		T (°C)	RH (%)	Weight (g)	W (mm)	L (mm)	SSD-weight in air (g)	SSD-weight in water (g)	Oven-dry weight (g)	Porosity (%)	Water absorption (%)	Avg. porosity (%)	Avg. water absorption (%)	Maximum load (kN)	UCS (MPa)	Avg. UCS (MPa)
Control	7	1	28	89	247.12	51.20	48.83	252.734	120.590	220.310	24.54	14.72	24.55	14.73	78.19	31.27	31.30
		2	28	89	247.23	51.55	48.14	252.840	120.592	220.318	24.59	14.76			79.16	31.90	
		3	28	89	247.12	51.17	50.09	252.726	120.595	220.311	24.53	14.71			78.75	30.72	
	28	1	28	89	247.25	49.44	49.86	253.535	129.021	224.578	23.26	12.89	23.28	12.91	88.76	36.01	35.55
		2	28	89	247.25	50.34	50.25	253.602	129.028	224.577	23.30	12.92			89.22	35.27	
		3	28	89	247.25	50.13	49.88	253.576	129.027	224.590	23.27	12.91			88.45	35.37	
	56	1	28	89	243.79	47.78	47.62	250.858	130.125	225.084	21.35	11.45	21.35	11.45	105.01	46.15	44.86
		2	28	89	243.79	47.76	49.25	250.875	130.126	225.089	21.36	11.46			106.10	45.11	
		3	28	89	243.79	48.25	50.65	250.862	130.125	225.084	21.35	11.45			105.84	43.31	
R10	7	1	28	88	230.48	50.80	50.33	245.491	130.646	222.406	20.10	10.38	20.10	10.38	85.77	33.55	33.79
		2	28	88	230.52	50.73	48.11	245.499	130.644	222.416	20.10	10.38			82.16	33.66	
		3	28	88	230.50	50.41	49.81	245.493	130.654	222.421	20.09	10.37			85.74	34.15	
	28	1	28	88	247.32	50.21	50.86	253.398	131.264	230.328	18.89	10.02	18.90	10.02	108.29	42.41	41.08
		2	28	88	247.32	51.19	51.98	253.416	131.266	230.322	18.91	10.03			107.25	40.31	
		3	28	88	247.33	49.47	50.93	253.410	131.261	230.321	18.90	10.02			102.13	40.54	
	56	1	28	88	240.94	49.71	49.76	247.204	129.789	226.707	17.46	9.04	17.17	9.04	127.18	51.42	52.24
		2	28	88	240.95	47.62	49.79	247.204	126.792	226.701	17.03	9.04			124.55	52.53	
		3	28	88	240.94	49.71	49.16	247.210	126.799	226.726	17.01	9.03			129.02	52.79	

Table 15 Compressive strength, apparent porosity, and water absorption of POBC mortars with different curing ages (Continue)

Mix	Age (days)		T (°C)	RH (%)	Weight (g)	W (mm)	L (mm)	SSD-weight in air (g)	SSD-weight in water (g)	Oven-dry weight (g)	Porosity (%)	Water absorption (%)	Avg. porosity (%)	Avg. water absorption (%)	Maximum load (kN)	UCS (MPa)	Avg. UCS (MPa)
								Pre-curing → Post-curing									
R20	7	1	28	88	235.79	50.65	51.77	243.296	122.373	220.500	18.85	10.34	19.00	10.43	82.88	31.61	32.11
		2	28	88	235.79	51.01	50.15	243.320	122.380	220.288	19.04	10.46			83.54	32.66	
		3	28	88	235.79	50.20	51.00	243.308	122.395	220.196	19.11	10.50			82.11	32.07	
	28	1	28	88	233.99	50.40	50.98	241.821	125.483	222.224	16.84	8.82	16.80	8.80	113.26	44.08	45.07
		2	28	88	233.99	49.92	50.28	241.822	125.489	222.256	16.82	8.80			115.00	45.82	
		3	28	88	233.99	50.20	49.30	241.830	125.468	222.341	16.75	8.77			112.14	45.31	
	56	1	28	88	234.96	50.95	49.10	244.095	123.931	225.099	15.81	8.44	15.54	8.28	134.99	53.96	52.94
		2	28	88	234.96	50.82	49.98	244.097	123.934	225.097	15.81	8.44			132.80	52.28	
		3	28	88	234.97	50.95	49.63	244.099	123.946	226.092	14.99	7.96			132.98	52.59	
R30	7	1	28	88	232.60	50.76	50.36	240.066	120.055	217.433	18.86	10.41	18.86	10.41	78.72	30.79	30.90
		2	28	88	232.61	50.77	49.33	240.068	120.060	217.445	18.85	10.40			77.45	30.92	
		3	28	88	232.62	50.76	50.16	240.069	120.071	217.432	18.86	10.41			78.85	30.97	
	28	1	28	88	244.74	50.78	51.32	242.417	122.250	223.025	16.14	8.69	15.67	8.40	99.54	38.20	39.45
		2	28	88	244.75	50.00	48.41	240.419	122.266	223.030	14.72	7.80			99.31	41.03	
		3	28	88	244.74	51.43	49.30	242.429	122.274	223.033	16.14	8.70			99.23	39.14	
	56	1	28	88	238.11	50.55	49.48	242.273	124.303	224.204	15.32	8.06	14.19	7.43	132.98	53.17	51.39
		2	28	88	238.12	50.59	49.50	242.274	124.307	224.209	15.31	8.06			129.26	51.62	
		3	28	88	238.14	50.00	50.44	242.285	124.319	228.205	11.94	6.17			124.54	49.38	

Table 15 Compressive strength, apparent porosity, and water absorption of POBC mortars with different curing ages (Continue)

Mix	Age (days)		T (°C)	RH (%)	Weight (g)	W (mm)	L (mm)	SSD-weight in air (g)	SSD-weight in water (g)	Oven-dry weight (g)	Porosity (%)	Water absorption (%)	Avg. porosity (%)	Avg. water absorption (%)	Maximum load (kN)	UCS (MPa)	Avg. UCS (MPa)
B10	7	1	28	85	239.10	48.79	49.05	244.502	118.951	217.623	21.41	12.35	21.77	12.35	63.12	26.38	26.30
		2	28	85	239.12	49.93	49.06	244.509	118.965	217.625	21.41	12.35			64.16	26.19	
		3	28	85	239.11	49.88	49.31	244.517	124.963	217.631	22.49	12.35			64.77	26.33	
	28	1	28	85	236.52	49.53	49.52	246.967	121.665	223.423	18.79	10.54	19.38	10.95	72.91	29.73	29.50
		2	28	85	236.53	50.13	49.71	247.966	121.667	222.484	20.18	11.45			72.95	29.27	
		3	28	85	236.53	50.47	49.74	246.980	120.668	222.759	19.18	10.87			74.02	29.49	
	56	1	28	85	247.47	50.91	50.04	254.322	129.206	231.331	18.38	9.94	18.35	9.93	103.44	40.60	41.02
		2	28	85	247.47	50.52	50.16	254.334	129.209	231.452	18.29	9.89			105.13	41.49	
		3	28	85	247.48	50.30	50.12	254.339	131.207	231.320	18.40	9.95			103.28	40.97	
B20	7	1	28	85	253.10	50.01	50.95	260.206	132.321	227.992	24.99	14.13	25.00	14.13	60.31	23.67	23.49
		2	28	85	253.10	50.98	50.99	260.209	131.326	227.993	25.00	14.13			60.45	23.25	
		3	28	85	253.10	51.09	50.89	260.211	131.339	227.996	25.00	14.13			61.21	23.54	
	28	1	28	85	245.01	51.04	51.25	250.252	131.824	224.401	21.83	11.52	21.80	11.52	73.70	28.17	29.01
		2	28	85	245.01	50.85	49.97	250.253	133.728	224.408	21.81	11.52			73.97	29.11	
		3	28	85	245.01	50.03	48.83	250.261	131.525	224.405	21.78	11.52			72.64	29.73	
	56	1	28	85	240.43	49.70	48.31	246.130	126.063	222.141	19.98	10.80	19.98	10.80	94.70	39.44	38.30
		2	28	85	240.43	48.37	50.04	246.145	126.080	222.145	19.99	10.80			93.97	38.82	
		3	28	85	240.45	50.48	51.45	246.127	126.074	222.165	19.96	10.79			95.12	36.62	

Table 15 Compressive strength, apparent porosity, and water absorption of POBC mortars with different curing ages (Continue)

| Mix | Pre-curing | | | | | Post-curing | | | | | | | | | | | |
	Age (days)		T (°C)	RH (%)	Weight (g)	W (mm)	L (mm)	SSD-weight in air (g)	SSD-weight in water (g)	Oven-dry weight (g)	Porosity (%)	Water absorption (%)	Avg. porosity (%)	Avg. water absorption (%)	Maximum load (kN)	UCS (MPa)	Avg. UCS (MPa)
B30	7	1	28	85	239.93	51.69	49.70	247.827	123.973	214.627	26.81	15.47	26.82	15.48	57.66	22.44	22.77
		2	28	85	239.93	51.52	49.88	247.845	123.978	214.625	26.82	15.48			58.55	22.78	
		3	28	85	239.94	50.17	49.66	247.859	123.979	214.626	26.83	15.48			57.54	23.10	
	28	1	28	85	237.53	50.79	48.27	244.000	132.601	215.016	26.02	13.48	25.85	13.39	64.61	26.35	26.04
		2	28	85	237.55	50.35	50.96	244.336	132.605	216.017	25.35	13.11			65.22	25.42	
		3	28	85	237.69	50.32	49.23	244.235	132.606	215.018	26.17	13.59			65.30	26.36	
	56	1	28	85	239.06	49.67	50.08	247.903	125.413	219.413	23.26	12.98	23.26	12.98	85.51	34.38	35.49
		2	28	85	239.08	49.55	50.17	247.905	125.416	219.419	23.26	12.98			86.84	34.93	
		3	28	85	239.09	48.09	49.92	247.909	125.419	219.416	23.26	12.99			89.21	37.16	
B5R5	7	1	28	89	239.20	50.06	50.90	246.879	126.964	221.331	21.31	11.54	21.31	11.54	73.39	28.80	29.02
		2	28	89	239.20	50.12	49.99	246.899	126.978	221.335	21.32	11.55			73.12	29.18	
		3	28	89	239.21	51.23	50.11	246.874	126.976	221.339	21.30	11.54			74.65	29.08	
	28	1	28	89	234.43	49.28	48.42	242.022	125.211	218.917	19.78	10.55	19.78	10.56	93.89	39.35	39.31
		2	28	89	234.44	50.19	48.70	242.025	127.215	218.916	19.78	10.56			96.56	39.50	
		3	28	89	234.45	50.30	50.37	242.027	126.214	218.920	19.78	10.55			98.99	39.07	
	56	1	28	89	248.08	50.64	49.67	256.411	120.956	233.738	16.74	9.70	16.74	9.70	102.10	40.59	40.15
		2	28	89	248.09	51.25	50.03	256.412	120.958	233.731	16.74	9.70			101.11	39.43	
		3	28	89	248.08	51.14	49.20	256.417	120.957	233.728	16.75	9.71			101.69	40.42	

Table 15 Compressive strength, apparent porosity, and water absorption of POBC mortars with different curing ages (Continue)

Mix	Age (days)		T (°C)	RH (%)	Weight (g)	W (mm)	L (mm)	SSD-weight in air (g)	SSD-weight in water (g)	Oven-dry weight (g)	Porosity (%)	Water absorption (%)	Avg. porosity (%)	Avg. water absorption (%)	Maximum load (kN)	UCS (MPa)	Avg. UCS (MPa)
B5R15	7	1	28	89	235.95	50.41	50.00	241.942	122.432	218.514	19.60	10.72	19.61	10.72	85.28	33.83	33.87
		2	28	89	235.95	49.46	50.28	241.949	122.435	218.519	19.60	10.72			84.21	33.86	
		3	28	89	235.95	50.17	50.01	241.956	122.447	218.516	19.61	10.73			85.10	33.92	
	28	1	28	89	239.46	50.21	48.81	245.718	125.205	223.634	18.32	9.88	17.77	9.55	95.67	39.04	39.37
		2	28	89	239.55	51.58	50.00	245.519	125.215	224.635	17.50	9.39			101.45	39.34	
		3	28	89	239.55	50.76	49.23	246.102	125.219	224.633	17.50	9.39			99.26	39.72	
	56	1	28	89	238.64	50.62	49.43	245.533	120.208	226.632	15.08	8.34	15.36	8.51	112.03	44.77	45.61
		2	28	89	238.66	49.21	49.43	245.542	120.209	225.624	15.89	8.83			111.00	45.63	
		3	28	89	238.66	49.43	48.95	245.551	120.216	226.625	15.10	8.35			112.31	46.42	
B15R5	7	1	28	89	239.66	51.26	50.17	244.794	124.013	217.189	22.86	12.71	22.86	12.71	63.70	24.77	24.50
		2	28	89	239.66	50.00	49.66	244.789	124.055	217.190	22.86	12.71			61.19	24.64	
		3	28	89	239.67	52.10	50.41	244.797	124.025	217.195	22.85	12.71			63.30	24.10	
	28	1	28	89	249.82	51.23	50.07	255.874	137.018	232.712	19.49	9.95	19.48	9.95	82.72	32.25	32.31
		2	28	89	249.83	50.51	50.86	255.875	137.000	232.716	19.48	9.95			82.41	32.08	
		3	28	89	249.83	50.60	50.08	255.879	137.014	232.721	19.48	9.95			82.60	32.60	
	56	1	28	89	244.52	51.36	48.12	250.826	128.828	229.376	17.58	9.35	17.60	9.36	101.61	41.11	40.32
		2	28	89	244.54	50.93	48.96	250.829	128.829	229.380	17.58	9.35			101.23	40.60	
		3	28	89	244.52	51.28	50.25	250.945	128.833	229.412	17.63	9.39			101.17	39.26	

Table 15 Compressive strength, apparent porosity, and water absorption of POBC mortars with different curing ages (Continue)

Mix	Age (days)		T (°C)	RH (%)	Weight (g)	W (mm)	L (mm)	SSD-weight in air (g)	SSD-weight in water (g)	Oven-dry weight (g)	Porosity (%)	Water absorption (%)	Avg. porosity (%)	Avg. water absorption (%)	Maximum load (kN)	UCS (MPa)	Avg. UCS (MPa)
B10R20	7	1	28	85	247.91	51.30	49.14	247.663	122.789	222.797	19.91	11.16	19.92	11.16	79.21	31.42	31.42
		2	28	85	247.92	51.95	50.07	247.669	122.791	222.798	19.92	11.16			81.00	31.14	
		3	28	85	247.91	51.77	47.87	247.675	122.794	222.796	19.92	11.17			78.55	31.70	
	28	1	28	85	243.65	50.22	49.66	248.871	124.046	225.869	18.43	10.18	18.33	10.18	88.62	35.53	35.45
		2	28	85	243.66	50.86	49.94	248.879	122.046	225.878	18.13	10.18			88.65	34.90	
		3	28	85	243.66	50.76	48.50	248.889	124.049	225.879	18.43	10.19			88.45	35.93	
	56	1	28	85	244.81	50.97	50.02	250.380	125.758	229.247	16.96	9.22	16.96	9.22	110.91	43.50	43.19
		2	28	85	244.81	51.17	49.86	250.380	125.765	229.254	16.95	9.22			110.55	43.33	
		3	28	85	244.81	51.90	49.91	250.391	125.754	229.257	16.96	9.22			110.69	42.73	
B20R10	7	1	28	87	239.37	52.12	50.94	244.310	121.283	214.922	23.89	13.67	23.89	13.67	72.51	27.31	27.89
		2	28	87	239.37	51.82	49.98	244.312	121.295	214.931	23.88	13.67			72.00	27.80	
		3	28	87	239.37	51.16	49.81	244.319	121.297	214.925	23.89	13.68			72.77	28.56	
	28	1	28	87	244.85	50.86	48.43	248.194	121.000	220.052	22.13	12.79	22.13	12.79	76.14	30.91	30.30
		2	28	87	244.86	51.25	49.58	248.199	121.046	220.054	22.13	12.79			74.52	29.33	
		3	28	87	244.86	49.89	49.23	248.195	121.002	220.059	22.12	12.79			75.28	30.65	
	56	1	28	87	247.61	51.28	49.34	253.250	127.568	229.755	18.69	10.23	18.70	10.23	95.13	37.60	37.72
		2	28	87	247.61	51.38	49.32	253.266	127.574	229.764	18.70	10.23			96.22	37.97	
		3	28	87	247.61	50.56	48.46	253.264	127.580	229.751	18.71	10.23			92.10	37.59	

Table 16 Properties of POBC mortars exposed to sulfuric acid solution

Mix	Age (days)		T (°C)	RH (%)	Oven-dry Weight* (g)	UCS (MPa) Ref. (Table 15)	W (mm)	L (mm)	Oven-dry Weight* (g)	Maximum load (kN)	UCS (MPa)	Loss in weight (%)	Loss in UCS (%)	Avg. loss in weight (%)	Avg. loss in UCS (%)
						Before expose to sulfuric acid solution			After expose to sulfuric acid solution						
Control	7	1	28	82	234.828	31.30	50.81	49.96	227.925	74.71	29.43	3.03	6.35	2.93	6.65
		2	28	82	239.420	31.30	50.82	49.46	232.407	73.82	29.37	3.02	6.57		
		3	28	82	244.488	31.30	50.33	49.36	237.967	72.64	29.24	2.74	7.04		
	28	1	28	82	246.935	35.55	50.04	49.77	240.771	83.36	33.47	2.56	6.21	2.59	6.24
		2	28	82	239.460	35.55	50.40	49.30	233.693	82.62	33.25	2.47	6.91		
		3	28	82	240.751	35.55	50.36	49.80	234.302	84.44	33.67	2.75	5.59		
	56	1	28	82	243.426	44.86	49.90	49.28	239.46	104.3	42.41	1.66	5.76	1.53	4.94
		2	28	82	243.468	44.86	49.71	49.40	239.033	103.63	42.20	1.86	6.29		
		3	28	82	241.000	44.86	49.26	49.82	238.397	107.13	43.65	1.09	2.76		
R10	7	1	28	82	240.037	33.56	49.88	49.88	232.905	76.79	30.86	3.06	8.75	2.90	6.26
		2	28	82	236.156	33.56	49.89	49.95	229.092	79.08	31.73	3.08	5.77		
		3	28	82	240.866	33.56	50.04	48.88	234.895	78.73	32.19	2.54	4.28		
	28	1	28	82	263.154	41.08	50.42	50.51	259.446	97.23	38.18	1.43	7.61	1.80	4.66
		2	28	82	252.356	41.08	50.50	49.94	247.781	99.14	39.31	1.85	4.51		
		3	28	82	250.590	41.08	50.33	50.00	245.357	101.49	40.33	2.13	1.87		
	56	1	28	82	247.763	48.13	49.85	50.11	245.231	120.21	48.04	1.03	0.18	0.81	3.84
		2	28	82	250.328	48.13	50.45	49.75	248.403	115.65	46.08	0.77	4.45		
		3	28	82	246.426	48.13	50.85	49.52	244.873	113.37	45.02	0.63	6.90		

*Oven-dry weight at 50 °C for 72 hours

Table 16 Properties of POBC mortars exposed to sulfuric acid solution (Continue)

Mix	Age (days)		T (°C)	RH (%)	Oven-dry Weight (g)	UCS (MPa) Ref. (Table 15)	W (mm)	L (mm)	Oven-dry Weight (g)	Maximum load (kN)	UCS (MPa)	Loss in weight (%)	Loss in UCS (%)	Avg. loss in weight (%)	Avg. loss in UCS (%)
					Before expose to sulfuric acid solution		After expose to sulfuric acid solution								
R20	7	1	28	85	240.585	32.11	50.95	49.62	233.504	75.67	29.93	3.03	7.29	2.82	5.97
		2	28	85	244.601	32.11	50.24	50.96	237.807	78.67	30.73	2.86	4.50		
		3	28	85	236.015	32.11	49.86	60.64	230.07	91.48	30.26	2.58	6.13		
	28	1	28	85	232.694	45.07	49.90	50.01	229.21	108.49	43.47	1.52	3.67	1.55	4.36
		2	28	85	233.443	45.07	50.12	50.17	229.852	107.66	42.82	1.56	5.27		
		3	28	85	235.995	45.07	50.15	50.08	232.361	108.69	43.28	1.56	4.14		
	56	1	28	85	246.426	52.94	50.31	49.69	245.09	125.66	50.27	0.55	5.33	0.68	2.90
		2	28	85	238.970	52.94	49.18	50.75	237.341	129.65	51.95	0.69	1.92		
		3	28	85	234.874	52.94	49.18	50.14	233.012	128.7	52.19	0.80	1.44		
R30	7	1	28	85	231.036	30.90	49.64	50.80	225.495	72.03	28.56	2.46	8.16	2.79	5.98
		2	28	85	236.827	30.90	50.85	50.21	230.165	75.62	29.62	2.89	4.32		
		3	28	85	223.169	30.90	50.21	49.59	216.655	72.94	29.29	3.01	5.47		
	28	1	28	85	242.154	39.45	50.24	49.79	240.058	97.35	38.92	0.87	1.38	1.20	3.61
		2	28	85	234.052	39.45	50.88	49.64	231.622	96.93	38.38	1.05	2.80		
		3	28	85	240.011	39.45	50.79	49.94	236.031	93.83	36.99	1.69	6.65		
	56	1	28	85	247.489	44.74	50.20	50.23	246.305	109.51	43.43	0.48	3.01	0.47	1.59
		2	28	85	245.149	44.74	49.52	50.87	244.682	111.75	44.36	0.19	0.85		
		3	28	85	248.782	44.74	50.46	50.33	246.966	112.59	44.33	0.74	0.92		

Table 16 Properties of POBC mortars exposed to sulfuric acid solution (Continue)

Mix	Age (days)		T (ºC)	RH (%)	Oven-dry Weight (g)	UCS (MPa) Ref. (Table 15)	W (mm)	L (mm)	Oven-dry Weight (g)	Maximum load (kN)	UCS (MPa)	Loss in weight (%)	Loss in UCS (%)	Avg. loss in weight (%)	Avg. loss in UCS (%)
					Before expose to sulfuric acid solution		**After expose to sulfuric acid solution**								
B10	7	1	28	85	241.097	26.30	50.35	49.19	234.329	59.34	23.96	2.89	9.77	3.00	7.24
		2	28	85	232.836	26.30	50.38	49.70	225.621	61.55	24.58	3.20	6.99		
		3	28	85	229.528	26.30	50.46	49.29	222.997	62.32	25.06	2.93	4.96		
	28	1	28	85	241.652	29.50	50.13	49.19	235.545	68.78	27.89	2.59	5.75	2.70	5.89
		2	28	85	245.077	29.50	50.62	49.95	239.156	70.29	27.80	2.48	6.10		
		3	28	85	243.094	29.50	50.25	49.24	235.940	68.96	27.87	3.03	5.83		
	56	1	28	85	226.655	41.02	50.05	49.60	224.130	98.41	39.64	1.13	3.47	0.97	4.43
		2	28	85	239.315	41.02	50.68	49.96	236.964	98.33	38.84	0.99	5.62		
		3	28	85	243.278	41.02	50.73	49.65	241.384	99.16	39.37	0.78	4.19		
B20	7	1	28	85	219.994	23.49	50.14	49.69	210.551	54.49	21.87	4.48	7.40	3.07	7.67
		2	28	85	223.986	23.49	50.00	49.68	219.255	53.75	21.64	2.16	8.55		
		3	28	85	215.660	23.49	49.93	49.77	210.265	54.52	21.94	2.57	7.06		
	28	1	28	85	237.981	29.01	49.02	49.97	232.087	67.20	27.43	2.54	5.73	2.68	7.04
		2	28	85	245.329	29.01	49.58	49.93	238.584	66.52	26.86	2.83	7.98		
		3	28	85	250.552	29.01	49.70	49.17	243.997	66.00	27.01	2.69	7.40		
	56	1	28	85	238.163	38.30	49.78	50.62	234.542	91.34	36.25	1.54	5.65	1.54	5.53
		2	28	85	230.270	38.30	50.81	49.92	226.764	92.28	36.27	1.55	5.58		
		3	28	85	229.040	38.30	49.02	50.15	225.602	89.36	36.35	1.52	5.36		

Table 16 Properties of POBC mortars exposed to sulfuric acid solution (Continue)

Mix	Age (days)		T (°C)	RH (%)	Oven-dry Weight (g)	UCS (MPa) Ref. (Table 15)	W (mm)	L (mm)	Oven-dry Weight (g)	Maximum load (kN)	UCS (MPa)	Loss in weight (%)	Loss in UCS (%)	Avg. loss in weight (%)	Avg. loss in UCS (%)
					Before expose to sulfuric acid solution		After expose to sulfuric acid solution								
B30	7	1	28	89	231.042	22.77	50.26	49.43	222.808	52.36	21.08	3.70	8.06	3.19	7.82
		2	28	89	224.795	22.77	50.43	49.60	219.040	53.17	21.26	2.63	7.14		
		3	28	89	226.404	22.77	50.71	49.33	219.259	52.62	21.04	3.26	8.27		
	28	1	28	89	240.749	26.04	50.19	50.40	233.985	62.27	24.62	2.89	5.80	2.99	7.59
		2	28	89	245.468	26.04	50.27	50.96	238.537	61.64	24.06	2.91	8.24		
		3	28	89	248.043	26.04	50.28	50.13	240.418	60.37	23.95	3.17	8.74		
	56	1	28	89	224.280	35.73	50.23	50.29	220.808	85.21	33.73	1.57	5.91	1.57	6.09
		2	28	89	234.840	35.73	49.25	50.47	231.189	83.46	33.58	1.58	6.40		
		3	28	89	237.051	35.73	50.68	50.47	233.382	86.23	33.71	1.57	5.97		
B5R5	7	1	28	89	232.178	29.02	50.62	49.27	229.099	67.73	27.16	1.34	6.87	6.70	2.90
		2	28	89	233.972	29.02	50.39	49.95	222.092	68.83	27.35	5.35	6.13		
		3	28	89	231.652	29.02	49.96	49.69	227.125	67.26	27.09	1.99	7.12		
	28	1	28	89	241.732	39.31	50.32	49.84	237.233	93.25	37.18	1.90	5.72	5.79	2.29
		2	28	89	243.176	39.31	50.79	49.62	237.541	93.42	37.07	2.37	6.04		
		3	28	89	243.487	39.31	50.83	49.75	237.313	94.13	37.22	2.60	5.60		
	56	1	28	89	240.068	42.51	49.88	50.76	237.195	103.24	40.78	1.21	4.27	4.36	1.14
		2	28	89	243.137	42.51	50.18	49.74	240.538	101.57	40.69	1.08	4.47		
		3	28	89	244.473	42.51	50.58	49.81	241.719	102.65	40.74	1.14	4.35		

Table 16 Properties of POBC mortars exposed to sulfuric acid solution (Continue)

Mix	Age (days)		T (°C)	RH (%)	Oven-dry Weight (g)	UCS (MPa) Ref. (Table 15)	W (mm)	L (mm)	Oven-dry Weight (g)	Maximum load (kN)	UCS (MPa)	Loss in weight (%)	Loss in UCS (%)	Avg. loss in weight (%)	Avg. loss in UCS (%)
					Before expose to sulfuric acid solution		After expose to sulfuric acid solution								
B5R15	7	1	28	84	240.024	33.87	50.81	49.11	227.546	79.72	31.95	5.48	6.02	2.69	6.43
		2	28	84	234.382	33.87	50.37	49.74	228.713	79.5	31.73	2.48	6.74		
		3	28	84	238.826	33.87	50.35	49.87	238.549	79.85	31.80	0.12	6.51		
	28	1	28	84	239.356	39.37	50.82	49.82	234.521	94.49	37.32	2.06	5.48	2.20	5.52
		2	28	84	240.360	39.37	50.46	49.16	235.642	93.18	37.56	2.00	4.80		
		3	28	84	236.024	39.37	50.26	49.59	230.156	92.3	37.03	2.55	6.30		
	56	1	28	84	244.957	45.61	50.68	49.68	243.053	110.7	43.97	0.78	3.73	0.86	4.07
		2	28	84	232.040	45.61	50.40	49.88	229.987	110.15	43.82	0.89	4.09		
		3	28	84	236.472	45.61	50.68	49.78	234.369	110.21	43.68	0.90	4.40		
B15R5	7	1	28	84	232.884	24.50	50.77	49.82	226.989	57.94	22.91	2.60	6.98	3.01	7.41
		2	28	84	235.383	24.50	50.39	49.45	230.754	56.46	22.66	2.01	8.15		
		3	28	84	244.023	24.50	49.56	50.50	233.679	57.27	22.88	4.43	7.09		
	28	1	28	84	234.718	32.31	50.17	49.58	228.761	74.57	29.98	2.60	7.77	2.61	6.71
		2	28	84	237.594	32.31	50.38	49.81	231.476	76.72	30.57	2.64	5.68		
		3	28	84	236.523	32.31	50.26	49.25	230.573	74.97	30.29	2.58	6.67		
	56	1	28	84	238.435	40.32	49.79	49.79	234.944	95.17	38.39	1.49	5.04	1.47	4.91
		2	28	84	236.565	40.32	49.87	50.42	233.214	96.68	38.45	1.44	4.87		
		3	28	84	242.624	40.32	49.81	50.12	239.051	96.03	38.47	1.49	4.83		

Table 16 Properties of POBC mortars exposed to sulfuric acid solution (Continue)

Mix	Age (days)		T (°C)	RH (%)	Oven-dry Weight (g)	UCS (MPa) Ref. (Table 15)	W (mm)	L (mm)	Oven-dry Weight (g)	Maximum load (kN)	UCS (MPa)	Loss in weight (%)	Loss in UCS (%)	Avg. loss in weight (%)	Avg. loss in UCS (%)
					Before expose to sulfuric acid solution		After expose to sulfuric acid solution								
B10R20	7	1	28	84	225.393	31.42	50.84	49.32	223.072	73.84	29.45	1.04	6.69	2.77	6.56
		2	28	84	229.728	31.42	50.74	49.48	223.611	73.27	29.18	2.74	7.66		
		3	28	84	232.146	31.42	50.30	49.44	222.056	74.18	29.83	4.54	5.33		
	28	1	28	84	228.063	35.45	50.61	49.60	223.229	83.95	33.44	2.17	6.02	2.49	6.19
		2	28	84	237.981	35.45	50.66	49.10	230.722	82.63	33.22	3.15	6.73		
		3	28	84	233.119	35.45	50.78	49.13	228.219	83.58	33.50	2.15	5.83		
	56	1	28	84	233.233	43.19	49.88	50.45	231.415	104.23	41.42	0.79	4.27	0.90	4.28
		2	28	84	234.902	43.19	50.43	49.41	232.652	103.45	41.52	0.97	4.03		
		3	28	84	227.716	43.19	50.96	50.44	225.552	106.18	41.31	0.96	4.55		
B20R10	7	1	28	87	233.632	27.89	50.38	49.85	227.575	62.7	24.97	2.66	11.71	3.01	7.58
		2	28	87	232.918	27.89	50.62	49.03	225.512	64.87	26.14	3.28	6.70		
		3	28	87	228.660	27.89	50.60	49.32	221.801	66.71	26.73	3.09	4.33		
	28	1	28	87	232.576	30.30	50.66	49.27	227.082	70.81	28.37	2.42	6.79	2.64	6.83
		2	28	87	233.207	30.30	50.63	49.33	227.205	71.04	28.44	2.64	6.51		
		3	28	87	226.120	30.30	50.37	49.00	219.817	69.77	28.27	2.87	7.17		
	56	1	28	87	229.844	37.72	49.88	50.45	226.375	90.52	35.97	1.53	4.86	1.52	4.93
		2	28	87	226.755	37.72	50.43	49.41	223.380	89.44	35.89	1.51	5.08		
		3	28	87	226.354	37.72	50.96	50.44	222.953	92.48	35.98	1.53	4.84		

Table 17 Properties of POBC mortars exposed to sodium sulfate solution

Mix	Age (days)		T (ºC)	RH (%)	Oven-dry Weight* (g)	UCS (MPa) Ref. (Table 15)	W (mm)	L (mm)	Oven-dry Weight* (g)	Maximum load (kN)	UCS (MPa)	Gain in weight (%)	Loss in UCS (%)	Avg. loss in weight (%)	Avg. loss in UCS (%)
					Before expose to sodium sulfate solution				After expose to sodium sulfate solution						
Control	7	1	28	82	236.755	34.36	50.35	50.70	238.032	86.28	33.80	0.54	1.67	0.45	1.51
		2	28	82	237.300	33.65	50.48	49.78	238.817	83.30	33.15	0.64	1.52		
		3	28	82	236.620	32.22	50.03	49.28	237.026	78.40	31.80	0.17	1.33		
	28	1	28	82	229.441	36.01	50.03	49.80	229.920	88.46	35.50	0.21	1.41	0.20	1.42
		2	28	82	236.951	35.27	50.39	49.24	237.381	86.18	34.73	0.18	1.55		
		3	28	82	230.043	35.37	50.32	49.77	230.520	87.45	34.92	0.21	1.30		
	56	1	28	82	242.780	40.00	50.24	49.67	243.054	98.67	39.54	0.11	1.17	0.13	1.15
		2	28	82	248.523	40.74	50.11	49.81	248.865	100.54	40.28	0.14	1.14		
		3	28	82	245.906	39.34	49.44	49.21	246.244	94.65	38.90	0.14	1.13		
R10	7	1	28	82	235.636	33.55	49.80	51.00	235.636	83.99	33.07	0.41	1.44	0.43	1.35
		2	28	82	233.992	33.66	48.86	50.17	233.992	81.34	33.18	0.50	1.45		
		3	28	82	238.908	33.48	50.14	49.61	238.908	82.34	33.10	0.39	1.15		
	28	1	28	82	251.490	42.41	50.43	50.45	251.490	106.92	42.03	0.13	0.92	0.15	0.97
		2	28	82	258.638	42.78	50.52	49.91	258.638	106.83	42.37	0.17	0.96		
		3	28	82	254.452	42.19	50.29	50.21	254.452	105.45	41.76	0.14	1.03		
	56	1	28	82	245.557	44.46	50.50	49.56	245.557	110.32	44.08	0.09	0.86	0.09	0.85
		2	28	82	248.470	44.34	49.74	50.48	248.470	110.19	43.89	0.10	1.04		
		3	28	82	252.500	44.85	50.46	49.33	252.500	83.99	44.56	0.10	0.64		

*Oven-dry weight at 50 °C for 72 hours

Table 17 Properties of POBC mortars exposed to sodium sulfate solution (Continue)

Mix	Age (days)		T (°C)	RH (%)	Before expose to sodium sulfate solution		After expose to sodium sulfate solution								
					Oven-dry Weight (g)	UCS (MPa) Ref. (Table 15)	W (mm)	L (mm)	Oven-dry Weight (g)	Maximum load (kN)	UCS (MPa)	Gain in weight (%)	Loss in UCS (%)	Avg. loss in weight (%)	Avg. loss in UCS (%)
R20	7	1	28	85	231.029	31.29	51.13	48.84	232.065	77.10	30.87	0.45	1.35	0.42	1.32
		2	28	85	231.773	31.09	51.55	49.85	232.706	78.82	30.67	0.40	1.37		
		3	28	85	229.817	31.29	51.04	48.54	230.777	76.58	30.91	0.42	1.23		
	28	1	28	85	240.476	41.83	50.21	49.02	240.894	101.82	41.37	0.17	1.11	0.14	0.89
		2	28	85	235.072	41.83	50.36	49.87	235.306	104.32	41.54	0.10	0.71		
		3	28	85	234.465	42.13	50.22	49.52	234.831	103.88	41.77	0.16	0.85		
	56	1	28	85	245.688	47.01	50.30	49.62	246.009	116.51	46.68	0.13	0.70	0.07	0.55
		2	28	85	237.942	47.40	50.99	49.30	238.032	118.59	47.18	0.04	0.47		
		3	28	85	240.777	47.84	50.48	49.89	240.875	119.92	47.62	0.04	0.48		
R30	7	1	28	85	230.270	34.71	50.02	49.88	231.112	85.59	34.30	0.36	1.17	0.41	1.30
		2	28	85	225.748	34.92	50.08	48.60	226.733	83.94	34.49	0.43	1.24		
		3	28	85	229.822	34.90	50.71	49.29	230.820	85.94	34.38	0.43	1.49		
	28	1	28	85	239.780	40.54	50.26	49.97	240.100	101.10	40.25	0.13	0.72	0.13	0.70
		2	28	85	245.823	39.45	50.48	49.28	246.042	97.52	39.20	0.09	0.64		
		3	28	85	238.308	39.14	50.64	49.52	238.716	97.40	38.84	0.17	0.76		
	56	1	28	85	239.670	42.33	50.88	49.68	239.708	106.65	42.19	0.02	0.34	0.03	0.32
		2	28	85	241.086	42.47	50.43	50.83	241.194	108.53	42.34	0.04	0.32		
		3	28	85	237.970	42.58	50.88	50.22	238.055	108.48	42.45	0.04	0.30		

Table 17 Properties of POBC mortars exposed to sodium sulfate solution (Continue)

Mix	Age (days)		T (°C)	RH (%)	Oven-dry Weight (g)	UCS (MPa) Ref. (Table 15)	W (mm)	L (mm)	Oven-dry Weight (g)	Maximum load (kN)	UCS (MPa)	Gain in weight (%)	Loss in UCS (%)	Avg. loss in weight (%)	Avg. loss in UCS (%)
					Before expose to sodium sulfate solution		After expose to sodium sulfate solution								
B10	7	1	28	85	238.197	25.34	50.68	50.25	239.315	63.63	24.99	0.47	1.41	0.45	1.40
		2	28	85	235.733	26.19	50.61	50.49	236.718	66.10	25.87	0.42	1.25		
		3	28	85	233.508	26.33	50.61	50.24	234.601	65.94	25.93	0.47	1.54		
	28	1	28	85	240.997	29.73	50.00	50.20	241.377	73.75	29.38	0.16	1.17	0.16	1.19
		2	28	85	247.950	29.27	49.91	50.11	248.473	72.57	29.02	0.21	0.89		
		3	28	85	250.105	29.49	50.01	50.22	250.392	72.95	29.05	0.11	1.51		
	56	1	28	85	226.719	40.60	50.52	49.70	227.016	101.00	40.23	0.13	0.94	0.12	0.98
		2	28	85	241.603	41.49	50.43	49.77	241.844	102.97	41.03	0.10	1.12		
		3	28	85	239.762	40.97	50.46	49.29	240.097	101.00	40.61	0.14	0.88		
B20	7	1	28	85	232.745	26.55	50.60	49.94	233.795	66.10	26.16	0.45	1.48	0.46	1.53
		2	28	85	231.742	26.07	50.63	49.97	232.902	64.98	25.68	0.50	1.52		
		3	28	85	231.334	25.58	50.66	49.80	232.362	63.54	25.19	0.44	1.58		
	28	1	28	85	245.071	28.17	49.93	49.99	245.510	69.45	27.82	0.18	1.26	0.18	1.28
		2	28	85	249.658	29.11	49.56	49.91	250.035	71.06	28.73	0.15	1.33		
		3	28	85	248.663	29.73	49.96	49.95	249.191	73.28	29.36	0.21	1.26		
	56	1	28	85	238.221	38.66	50.12	50.06	238.567	95.90	38.22	0.15	1.16	0.16	1.21
		2	28	85	236.711	36.56	50.40	49.68	237.129	90.26	36.05	0.18	1.41		
		3	28	85	228.610	35.91	50.80	49.40	228.941	89.18	35.54	0.14	1.06		

Table 17 Properties of POBC mortars exposed to sodium sulfate solution (Continue)

Mix	Age (days)		T (°C)	RH (%)	Oven-dry Weight (g)	UCS (MPa) Ref. (Table 15)	W (mm)	L (mm)	Oven-dry Weight (g)	Maximum load (kN)	UCS (MPa)	Gain in weight (%)	Loss in UCS (%)	Avg. loss in weight (%)	Avg. loss in UCS (%)
					Before expose to sodium sulfate solution		After expose to sodium sulfate solution								
B30	7	1	28	89	227.188	22.44	50.86	50.62	228.292	56.91	22.10	0.48	1.54	0.48	1.56
		2	28	89	225.960	22.78	50.84	50.68	226.929	57.98	22.50	0.43	1.25		
		3	28	89	224.634	23.10	50.67	50.61	225.847	58.12	22.66	0.54	1.90		
	28	1	28	89	235.013	26.35	50.20	50.19	235.482	65.50	26.00	0.20	1.37	0.21	1.39
		2	28	89	232.680	25.42	50.15	50.19	233.085	63.08	25.06	0.17	1.43		
		3	28	89	247.533	26.36	50.29	50.02	248.157	65.41	26.00	0.25	1.37		
	56	1	28	89	239.169	33.70	50.59	49.63	239.525	83.55	33.28	0.15	1.27	0.16	1.32
		2	28	89	236.634	32.94	50.11	49.76	237.073	81.05	32.50	0.19	1.33		
		3	28	89	223.559	34.31	50.20	50.68	223.909	86.12	33.85	0.16	1.35		
B5R5	7	1	28	89	235.607	30.59	49.87	49.87	236.610	74.96	30.14	0.42	1.50	0.44	1.50
		2	28	89	235.163	29.18	49.79	49.85	236.297	71.39	28.76	0.48	1.46		
		3	28	89	235.854	29.08	49.91	49.85	236.846	71.25	28.64	0.42	1.54		
	28	1	28	89	234.514	39.35	50.46	49.78	234.858	97.56	38.84	0.15	1.31	0.15	1.23
		2	28	89	243.874	39.50	50.38	49.97	244.259	98.38	39.08	0.16	1.09		
		3	28	89	241.384	39.07	50.39	49.82	241.748	96.83	38.57	0.15	1.30		
	56	1	28	89	242.204	42.58	49.69	49.81	242.512	104.22	42.11	0.13	1.12	0.12	1.11
		2	28	89	238.784	42.16	50.35	49.84	239.060	104.65	41.70	0.12	1.11		
		3	28	89	245.870	42.80	49.94	50.28	246.179	106.29	42.33	0.13	1.11		

Table 17 Properties of POBC mortars exposed to sodium sulfate solution (Continue)

Mix	Age (days)		T (°C)	RH (%)	Before expose to sodium sulfate solution Oven-dry Weight* (g)	UCS (MPa) Ref. (Table 15)	After expose to sodium sulfate solution W (mm)	L (mm)	Oven-dry Weight* (g)	Maximum load (kN)	UCS (MPa)	Gain in weight (%)	Loss in UCS (%)	Avg. loss in weight (%)	Avg. loss in UCS (%)
B5R15	7	1	28	84	243.379	24.77	50.31	49.75	244.506	61.03	24.38	0.46	1.58	0.46	1.52
		2	28	84	238.364	24.64	50.22	49.91	239.461	60.75	24.24	0.46	1.68		
		3	28	84	240.271	24.10	50.11	49.68	241.405	59.23	23.79	0.47	1.30		
	28	1	28	84	239.986	32.91	49.54	49.42	240.371	79.55	32.49	0.16	1.27	0.15	1.24
		2	28	84	242.297	32.72	49.93	49.98	242.652	80.62	32.31	0.15	1.29		
		3	28	84	223.785	32.60	49.52	49.95	224.127	79.70	32.22	0.15	1.16		
	56	1	28	84	236.176	39.47	50.32	50.50	236.487	99.24	39.05	0.13	1.08	0.13	1.14
		2	28	84	237.815	39.78	50.37	49.84	238.107	98.77	39.34	0.12	1.12		
		3	28	84	233.534	39.26	50.50	50.12	233.856	98.16	38.78	0.14	1.24		
B15R5	7	1	28	84	243.379	24.77	50.31	49.75	244.506	61.03	24.38	0.46	1.58	0.46	1.52
		2	28	84	238.364	24.64	50.22	49.91	239.461	60.75	24.24	0.46	1.68		
		3	28	84	240.271	24.10	50.11	49.68	241.405	59.23	23.79	0.47	1.30		
	28	1	28	84	239.986	32.91	49.54	49.42	240.371	79.55	32.49	0.16	1.27	0.15	1.24
		2	28	84	242.297	32.72	49.93	49.98	242.652	80.62	32.31	0.15	1.29		
		3	28	84	223.785	32.60	49.52	49.95	224.127	79.70	32.22	0.15	1.16		
	56	1	28	84	236.176	39.47	50.32	50.50	236.487	99.24	39.05	0.13	1.08	0.13	1.14
		2	28	84	237.815	39.78	50.37	49.84	238.107	98.77	39.34	0.12	1.12		
		3	28	84	233.534	39.26	50.50	50.12	233.856	98.16	38.78	0.14	1.24		

Table 17 Properties of POBC mortars exposed to sodium sulfate solution (Continue)

Mix	Age (days)		T (°C)	RH (%)	Oven-dry Weight (g)	UCS (MPa) Ref. (Table 15)	W (mm)	L (mm)	Oven-dry Weight (g)	Maximum load (kN)	UCS (MPa)	Gain in weight (%)	Loss in UCS (%)	Avg. loss in weight (%)	Avg. loss in UCS (%)
					Before expose to sodium sulfate solution		After expose to sodium sulfate solution								
B10R20	7	1	28	84	237.489	31.42	50.56	49.47	238.512	77.49	30.98	0.43	1.42	0.43	1.41
		2	28	84	236.514	31.14	50.68	49.36	237.508	76.89	30.74	0.42	1.31		
		3	28	84	236.102	31.70	50.62	49.56	237.143	78.35	31.23	0.44	1.49		
	28	1	28	84	240.611	33.50	50.15	49.87	240.965	82.93	33.16	0.15	1.02	0.15	1.08
		2	28	84	239.213	33.56	50.00	49.84	239.570	82.64	33.16	0.15	1.19		
		3	28	84	234.909	35.93	50.47	49.49	235.251	88.84	35.57	0.15	1.01		
	56	1	28	84	236.223	40.36	49.85	50.72	236.465	101.13	40.00	0.10	0.90	0.10	0.91
		2	28	84	231.264	40.98	50.05	49.94	231.500	101.34	40.54	0.10	1.07		
		3	28	84	238.522	40.42	50.41	49.88	238.768	100.85	40.11	0.10	0.77		
B20R10	7	1	28	87	234.042	27.31	50.33	50.12	235.144	67.84	26.89	0.47	1.55	0.46	1.54
		2	28	87	235.556	27.80	50.27	50.15	236.631	69.02	27.38	0.45	1.54		
		3	28	87	235.594	28.56	50.24	50.16	236.682	70.89	28.13	0.46	1.51		
	28	1	28	87	241.060	30.91	50.56	50.21	241.458	77.53	30.54	0.16	1.22	0.16	1.31
		2	28	87	232.912	29.33	50.51	50.30	233.305	73.54	28.95	0.17	1.32		
		3	28	87	229.416	30.65	50.38	50.25	229.780	76.53	30.23	0.16	1.39		
	56	1	28	87	232.405	37.60	49.85	50.54	232.740	93.64	37.17	0.14	1.16	0.14	1.18
		2	28	87	228.021	37.97	50.05	49.91	228.345	93.78	37.54	0.14	1.14		
		3	28	87	234.365	37.59	50.41	50.44	234.701	94.42	37.13	0.14	1.23		

APPENDIX G

Properties of POBC concretes

Table 18 The RCPT results of POBC concrete with different binary and ternary mixtures and curing ages

	Ages		28 days		56 days	
Control	Diameter (mm)	1	107.84		107.43	
		2	107.93		107.12	
		Average	107.89		107.28	
	Time elapsed (min)	0	0.140	0.140	0.130	0.130
		30	0.170	0.340	0.130	0.260
		60	0.180	0.360	0.140	0.280
		90	0.180	0.360	0.140	0.280
		120	0.185	0.370	0.150	0.300
		150	0.190	0.380	0.150	0.300
		180	0.190	0.380	0.160	0.320
		210	0.190	0.380	0.170	0.340
		240	0.190	0.380	0.180	0.360
		270	0.190	0.380	0.180	0.360
		300	0.190	0.380	0.190	0.380
		330	0.190	0.380	0.190	0.380
		360	0.190	0.190	0.190	0.190
	Q_x (Coulombs)		3,978		3,492	
	Q_s (Coulombs)		3,085		2,739	

Table 18 The RCPT results of POBC concrete with different binary and ternary mixtures and curing ages (Continue)

	Ages		28 days		56 days	
R10	Diameter (mm)	1	107.89		107.45	
		2	107.90		107.87	
		Average	107.90		107.66	
	Time elapsed (min)	0	0.060	0.060	0.045	0.045
		30	0.060	0.120	0.045	0.090
		60	0.060	0.120	0.045	0.090
		90	0.070	0.140	0.045	0.090
		120	0.070	0.140	0.045	0.090
		150	0.070	0.140	0.045	0.090
		180	0.070	0.140	0.045	0.090
		210	0.070	0.140	0.045	0.090
		240	0.080	0.160	0.045	0.090
		270	0.080	0.160	0.045	0.090
		300	0.080	0.160	0.045	0.090
		330	0.100	0.200	0.045	0.090
		360	0.100	0.100	0.045	0.045
	Q_x (Coulombs)		1,602		972	
	Q_s (Coulombs)		1,242		757	

Table 18 The RCPT results of POBC concrete with different binary and ternary mixtures and curing ages (Continue)

	Ages		28 days		56 days	
R20	Diameter (mm)	1	107.23		107.87	
		2	107.46		107.80	
		Average	107.35		107.84	
	Time elapsed (min)	0	0.040	0.040	0.025	0.025
		30	0.050	0.100	0.030	0.060
		60	0.050	0.100	0.035	0.070
		90	0.060	0.120	0.035	0.070
		120	0.060	0.120	0.035	0.070
		150	0.060	0.120	0.035	0.070
		180	0.060	0.120	0.035	0.070
		210	0.060	0.120	0.035	0.070
		240	0.070	0.140	0.035	0.070
		270	0.100	0.200	0.035	0.070
		300	0.100	0.200	0.035	0.070
		330	0.100	0.200	0.035	0.070
		360	0.100	0.100	0.035	0.035
	Q_x (Coulombs)		1,512		738	
	Q_s (Coulombs)		1,184		573	

Table 18 The RCPT results of POBC concrete with different binary and ternary mixtures and curing ages (Continue)

	Ages		28 days		56 days	
R30	Diameter (mm)	1	107.33		107.74	
		2	107.42		107.78	
		Average	107.38		107.76	
	Time elapsed (min)	0	0.030	0.030	0.020	0.020
		30	0.030	0.060	0.020	0.040
		60	0.030	0.060	0.020	0.040
		90	0.030	0.060	0.020	0.040
		120	0.030	0.060	0.020	0.040
		150	0.030	0.060	0.020	0.040
		180	0.030	0.060	0.020	0.040
		210	0.030	0.060	0.020	0.040
		240	0.030	0.060	0.020	0.040
		270	0.030	0.060	0.020	0.040
		300	0.030	0.060	0.020	0.040
		330	0.030	0.060	0.020	0.040
		360	0.030	0.030	0.020	0.020
	Q_x (Coulombs)		648		432	
	Q_s (Coulombs)		507		336	

Table 18 The RCPT results of POBC concrete with different binary and ternary mixtures and curing ages (Continue)

	Ages		28 days		56 days	
B10	Diameter (mm)	1	107.29		107.68	
		2	107.35		107.90	
		Average	107.32		107.79	
	Time elapsed (min)	0	0.220	0.220	0.190	0.190
		30	0.270	0.540	0.220	0.440
		60	0.305	0.610	0.240	0.480
		90	0.340	0.680	0.250	0.500
		120	0.370	0.740	0.260	0.520
		150	0.380	0.760	0.260	0.520
		180	0.400	0.800	0.270	0.540
		210	0.420	0.840	0.270	0.540
		240	0.430	0.860	0.270	0.540
		270	0.450	0.900	0.270	0.540
		300	0.460	0.920	0.270	0.540
		330	0.480	0.960	0.270	0.540
		360	0.480	0.480	0.270	0.270
	Q_x (Coulombs)		8,379		5,544	
	Q_s (Coulombs)		6,566		4,306	

Table 18 The RCPT results of POBC concrete with different binary and ternary mixtures and curing ages (Continue)

	Ages		28 days		56 days	
B20	Diameter (mm)	1	107.94		108.10	
		2	107.72		108.03	
		Average	107.83		108.07	
	Time elapsed (min)	0	0.260	0.260	0.190	0.190
		30	0.320	0.640	0.220	0.440
		60	0.360	0.720	0.240	0.480
		90	0.390	0.780	0.260	0.520
		120	0.400	0.800	0.270	0.540
		150	0.405	0.810	0.280	0.560
		180	0.420	0.840	0.280	0.560
		210	0.420	0.840	0.280	0.560
		240	0.420	0.840	0.280	0.560
		270	0.420	0.840	0.290	0.580
		300	0.420	0.840	0.290	0.580
		330	0.420	0.840	0.290	0.580
		360	0.420	0.420	0.290	0.290
	Q_x (Coulombs)		8,523		5,796	
	Q_s (Coulombs)		6,615		4,479	

Table 18 The RCPT results of POBC concrete with different binary and ternary mixtures and curing ages (Continue)

Ages			28 days		56 days	
Diameter (mm)		1	107.61		108.05	
		2	107.67		106.89	
		Average	107.64		107.47	
B30	Time elapsed (min)	0	0.300	0.300	0.220	0.220
		30	0.360	0.720	0.240	0.480
		60	0.420	0.840	0.260	0.520
		90	0.450	0.900	0.270	0.540
		120	0.470	0.940	0.280	0.560
		150	0.470	0.940	0.295	0.590
		180	0.470	0.940	0.300	0.600
		210	0.470	0.940	0.300	0.600
		240	0.470	0.940	0.310	0.620
		270	0.470	0.940	0.310	0.620
		300	0.470	0.940	0.310	0.620
		330	0.470	0.940	0.310	0.620
		360	0.470	0.470	0.320	0.320
	Q_x (Coulombs)		9,675		6,219	
	Q_s (Coulombs)		7,536		4,860	

Table 18 The RCPT results of POBC concrete with different binary and ternary mixtures and curing ages (Continue)

	Ages		28 days		56 days	
B5R5	Diameter (mm)	1	108.05		106.91	
		2	108.08		106.86	
		Average	108.07		106.89	
	Time elapsed (min)	0	0.010	2.000	0.080	0.080
		30	0.130	0.130	0.100	0.200
		60	0.140	0.280	0.100	0.200
		90	0.150	0.300	0.100	0.200
		120	0.170	0.340	0.100	0.200
		150	0.180	0.360	0.120	0.240
		180	0.185	0.370	0.120	0.240
		210	0.190	0.380	0.120	0.240
		240	0.190	0.380	0.120	0.240
		270	0.190	0.380	0.120	0.240
		300	0.190	0.380	0.120	0.240
		330	0.190	0.380	0.120	0.240
		360	0.190	0.380	0.120	0.120
	Q_x (Coulombs)		3,825		2,412	
	Q_s (Coulombs)		2,956		1,905	

Table 18 The RCPT results of POBC concrete with different binary and ternary mixtures and curing ages (Continue)

	Ages		28 days		56 days	
B5R15	Diameter (mm)	1	107.93		106.91	
		2	108.25		106.86	
		Average	108.09		106.89	
	Time elapsed (min)	0	0.040	0.040	0.035	0.035
		30	0.040	0.080	0.040	0.080
		60	0.050	0.100	0.040	0.080
		90	0.050	0.100	0.040	0.080
		120	0.050	0.100	0.040	0.080
		150	0.050	0.100	0.040	0.080
		180	0.050	0.100	0.040	0.080
		210	0.050	0.100	0.045	0.090
		240	0.050	0.100	0.045	0.090
		270	0.050	0.100	0.045	0.090
		300	0.050	0.100	0.045	0.090
		330	0.050	0.100	0.045	0.090
		360	0.050	0.050	0.045	0.045
	Q_x (Coulombs)		1,053		909	
	Q_s (Coulombs)		813		718	

Table 18 The RCPT results of POBC concrete with different binary and ternary mixtures and curing ages (Continue)

	Ages		28 days		56 days	
B15R5	Diameter (mm)	1	107.76		106.78	
		2	107.61		106.83	
		Average	107.69		106.81	
	Time elapsed (min)	0	0.085	0.085	0.050	0.050
		30	0.100	0.200	0.050	0.100
		60	0.100	0.200	0.050	0.100
		90	0.100	0.200	0.050	0.100
		120	0.110	0.220	0.050	0.100
		150	0.110	0.220	0.060	0.120
		180	0.120	0.240	0.060	0.120
		210	0.120	0.240	0.060	0.120
		240	0.120	0.240	0.070	0.140
		270	0.120	0.240	0.070	0.140
		300	0.120	0.240	0.070	0.140
		330	0.121	0.242	0.070	0.140
		360	0.122	0.122	0.080	0.080
	Q_x (Coulombs)		2,420		1,305	
	Q_s (Coulombs)		1,884		1,032	

Table 18 The RCPT results of POBC concrete with different binary and ternary mixtures and curing ages (Continue)

Ages			28 days		56 days	
Diameter (mm)		1	106.55		106.57	
		2	107.10		107.04	
		Average	106.83		106.81	
B10R20	Time elapsed (min)	0	0.040	0.040	0.035	0.035
		30	0.040	0.080	0.035	0.070
		60	0.041	0.082	0.035	0.070
		90	0.041	0.082	0.035	0.070
		120	0.041	0.082	0.035	0.070
		150	0.041	0.082	0.035	0.070
		180	0.041	0.082	0.035	0.070
		210	0.041	0.082	0.035	0.070
		240	0.041	0.082	0.035	0.070
		270	0.041	0.082	0.035	0.070
		300	0.041	0.082	0.035	0.070
		330	0.041	0.082	0.035	0.070
		360	0.041	0.041	0.035	0.035
Q_x (Coulombs)			883		756	
Q_s (Coulombs)			698		598	

Table 18 The RCPT results of POBC concrete with different binary and ternary mixtures and curing ages (Continue)

	Ages		28 days		56 days	
B20R10	Diameter (mm)	1	106.86		107.27	
		2	107.62		107.52	
		Average	107.24		107.40	
	Time elapsed (min)	0	0.080	0.080	0.055	0.055
		30	0.090	0.180	0.060	0.120
		60	0.100	0.200	0.060	0.120
		90	0.100	0.200	0.060	0.120
		120	0.105	0.210	0.060	0.120
		150	0.110	0.220	0.060	0.120
		180	0.120	0.240	0.060	0.120
		210	0.120	0.240	0.060	0.120
		240	0.120	0.240	0.060	0.120
		270	0.120	0.240	0.060	0.120
		300	0.120	0.240	0.060	0.120
		330	0.121	0.242	0.060	0.120
		360	0.140	0.140	0.060	0.060
	Q_x (Coulombs)		2,405		1,292	
	Q_s (Coulombs)		1,887		1,011	

Table 19 Capillary water absorption of 28-day POBC concrete with different binary and ternary mixtures

Mix designation	Avg. Cross-sectional area (mm^2)	Mass (kg)		ΔMass/area*10^5	ΔMass/area/time$^{0.5}$
		Weighted at 0 h	Weighted at 72 h		
Control	9,136.75	1.051	1.061	0.109	0.12
R10	9,138.44	1.026	1.034	0.088	0.10
R20	9,045.51	0.964	0.971	0.077	0.09
R30	9,050.57	0.984	0.990	0.066	0.07
B10	9,041.30	0.970	0.980	0.111	0.14
B20	9,127.43	0.989	1.005	0.175	0.21
B30	9,095.30	1.024	1.041	0.187	0.22
B5R5	8,998.38	1.018	1.025	0.078	0.10
B5R15	9,171.50	1.036	1.042	0.065	0.08
B15R5	9,102.90	1.018	1.025	0.077	0.09
B10R20	9,126.59	1.003	1.009	0.066	0.08
B20R10	9,027.82	1.018	1.025	0.078	0.09

Table 20 Capillary water absorption of 56-day POBC concrete with different binary and ternary mixtures

Mix designation	Avg. Cross-sectional area (mm^2)	Mass (kg)		ΔMass/area*10^5	ΔMass/area/time$^{0.5}$
		Weighted at 0 h	Weighted at 72 h		
Control	9,007.64	1.039	1.047	0.096	0.10
R10	9,139.29	1.041	1.047	0.075	0.08
R20	9,122.36	1.018	1.023	0.064	0.07
R30	9,118.97	1.019	1.024	0.056	0.06
B10	9,058.16	1.004	1.013	0.103	0.11
B20	8,945.52	1.086	1.095	0.108	0.12
B30	8,969.00	1.014	1.027	0.151	0.17
B5R5	8,963.96	1.055	1.062	0.079	0.09
B5R15	9,061.53	1.042	1.048	0.067	0.07
B15R5	8,958.93	1.031	1.037	0.078	0.08
B10R20	8,994.19	1.003	1.008	0.066	0.07
B20R10	9,075.03	1.036	1.042	0.071	0.08

Table 21 Indirect tensile strength of 28-day POBC concrete with different binary and ternary mixtures

Mixes	Diameter (mm)			L, Thickness (mm)			P (N)	2P (N)	Pi*(D)*(L)	σt
	Top	Bottom	Avg.	Left	Right	Avg.				(MPa)
Control	112.84	107.93	110.39	52.74	55.63	54.19	25,960	51,920	18,798.09	2.76
R10	107.89	107.90	107.90	51.43	50.82	51.13	32,180	64,360	17,336.41	3.71
R20	107.23	107.46	107.35	50.78	50.39	50.59	25,340	50,680	17,065.86	2.97
R30	107.33	107.42	107.38	51.35	52.20	51.78	22,190	44,380	17,472.21	2.54
B10	107.29	107.35	107.32	51.70	49.41	50.56	24,860	49,720	17,051.77	2.92
B20	107.94	107.72	107.83	51.90	50.79	51.35	24,110	48,220	17,400.53	2.77
B30	107.61	107.67	107.64	52.34	52.33	52.34	19,870	39,740	17,704.78	2.24
B5R5	108.05	108.08	108.07	50.79	50.75	50.77	24,400	48,800	17,243.16	2.83
B5R15	107.93	108.25	108.09	52.25	52.53	52.39	25,850	51,700	17,797.48	2.90
B15R5	107.70	107.61	107.66	51.25	51.82	51.54	24,710	49,420	17,436.57	2.83
B10R20	106.55	107.10	106.83	51.29	51.26	51.28	27,970	55,940	17,214.85	3.25
B20R10	106.86	107.62	107.24	51.76	52.02	51.89	24,590	49,180	17,489.01	2.81

Table 22 Indirect tensile strength of 56-day POBC concrete with different binary and ternary mixtures

Mixes	Diameter (mm)			L, Thickness (mm)			P (N)	2P (N)	Pi*(D)*(L)	σt
	Top	Bottom	Avg.	Left	Right	Avg.				(MPa)
Control	107.43	107.12	107.28	52.44	52.26	52.35	27,250	54,500	17,649.80	3.09
R10	107.45	107.90	107.68	51.11	52.57	51.84	33,350	66,700	17,543.03	3.80
R20	107.87	107.80	107.84	52.95	53.21	53.08	28,570	57,140	17,989.34	3.18
R30	107.74	107.78	107.76	52.65	51.35	52.00	25,840	51,680	17,611.06	2.93
B10	107.59	107.42	107.51	50.84	51.24	51.04	27,310	54,620	17,245.03	3.17
B20	106.69	106.75	106.72	52.66	51.59	52.13	26,310	52,620	17,483.02	3.01
B30	108.05	106.89	107.47	53.80	53.53	53.67	26,880	53,760	18,126.04	2.97
B5R5	106.90	106.86	106.88	51.58	52.34	51.96	26,560	53,120	17,453.81	3.04
B5R15	106.78	106.83	106.81	52.07	52.22	52.15	30,950	61,900	17,503.66	3.54
B15R5	107.85	107.44	107.65	52.05	52.59	52.32	27,010	54,020	17,700.53	3.05
B10R20	106.57	107.04	106.81	52.19	51.90	52.05	29,010	58,020	17,470.09	3.32
B20R10	107.27	107.52	107.40	53.57	52.20	52.89	26,810	53,620	17,850.12	3.00

VITAE

Name   Miss Kamolchanok Kueaket

Student ID 6010120097

Educational Attainment

Degree	Name of Institution	Year of Graduation
Bachelor of Science (Geoscience) (First-class honor)	Mahidol University, Kanchanaburi campus	2016

Scholarship Awards during Enrollment

1. Graduate Engineering Scholarship, Faculty of Engineering, Prince of Songkla University, 2017
2. PSU.GS. Research Grant for Thesis, PSU Graduate School, Prince of Songkla University, 2019

Work – Position and Address

2020 - Present: Mining industrial technical officer

    Primary Industries and Mines Group, Provincial Industry Office, Phang-nga

    490 Petchakasem road, Tambon Tai-Chang,

    Ampoe Mueang Phang-nga, Phang-nga,

    Thailand, 82000

List of Publications and Proceedings

1. Kueaket, K., & Tonnayopas, D. (2018). Enhanced properties of palm oil boiler clinker concrete with Sang Yod rice husk ash. *Proceeding of 7th International Conference on Applied Sciences and Engineering (ICASEA, 2018)*, Kota Kinabalu, Sabah, Malaysia, 29-38.
2. Kueaket, K., & Tonnayopas, D. (2019). Palm oil boiler clinker properties used as a green aggregate for construction. *Proceeding of the 13th International Conference on Mining, Materials, and Petroleum Engineering (CMMP 2019)*, Krabi, Thailand, 86-91.
3. Kueaket, K., & Tonnayopas, D. (2021). Compressive strength and durability performance of mortar containing palm oil boiler clinker aggregate, rice husk ash, and calcium bentonite. *Journal of Applied Engineering Science*, 19(1), 193-203. doi: 10.5937/jaes0-27580
4. Kueaket, K., & Tonnayopas, D. (2021). Sustainable mortar and concrete made from palm oil boiler clinker aggregate comprising rice husk ash and calcium bentonite: Compressive strength and durability assessment. *Journal of Applied Science*, 20(1), 39-55. doi: 10.14416/j.appsci.2021.01.004